www.cardiol.br

www.dicsbc.org

ABC Imagem Cardiovascular

Sociedade Brasileira de Cardiologia • ISSN 2675-312X • Volume 35, Nº 4, October/November/December 2022

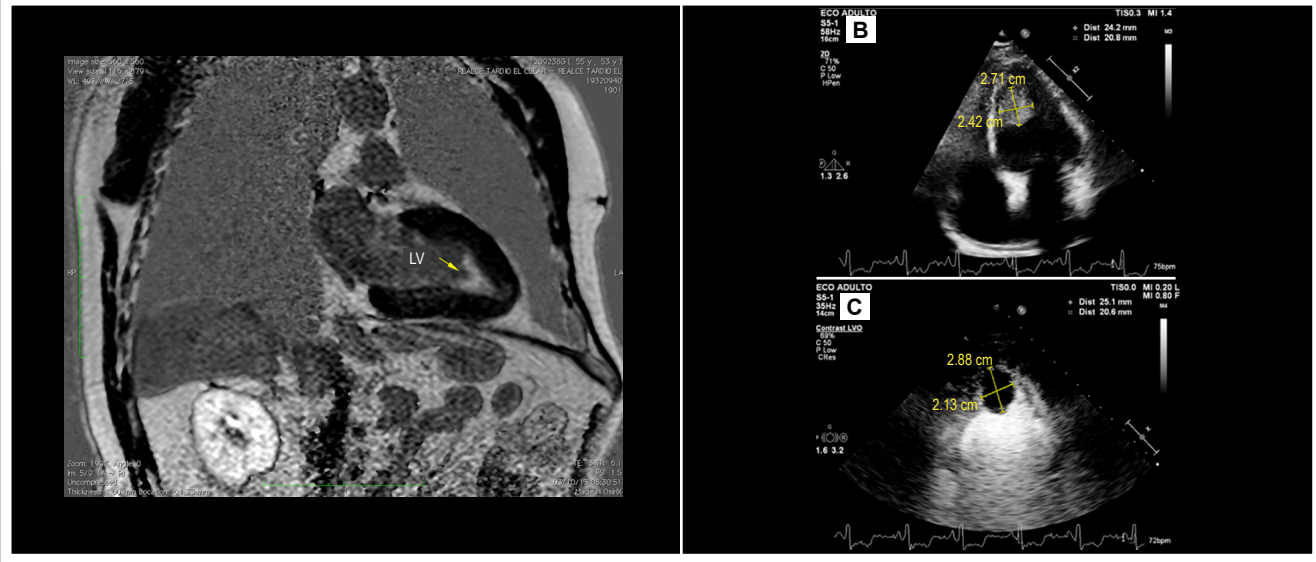

Arquivos Brasileiros de Cardiologia - Imagem Cardiovascular

Volume 35, Nº 4, October/November/December 2022

Indexing source: LILACS - Literatura Latino-Americana e do Caribe em Ciências da Saúde - www.bireme.br, LATINDEX - Sistema Regional de Información en Línea para Revistas Científicas de América Latina, El Caribe, España y Portugal - www.latindex.unam.mx

Department of Cardiovascular Imaging/ Brazilian Society of Cardiology
Rua Barata Ribeiro nº 380 cj.54
01308-000 - São Paulo - SP - Brasil
Fone/Fax: +55 (11) 3259-2988
Fones: +55 (11) 3120-3363
+55 (11) 3259-2988 / +55 (11) 2589-4168

Editorial Coordination
Atha Comunicação e Editora
Rua Machado Bittencourt, 190 - conj. 409
São Paulo, SP, Brasil
Tel.: (11) 50879502

Editorial Support
revista@dicsbc.com

www.cardiol.br
www.dicsbc.org
ABC Imagem Cardiovascular

Contents - *Sumário*

Click on the title to read the article

www.cardiol.br
www.dicsbc.org
ABC Imagem Cardiovascular

www.cardiol.br
www.dicsbc.org
ABC Imagem Cardiovascular

Editorial Board Imagem Cardiovascular

National Editorial Board

Brivaldo Markman Filho - Hospital das Clínicas da Universidade Federal de Pernambuco – PE

Bruna Morhy Borges Leal Assunção - Hospital Sírio Libanês e Instituto do Câncer do Estado de São Paulo (ICESP), São Paulo - SP

Caio Cesar Jorge Medeiros - Hospital São Luiz, São Paulo - SP

Carlos Eduardo Rochitte - Instituto do Coração do Hospital das Clínicas da Faculdade de Medicina da Universidade de São Paulo (INCOR/FMUSP), São Paulo - SP

Carlos Eduardo Suaide Silva - DASA (Diagnósticos da América) São Paulo - SP

Carlos Eduardo Tizziani Oliveira Lima - Hospital Casa de Saúde de Campinas, Campinas – SP

Cecília Beatriz Bittenciurt Viana Cruz - Instituto do Coração Hospital das Clínicas da Faculdade de Medicina da Universidade de São Paulo (INCOR/FMUSP), Hospital Sírio Libanês e Instituto do Câncer do Estado de São Paulo (ICESP), São Paulo - SP

Cintia Galhardo Tressino - Instituto Dante Pazzanese e Grupo DASA, São Paulo - SP

Claudia Cosentino Gallafrio - Hospital do GRAACC - Universidade Federal de São Paulo/Hospital Israelita Albert Einstein/Grupo DASA São Paulo - Alta diagnósticos, São Paulo – SP

Claudia Pinheiro de Castro Grau - Instituto do Coração Hospital das Clínicas da FMUSP e Hospital e Maternidade São Luiz, São Paulo - SP

Claudia Gianini Monaco - Hospital Israelita Albert Einstein, São Paulo - SP

Cláudio Henrique Fischer – Universidade Federal de São Paulo (UNIFESP) e Hospital Israelita Albert Einstein, São Paulo - SP

Cláudio Leinig Pereira da Cunha - Universidade Federal do Paraná, Curitiba - PR

Claudio Tinoco Mesquita - Universidade Federal Fluminense (UFF), Rio de Janeiro - RJ

Clerio Francisco de Azevedo Filho - Universidade do Estado do Rio de Janeiro (UERJ), Rio de Janeiro – RJ

David Costa de Souza Le Bihan - Instituto Dante Pazzanese da Cardiologia, São Paulo - SP

Djair Brindeiro Filho - Serviço de Ecocardiografia do Recife Ltda. e Real Hospital Português de Beneficência em Pernambuco - PE

Edgar Bezerra Lira Filho - Hospital das Clínicas, FMUSP; Hospital Israelita Albert Einstein, São Paulo – SP

Edgar Daminello - Hospital Israelita Albert Einstein, São Paulo – SP

Eliza de Almeida Gripp - Hospital Pró Cardíaco e do Hospital Universitário Antônio Pedro (UFF), Rio de Janeiro - RJ

Eliza Kaori Uenishi - Instituto do Coração do Hospital das Clínicas da Faculdade de Medicina da Universidade de São Paulo (INCOR/FMUSP), São Paulo - SP

Estela Suzana Kleiman Horowitz - Fundação Universitária de Cardiologia, Porto Alegre – RS

Fabio de Cerqueira Lario - Hospital Alemão Oswaldo Cruz, São Paulo – SP

Fabio Villaça Guimarães Filho - Faculdade de Medicina de Marília/Instituto do Coração de Marília, Marília – SP

Fernando Antônio de Portugal Morcerf - Ecor Ecocardiografia Ltda, Rio de Janeiro – RJ

Frederico José Neves Mancuso - Escola Paulista de Medicina - Universidade Federal de São Paulo (UNIFESP/EPM), São Paulo - SP

Gabriel Leo Blacher Grossman - Hospital Moinhos de Vento e Clínica Cardionuclear, Rio Grande do Sul – RS

Gabriela Liberato - Instituto do Coração do Hospital das Clínicas da Faculdade de Medicina da Universidade de São Paulo (INCOR/FMUSP), São Paulo - SP

Gabriela Nunes Leal - Hospital das Clínicas da Faculdade de Medicina da Universidade de São Paulo (HC-FMUSP), São Paulo - SP

Giordano Bruno de Oliveira Parente - Hospital Agamenon Magalhães, Recife - PE

Gláucia Maria Penha Tavares - Instituto do Coração do Hospital das Clínicas da Faculdade de Medicina da Universidade de São Paulo (INCOR/FMUSP) e Hospital Israelita Albert Einstein, São Paulo - SP

Henry Abensur - Departamento de Ecocardiografia, A Beneficência Portuguesa de São Paulo, São Paulo - SP

Ibraim Masciarelli Francisco Pinto - Instituto Dante Pazzanese de Cardiologia, São Paulo - SP

Ilan Gottlieb - Casa de Saúde São José e Clínica São Vicente, Rio de Janeiro - SP

Iran de Castro - Instituto de Cardiologia do Rio Grande do Sul (IC/FUC), Porto Alegre - RS

Isabel Cristina Britto Guimaraes - Hospital Ana Neri, Universidade Federal da Bahia, Bahia - BA

Ivan Romero Rivera - Universidade Federal de Alagoas, Maceió - AL

Jaime Santos Portugal - Proecho - Cardiologia Serviços Médicos Ltda, Rio de Janeiro - RJ

Jeane Mike Tsutsui - Instituto do Coração do Hospital das Clínicas da Faculdade de Medicina da Universidade de São Paulo (INCOR/FMUSP), Fleury Medicina e Saúde, São Paulo – SP

João Marcos Bemfica Barbosa Ferreira - Universidade do Estado do Amazonas, Amazonas - AM

José de Arimatéia Batista Araujo-Filho - Hospital Sírio-Libanês, São Paulo, Brasil. Memorial Sloan-Kettering Cancer Center, Nova Iorque – Estados Unidos.

José Lázaro de Andrade - Hospital Sírio Libanês, São Paulo – SP

José Luis de Castro e Silva Pretto - Hospital São Vicente de Paulo/Hospital de Clínicas de Passo Fundo, Rio Grade do Sul - RS

José Luiz Barros Pena - Hospital Felício Rocho, Belo Horizonte - MG

José Maria Del Castillo - Pronto Socorro Cardiológico de Pernambuco (PROCAPE - UPE), Recife – PE

José Olimpio Dias Júnior - Hospital Mater Dei, Belo Horizonte - MG

José Sebastião de Abreu - Clinicárdio de Fortaleza e Cardioexata, Fortaleza – PE

José Roberto Matos-Souza - Faculdade de Medicina da UNICAMP, São Paulo - SP

Joselina Luzia Menezes Oliveira - Fundação São Lucas, Aracaju – SE

Jorge Andion Torreão - Hospital Cárdio Pulmonar, Bahia – BA

Juliana Fernandes Kelendjian - CDI Centro de Diagnóstico por Imagem, Goiânia - GC

Laise Antonia Bonfim Guimarães - Sociedade Beneficente Israelita Brasileira de Ensino e Pesquisa Albert Einstein, são Paulo – SP

Lara Cristiane Terra Ferreira Carreira - Cardiologia Nuclear de Curitiba e Hospital Nossa Senhora do Pilar, Curitiba, Paraná – PR

Leina Zorzanelli - Instituto do Coração do Hospital das Clínicas da Faculdade de Medicina da Universidade de São Paulo (INCOR/FMUSP), São Paulo - SP

Lilian Maria Lopes - ECOKIDGRAFIA - Serviços Médicos Ecodoppler, São Paulo – SP

Liz Andréa Baroncini - Hospital da Cruz Vermelha e Instituto Saber e Aprender, Paraná - PR

Luciano Aguiar Filho - Hospital Salvaluz, DIAGMED (Tomografia e Ressonância Cardíaca), Hospital Municipal de Barueri e Instituto Dante Pazzanese de Cardiologia, São Paulo -SP

Luciano Herman Juaçaba Belém - Instituto Nacional de Cardiologia, Rio de Janeiro - RJ

Luiz Darcy Cortez Ferreira - OMNI - CCNI - Medicina Diagnóstica, São Paulo - SP

Luiz Felipe P. Moreira - Instituto do Coração do Hospital das Clínicas da Faculdade de Medicina da Universidade de São Paulo (INCOR/FMUSP), São Paulo - SP

Manuel Adán Gil – Universidade Federal de São Paulo – Escola Paulista de Medicina, São Paulo – SP

Marcela Momesso Peçanha - Instituto Dante Pazzanese de Cardiologia, São Paulo – SP

Marcelo Dantas Tavares - Universidade Federal da Paraíba, Paraíba - PB

Marcelo Haertel Miglioranza - Instituto de Cardiologia do Rio Grande do Sul, Rio Grande do Sul - RS

Marcelo Luiz Campos Vieira - Instituto do Coração do Hospital das Clínicas da Faculdade de Medicina da Universidade de São Paulo (InCor-HCFMUSP) e Hospital Israelita Albert Einstein, São Paulo - SP

Marcelo Souza Hadlich - Instituto Nacional de Cardiologia, INC., Hospital da Unimed-Rio, ACSC - Casa de Saúde São José, RioImagem CDI, Rede D´Or de Hospitais, Rede Labs D'Or, Rio de Janeiro – RJ

Marcia Azevedo Caldas - Faculdade de Medicina de Campos, Rio de Janeiro - RJ

Marcia de Melo Barbosa – ECOCENTER, Belo Horizonte – MG

Marcia Ferreira Alves Barberato - CardioEco – Centro de Diagnóstico Cardiovascular, Curitiba - PR

Márcio Silva Miguel Lima - Instituto do Coração do Hospital das Clínicas da Faculdade de Medicina da Universidade de São Paulo (InCor-HCFMUSP), São Paulo – SP

Marcio Sommer Bittencourt - Hospital Universitário de São Paulo/Hospital Israelita Albert Einstein, São Paulo - SP

Márcio Vinícius Lins de Barros - Faculdade de Saúde e Ecologia Humana FASEH, Vespasiano - MG

Marcos Valério Coimbra de Resende - Hospital Samaritano Paulista, São Paulo – SP

Maria Clementina Di Giorgi - Instituto do Coração do Hospital das Clínicas da Faculdade de Medicina da Universidade de São Paulo (InCor-HCFMUSP), São Paulo – SP

International Editorial Board

Department of Cardiovascular Imaging

President
André Luiz Cerqueira de Almeida - BA

Vice President of Echocardiography
Alex dos Santos Félix - RJ

Vice President of Nuclear Cardiology
Simone Cristina Soares Brandão - PE

Vice President of Vascular Echography
José Aldo Ribeiro Teodoro - SP

Vice President of Magnetic Resonance Imaging
Otávio Rizzi Coelho Filho - SP

Vice President of Computed Tomography
Márcio Sommer Bittencourt - SP

Vice President of Congenital Heart Disease and Pediatric Cardiology
Adriana Mello Rodrigues dos Santos - MG

Managing Director
Silvio Henrique Barberato - PR

Financial Director
Mohamed Hassan Saleh - SP

Journal Director
Daniela do Carmo Rassi Frota - GO

Board of Trustees

President
Fábio Villaça Guimarães Filho - SP

Members
Afonso Akio Shiozaki - PR
Bruna Morhy Borges Leal Assunção - SP
David Costa de Souza Le Bihan - SP
Jorge Andion Torreão - BA
José Luiz Barros Pena - MG
José Olimpio Dias Júnior - MG
Rafael Willain Lopes - SP

Scientific Committee

Coordinator
Alex dos Santos Félix - RJ

Members
Simone Cristina Soares Brandão - PE
José Aldo Ribeiro Teodoro - SP
Otávio Rizzi Coelho Filho - SP
Márcio Sommer Bittencourt - SP

Qualification Committee

Coordinator
Andrea de Andrade Vilela - SP

Adult Echo Members
Antônio Amador Calvilho Júnior - SP
Candice Machado Porto - BA
Eliza de Almeida Gripp - RJ
João Carlos Moron Saes Braga - SP
Rafael Modesto Fernandes – BA
Rudyney Eduardo Uchoa de Azevedo – SP
Sandra Nívea dos Reis Saraiva Falcão - CE

Congenital Echo Members
Carlos Henrique de Marchi - SP
Daniela Lago Kreuzig - SP
Halsted Alarcão Gomes Pereira da Silva - SP
Márcio Miranda Brito - TO

Seniors
Fábio Villaça Guimarães Filho - SP
Maria Estefânia Bosco Otto - DF
Solange Bernades Tatani - SP

Communication, Information and Internet Committee

Coordinator
José Roberto Matos Souza - SP

Members
Fabio Roston
Issam Shehadeh

Committee of Institutional Relations, Fees and Advocacy

Coordinator
Marcelo Haertel Miglioranza - RS

Members
Wagner Pires de Oliveira Júnior - DF

Committee of Education and Accreditation

Coordinator
Edgar Bezerra de Lira Filho - SP

Intersociety Committee

Coordinator
Marcelo Luiz Campos Vieira - SP

DIC Youth Committee

Coordinator
Eliza de Almeida Gripp - RJ

Positioning and Guidelines Committee

Coordinator
Marcelo Dantas Tavares de Melo - PB

Consultant
José Luiz Barros Pena - MG

Representatives

ASE
José Luiz Barros Pena - MG

EACVI
Alex dos Santos Félix - RJ

SISIAC
Ana Cristina de Almeida Camarozano - PR

Board of Former Presidents
Jorge Eduardo Assef - SP
Arnaldo Rabischoffsky - RJ
Samira Saady Morhy - SP
Marcelo Luiz Campos Vieira - SP
Carlos Eduardo Rochitte -SP

Board of Directors – Year 2022 (Brazilian Society of Cardiology)

North/Northeast
Nivaldo Menezes Filgueiras Filho (BA)
Sérgio Tavares Montenegro (PE)

East
Denilson Campos de Albuquerque (RJ)
Andréa Araujo Brandão (RJ) – Vice-presidente do Conselho Administrativo

State of São Paulo
Celso Amodeo (SP)
João Fernando Monteiro Ferreira (SP) – Presidente do Conselho Administrativo

Center
Carlos Eduardo de Souza Miranda (MG)
Weimar Kunz Sebba Barroso de Souza (GO)

South
Paulo Ricardo Avancini Caramori (RS)
Gerson Luiz Bredt Júnior (PR)

Editor of ABC Cardiol (2022-2025)
Carlos Eduardo Rochitte

Editor of IJCS (2022-2025)
Claudio Tinoco Mesquita

Presidents of State and Regional Chapters

SBC/AL – Pedro Henrique Oliveira de Albuquerque
SBC/BA – Joberto Pinheiro Sena
SBC/DF – Fausto Stauffer Junqueira de Souza
SBC/ES – Tatiane Mascarenhas Santiago Emerich
SBC/GO – Humberto Graner Moreira
SBC/MA – Francisco de Assis Amorim de Aguiar Filho
SBC/MG – Antônio Fernandino de Castro Bahia Neto
SBC/MS – Mauro Rogério de Barros Wanderley Júnior
SBC/NNE – José Albuquerque de Figueiredo Neto
SBC/PB – Guilherme Veras Mascena
SBC/PE – Carlos Japhet Da Matta Albuquerque
SBC/PI – Jônatas Melo Neto
SBC/PR – Olímpio R. França Neto
SOCERJ – Ronaldo de Souza Leão Lima
SBC/RN – Antônio Amorim de Araújo Filho
SOCERGS – Fábio Cañellas Moreira
SOCESP – Ieda Biscegli Jatene

Departments and Study Groups

SBC/DA – Marcelo Heitor Vieira Assad
SBC/DCC – Bruno Caramelli
SBC/DCC/CP – Cristiane Nunes Martins
SBC/DCM – Maria Cristina Costa de Almeida
SBC/DECAGE – José Carlos da Costa Zanon
SBC/DEIC – Mucio Tavares de Oliveira Junior
SBC/DEMCA – Álvaro Avezum Junior
SBC/DERC – Ricardo Quental Coutinho
SBC/DFCVR – Elmiro Santos Resende
SBC/DHA – Lucélia Batista Neves Cunha Magalhães
SBC/DIC – André Luiz Cerqueira de Almeida
SBCCV – João Carlos Ferreira Leal
SOBRAC – Fatima Dumas Cintra
SBHCI – Ricardo Alves da Costa
DCC/GECIP – Marcelo Luiz da Silva Bandeira
DCC/GECOP – Maria Verônica Câmara dos Santos
DCC/GEPREVIA – Isabel Cristina Britto Guimarães
DCC/GAPO – Luciana Savoy Fornari
DCC/GEAT – Carlos Vicente Serrano Junior
DCC/GECETI – João Luiz Fernandes Petriz
DCC/GEDORAC – Sandra Marques e Silva
DCC/GEECG – Nelson Samesima
DCC/GERTC – Adriano Camargo de Castro Carneiro
DEIC/GEICPED – Estela Azeka
DEIC/GEMIC – Marcus Vinicius Simões
DEIC/GETAC – Silvia Moreira Ayub Ferreira
DERC/GECESP – Marconi Gomes da Silva
DERC/GECN – Lara Cristiane Terra Ferreira Carreira
DERC/GERCPM – Pablo Marino Corrêa Nascimento

How to Perform a Diagnostic and Prognostic Analysis of Hypertrophic Cardiomyopathy in 2022: Should we Divide to Improve Treatment?

Cardiomiopatia Hipertrófica: Como Realizar uma Análise Diagnóstica e Prognóstica em 2022. Dividir para Tratar Melhor?

Alexandra Toste[1,2], *Nuno Cardim*[1,2]

[1]*Luz Hospital – Center for Hereditary Heart Diseases and Hypertrophic Cardiomyopathy, São Paulo, SP, Brazil.* [2]*Nova Medical School, Lisboa, Portugal.*

Hypertrophic cardiomyopathy (HCM), the most common genetic heart disease, has an estimated prevalence in the general population of 1:500–1:200.[1] The diagnosis is based on the presence of left ventricular hypertrophy (LVH) that is not fully explained by loading conditions, and HCM occurs in the absence of other cardiac, systemic, or metabolic disease or in the context of a multiorgan syndrome associated with LVH.[2]

Despite being considered a genetic disease, the initial diagnosis of HCM does not require genetic testing. The diagnostic power of current genetic panels is modest, just 46%;[3] therefore, failure to detect a mutation does not exclude the diagnosis. Current guidelines recommend genetic testing, especially when the possibility of cascading familial genetic screening is anticipated or in cases in which the clinical presentation suggests a specific non-sarcomeric etiology potentially treatable with specific therapy, such as Anderson-Fabry disease, Danon disease, or familial amyloidosis.[4]

The diagnosis of HCM is determined using transthoracic echocardiography in most cases, the first-choice imaging modality. Although the current diagnostic criteria are based exclusively on increased wall thickness, HCM also involves structural cardiomyocyte derangement, interstitial fibrosis, microvascular remodeling, and microcirculatory dysfunction, changes that may precede increased left ventricular (LV) wall thickness.[5] Thus, cardiac magnetic resonance (CMR) imaging can play a much more precise and sensitive role in tissue characterization along with late gadolinium enhancement, T1 mapping, fractal analysis, diffusion tensor imaging, transit time, and segmental perfusion defect assessment. Some of these techniques have been implemented in clinical practice, while others are still being investigated.

HCM is a disease with great phenotypic and clinical heterogeneity ranging from long-term asymptomatic disease to being a cause of sudden death in young adults and athletes.[6] HCM can progress according to several profiles: heart failure (HF) with preserved ejection fraction due to diastolic dysfunction and/or obstruction; HF with reduced ejection fraction; atrial fibrillation (AF) and stroke; ventricular arrhythmias; and sudden cardiac death (SCD). The predictors of each of these profiles remain unclear exception made for the profile of ventricular arrhythmias and SCD. This area has been the subject of research in recent years for which quite robust sudden death risk stratification strategies have been developed.

Indeed, the European model,[6] incorporated into the 2014 European recommendations, estimates the five-year risk of sudden death of a specific patient using mathematical models and considering seven clinical and imaging variables (age, maximum LV thickness, left atrial diameter, maximum LV outflow gradient, family history of SCD, unexplained syncope, and non-sustained ventricular tachycardia [NVT]). On the other hand, the American strategy,[7] which was recently optimized, includes new risk factors in the SCD risk stratification, such as the presence of apical aneurysms with fibrosis, extensive late enhancement on CMR (usually ≥15% of LV mass), and LV systolic dysfunction (defined as an ejection fraction < 50%). The presence of a new or classic risk factor (family history of SCD in a first-degree relative, massive hypertrophy ≥ 30 mm, unexplained syncope events, NVT) may be an indication for an implantable cardioverter-defibrillator, with different strengh levels of evidence.

However, the prognostic assessment of patients with HCM goes beyond SCD risk stratification. Progression to other profiles represent a large part of the current morbidity and mortality of this disease. The international Sarcomeric Human Cardiomyopathy Registry (SHaRe),[3] which involved 4,591 HCM patients with a median follow-up of 5.4 years and >24,000 patient-years, identified two major predictors of adverse events: sarcomeric mutation status and age at diagnosis.

Survival analysis showed that groups with pathogenic mutation, probably pathogenic or variant of uncertain significance, had events at younger ages and a higher incidence of compound events — HF and AF — than the group with no identified mutation (SARC-). On the other hand, the group with a pathogenic or likely pathogenic mutation (SARC+) had a higher risk of malignant ventricular arrhythmias compared to the SARC- group.

At the same time, patients with nonfamilial HCM (SARC- and no family history of HCM) had a lower risk of mortality

Keywords

Hypertrophic Cardiomyopathy; Genetics; Sarcomere-Positive, Nonfamilial; Diagnosis; Prognosis.

Mailing Address: Alexandra Toste •

E-mail: alexandra.toste6@gmail.com

Manuscript received 8/8/2022; revised 8/15/2022; accepted 9/20/2022

Editor responsible for the review: Daniela do Carmo Rassi Frota

DOI: 10.47593/2675-312X/20223504eed_23i

and compound events than the other groups, and the age-adjusted mortality rate of this group was similar to that of the general population.

Regarding age, the age-adjusted mortality rate was four times higher in young patients (20–29 years old) and three times higher in patients 50–69 years than in the general population, with HF and non-cardiac mortality being the main causes of death. Surprisingly, SCD represented only 16% of these deaths. Regardless of age, most HCM-related complications occurred late (at 50–70 years) and involved HF and AF.

Evidence suggests the existence of two major HCM subtypes based on the identification of sarcomeric mutations.[8,9] SARC+ patients are younger at the time of diagnosis, have a higher degree of hypertrophy that is typically asymmetric, and have a more frequent family history of HCM and SCD with a worse prognosis. On the contrary, SARC- patients more often present with a sigmoid interventricular septum, less fibrosis, and more comorbidities such as hypertension and obesity; and seem to follow a more benign clinical course (Figure 1).

These findings suggest that genetic testing may play an important role in the diagnosis and prognosis of these patients, distinguishing two very different HCM subgroups that probably require different prevention, treatment, and screening strategies. Considering this new approach to HCM, genetic studies will play an even more important role in disease management, increasing our understanding of HCM from a molecular point of view and enabling the more accurate treatment of these patients. In short, we should divide cases to better treat them.

Authors' contributions

Manuscript writing: Toste A; critical review of the manuscript for important intellectual content: Cardim N.

Conflict of interest

The authors have declared that they have no conflict of interest.

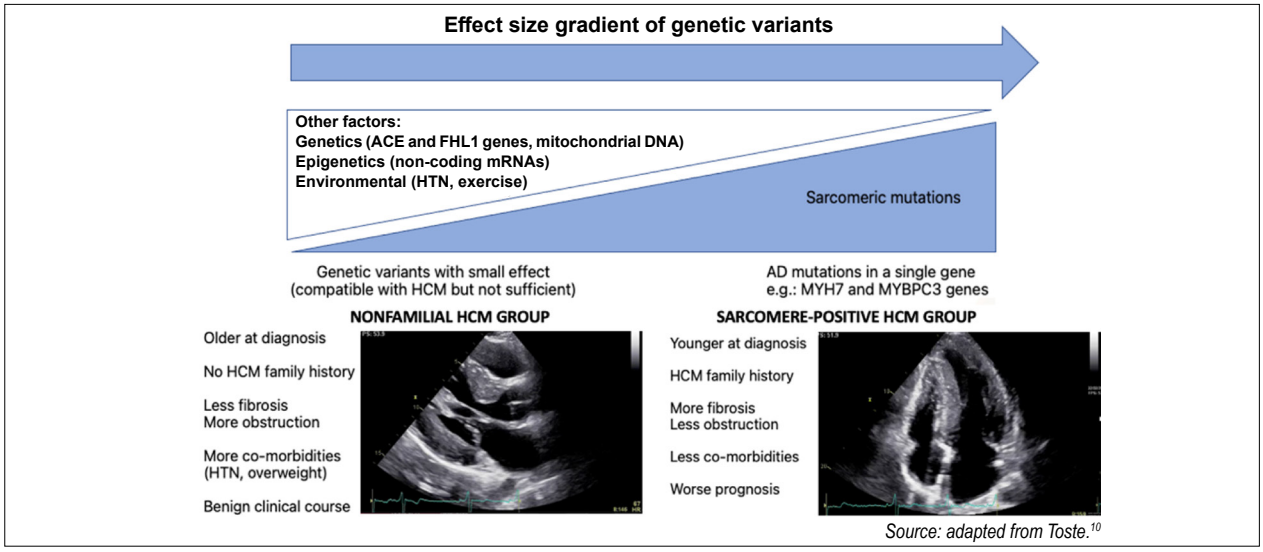

Figure 1 – *Main characteristics by HCM subgroup.*

References

1. Semsarian C, Ingles J, Maron MS, Maron BJ. New perspectives on the prevalence of hypertrophic cardiomyopathy. J Am Coll Cardiol. 2015;65(12):1249-54. doi: https://doi.org/10.1016/j.jacc.2015.01.019

2. Cardim N, Galderisi M, Edvardsen T, Plein S, Popescu BA, D'Andrea A, et al. Role of multimodality cardiac imaging in the management of patients with hypertrophic cardiomyopathy: an expert consensus of the European Association of Cardiovascular Imaging Endorsed by the Saudi Heart Association. Eur Heart J Cardiovasc Imaging. 2015;16(3):280. doi: https://doi.org/10.1093/ehjci/jeu291

3. Ho CY, Day SM, Ashley EA, Michels M, Pereira AC, Jacoby D, et al. Genotype and Lifetime Burden of Disease in Hypertrophic Cardiomyopathy: Insights from the Sarcomeric Human Cardiomyopathy Registry (SHaRe). Circulation. 2018;138(14):1387-98. doi: https://doi.org/10.1161/CIRCULATIONAHA.117.033200

4. Sousa A, Moldovan O, Lebreiro A, Bourbon M, António N, Rato Q, et al. Recomendações para a realização de testes genéticos em cardiologia – revisão das principais diretrizes internacionais. Rev Port Cardiol. 2020;39(10):597-610.

5. Ho CY, Abbasi SA, Neilan TG, Shah RV, Chen Y, Heydari B, et al. T1 measurements identify extracellular volume expansion in hypertrophic cardiomyopathy sarcomere mutation carriers with and without left ventricular hypertrophy. Circ Cardiovasc Imaging. 2013;6(3):415-22. doi: https://doi.org/10.1161/CIRCIMAGING.112.000333

6. O'Mahony C, Jichi F, Pavlou M, Monserrat L, Anastasakis A, Rapezzi C, et al.; Hypertrophic Cardiomyopathy Outcomes Investigators. A novel clinical risk prediction model for sudden cardiac death in hypertrophic cardiomyopathy (HCM risk-SCD). Eur Heart J. 2014;35(30):2010-20. doi: 10.1093/eurheartj/eht439

7. Ommen SR, Mital S, Burke MA, Day SM, Deswal A, Elliott P, et al. 2020 AHA/ACC Guideline for the Diagnosis and Treatment of Patients With Hypertrophic Cardiomyopathy: A Report of the American College of Cardiology/American Heart Association Joint Committee on Clinical Practice Guidelines. Circulation. 2020;142(25):e558-e631. doi: https://doi.org/10.1161/CIR.0000000000000937. Erratum in: Circulation. 2020;142(25):e633.

8. Lopes LR, Syrris P, Guttmann OP, O'Mahony C, Tang HC, Dalageorgou C, et al. Novel genotype-phenotype associations demonstrated by high-throughput sequencing in patients with hypertrophic cardiomyopathy. Heart. 2015;101(4):294-301. doi: https://doi.org/10.1136/heartjnl-2014-306387

9. Ingles J, Burns C, Bagnall RD, Lam L, Yeates L, Sarina T, et al. Nonfamilial Hypertrophic Cardiomyopathy: Prevalence, Natural History, and Clinical Implications. Circ Cardiovasc Genet. 2017;10(2):e001620. doi: https://doi.org/10.1161/CIRCGENETICS.116.001620

10. Toste A. Advances in hypertrophic cardiomyopathy: What the cardiologist needs to know. Rev Port Cardiol. 2022;41(6):499-509. doi: https://doi.org/10.1016/j.repc.2021.05.015

DIC-SBC Women's Group

Grupo de Mulheres do DIC-SBC

Samira Saady Morhy[1], *Marly Uellendahl*[2,3]

[1]*Hospital Israelita Albert Einstein, São Paulo, SP, Brazil;* [2]*Diagnóstico da América S/A (DASA), São Paulo, SP, Brazil;* [3]*Federal University of São Paulo, São Paulo, Brazil (UNIFESP), São Paulo, SP, Brazil.*

The first meeting of the DIC-SBC Women's Group was held at the 11th Conference of the Department of Cardiovascular Imaging (DIC) of the Brazilian Society of Cardiology (Sociedade Brasileira de Cardiologia [SBC], in São Paulo, August 28–31, 2022.

This meeting aimed to organize a work group to encourage and develop greater participation of female DIC members, speakers in scientific activities, guideline authors, and members of the Board of Directors.

In the last century, the number of female physicians has significantly increased in Brazil: they comprised 22.3% in 1910, only 13% in 1960, and 46.6% in 2020 (Table 1).[1]

Table 1 – Number of physicians in Brazil by sex.

Year	Women	Men
1910	2,956 (22.3)	10,314 (77.7)
1960	4,519 (13.0)	30,273 (87.0)
2020	222,942 (46.6)	255,040 (53.4)

Source: Scheffer et al.[1]

Analysis of the number of new physician registrations in the Medical Councils by sex revealed 50.4% in 2009 and 57.5% in 2020 (Figure 1).[1]

However, a funnel is noted in the analysis of the participation of women in medical societies, as despite the increased number of new registrations throughout Brazil, the SBC includes a majority of men and only 31% women (Figure 2).

The difference in male and female members of the DIC was smaller than that of the SBC, but women still comprised a minority at 43% (Figure 3).

The participation of women on the DIC Board of Directors is even lower at 14.8% (Figure 4). Since the inception of the DIC in 1988, of the 17 presidents, only two were women: Dr. Marcia Barbosa, from Minas Gerais, in the 2008–2009 biennium; and Dr. Samira Saady Morhy, from São Paulo, in the 2016–2017 biennium.

In this inaugural meeting of the DIC Women's Group, approximately 26 DIC members participated, and issues impacting the participation of women in Societies were discussed,

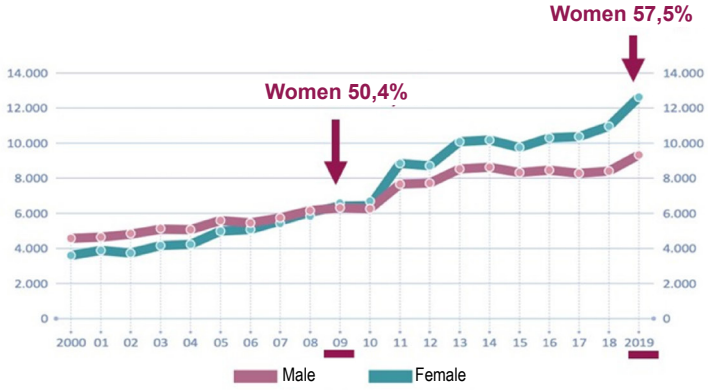

Source: Scheffer M et al, Demografia Médica no Brasil 2020.[1]

Figure 1 – *Evolution of new physicians in Brazil by sex.*

Keywords

Gender Inequality; Women in the Labor Market; Role of Women.

Mailing Address: Samira Saady Morhy •
R. Pintassilgo, 458. Ap 53, Moema, São Paulo, SP, Brazil,
Postal Code: 04514-032.
E-mail: samirasaady@gmail.com
Manuscript received 9/13/2022; revised 9/30/2022; accepted 10/30/2022

Editor responsible for the review: Daniela do Carmo Rassi Frota

DOI: 10.47593/2675-312X/20223504eed_33i

Editorial

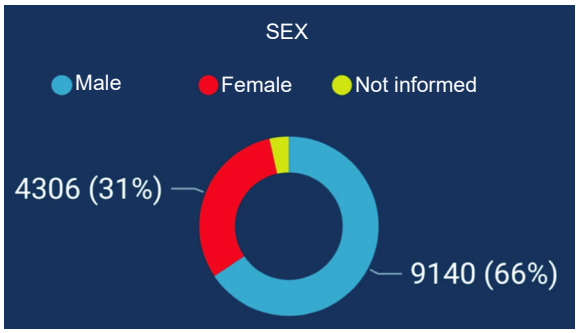

Source: Website of the Brazilian Society of Cardiology www.cardiol.br.

Figure 2 – *Proportion of Brazilian Society of Cardiology members by sex.*

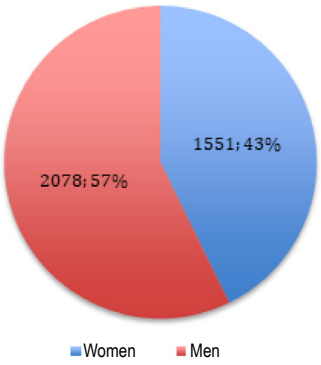

Source: DIC Secretariat www.dicsbc.com.br.

Figure 3 – *Proportion of Cardiovascular Imaging Department (DIC) of the Brazilian Society of Cardiology (SBC) members by sex.*

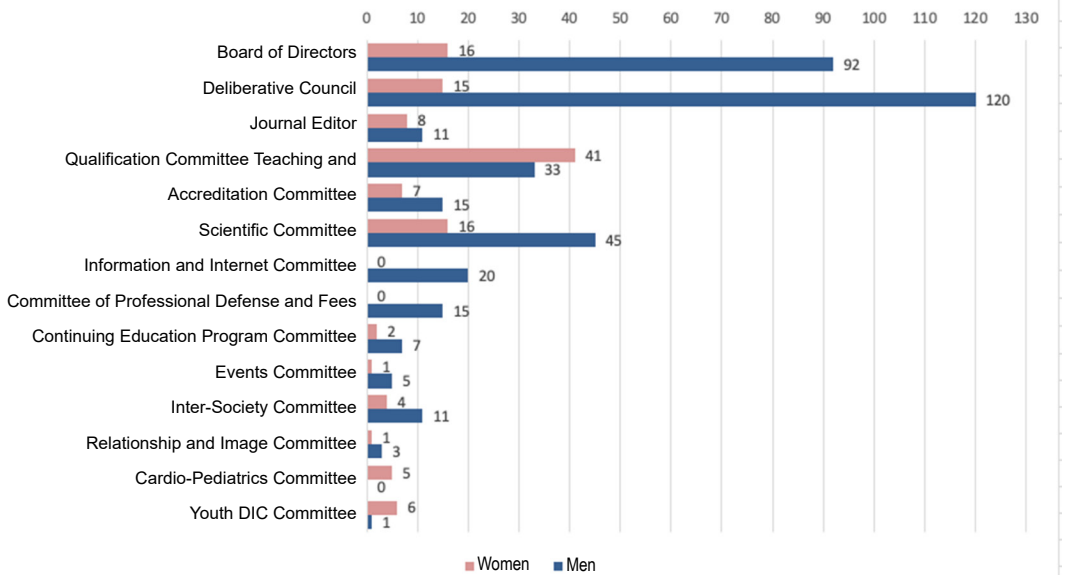

Source: DIC Secretariat www.dicsbc.com.br.

Figure 4 – *Women's participation in the Board of the Department of Cardiovascular Imaging (DIC) of the Brazilian Society of Cardiology (SBC) since its inception.*

such as difficulty dividing their time between family and profession, different types of harassment, impostor syndrome, and others. (Figure 5)

Sex-based equity for the next boards, scientific events, and guidelines was proposed to the current Board of Directors.

We count on all DIC women to help us with this work group!

Authors' contributions

Manuscript design and writing: Morhy SS and Uellendahl M.

Conflict of interest

The authors have declared that they have no conflict of interest.

Figure 5 – *Participants at the opening meeting of the DIC-SBC Group of Women held on July 30, 2022 at the 11th Conference of the Cardiovascular Imaging Department of the Brazilian Society of Cardiology.*

Reference

1. Scheffer M, Cassenote A, Guerra A, Guilloux AG, Brandão AP, Miotto BA. Demografia médica no Brasil 2020. São Paulo: Departamento de Medicina Preventiva da Faculdade de Medicina da USP; Conselho Federal de Medicina, 2020 [citado 2022 Set 26]. Disponível em: https://www.fm.usp.br/fmusp/conteudo/DemografiaMedica2020_9DEZ.pdf

Difficulty Introducing Contrast Echocardiography in Daily Clinical Practice in South America: A Matter of Economy?

Por Que é Tão Difícil Introduzir a Ecocardiografia com Contraste na Prática Clínica Diária na América do Sul: Uma Questão de Economia?

Ricardo Ronderos[1,2,3]

[1]*ICBA - Instituto Cardiovascular Buenos Aires Argentina, Buenos Aires, Argentina.* [2]*Instituto de Cardiología La Plata, La Plata, Argentina.* [3]*Universidad Nacional de La Plata, La Plata, Argentina.*

Contrast echocardiography has shown invaluable utility in the clinical setting during the last 20 years. Most studies have demonstrated its successful application in different clinical scenarios. Ultrasound contrast agents (UCA) have evolved incredibly since their first-generation iterations at the end of the last century. From weak and short-term duration agents like Levovist™ to the development of fluorocarbons with simple storage requirements like Definity™ and Sonovue™, significant improvements have been achieved and the logistics in echocardiography labs became easier. Nevertheless, their clinical application did not increase as expected, especially in South America.

To analyze this fact, we must consider the probability of a new diagnostic technique becoming a regular and widespread diagnostic tool. A new diagnostic technique should be superior to its predecessors and available in different clinical scenarios; feature simple instrumentation, simple interpretation, well-defined normal patterns; be attractive and comprehensive in terms of image quality; and be cost-effective to ensure acceptance by health system financiers.[1,2] (Figure 1)

A disruptive technology is the one that proves necessary over time, garners increased interest, and fulfills market expectations. Therefore, it must not only be needed; it must achieve success and acceptance. Hence, let us analyze UCA development and applications from this point of view.

First, the available contrast agents improved from requiring difficult storage with freezing to a simple powder vial that can be storage in the echocardiography lab. Nevertheless, an intravenous catheter should be placed during the echo exam to inject the contrast; this simple change created difficulty, especially in South America, where physicians work alone taking images without technicians in daily practice.

Doctors must perform this simple but time-consuming procedure during echocardiography exam. Second, to prepare the UCA for injection, more time is needed, and for many contrasts, extra devices are needed; for others, an infusion pump should be added. All these facts significantly increase the time required for echocardiography. All these issues increase the cost, which is not reflected in reimbursement.[3,4]

Second, to apply contrast during echocardiography, the proper machine settings must be selected according to the involved study and/or contrast application. Imaging interpretation, despite the simplification of image acquisition and rendering, requires a learning curve that is longer if contrast studies are infrequently performed in the echocardiography lab.[4] The dearth of studies due to high time requirement, logistical problems, UCA cost and reimbursement problems make an explosive combination that works against the learning curve in busy echocardiography labs.

To obtain a good and diagnostic contrast echocardiogram, excellent quality pictures must be achieved; therefore, if training is incomplete, success is impossible. I remember a personal experience in which one of the most powerful companies distributed a marketing survey in Argentina. Almost 65% of responding physicians reported that they were not interested in using UCA in daily clinical practice. Why? Because of all these topics listed above!

Third, let us consider the market point of view. The South American market, except for Brazil, is not large enough to provide UCA to the region. If the market is limited and the physicians who must use the product are not excited, the product cannot be successful. The Brazilian market is large and probably requires significant effort to cover the entire region, but the same difficulties occurred in Brazil as in Argentina, Colombia, and Chile.

At the beginning of the 21st century, I had the opportunity to lead an amazing group of specialists to develop guidelines for contrast use in clinical practice. Almost all Latin American countries participated in this initiative sponsored by the National University of La Plata and Bristol Myers Squibb. The results were published almost simultaneously by Argentinian, Brazilian, Mexican, and other Latin American Societies of Cardiology Journals.[5,6] Despite these publications, most markets in Latin America still lack UCA products.

Therefore, market and physician acceptance matter.

A disruptive technology is one expected by the market that solves problems or simplify solutions compared to former products. (Figure 1)

Keywords

Echocardiography; Contrast Echocardiography; Cost-Benefit Analysis.

Mailing Address: Ricardo E Ronderos •
Calle 6 No 212 La Plata 1900 Argentina.
E-mail: trotare@hotmail.com
Manuscript received 08/15/2022; revised 8/17/2022; accepted 8/18/2022

Editor responsible for the review: Daniela do Carmo Rassi Frota

DOI: 10.47593/2675-312X/20223504eed_16i

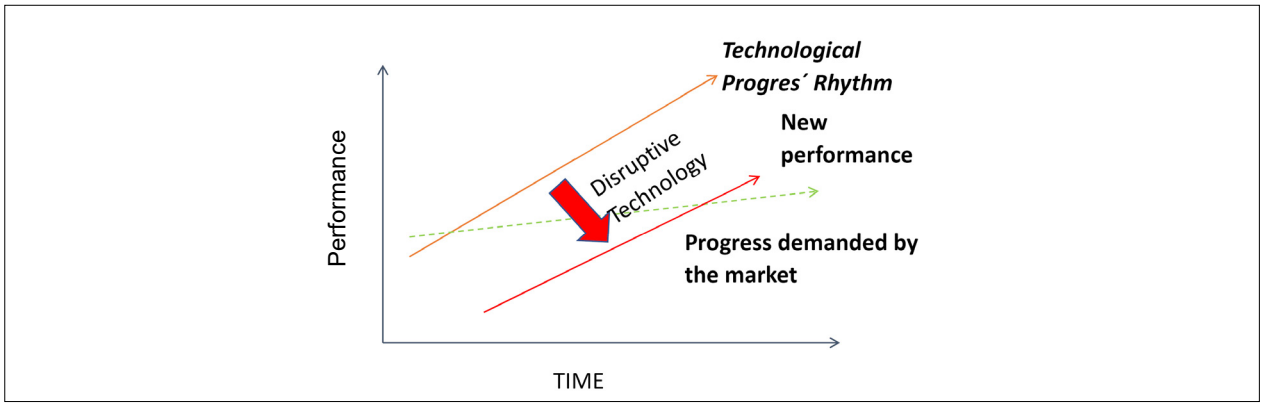

Figure 1 – *Impact of disruptive technology in medicine.*

Most papers showed no inferiority of contrast echocardiography myocardial studies versus nuclear medicine examinations. Single-photon emission computed tomography studies are used in routine medical practice despite randomized studies being seldom performed and well accepted and used widely.[7-10]

Radioisotopes are marketed by companies that also produce UCA, most of which (such as BMS and Lanteus) sold the UCA areas to money funds. Thus, it seems more sensible to continue studies of myocardial perfusion diagnosis than to pursue a non-widely accepted field such as contrast echocardiography. Moreover, the advent of multislice computed tomography to provide atherosclerotic plaque images in the context of a well-established diagnostic machine business seem to complete a not friendly context.[11]

The last few decades involved automatic quantification and automatic image acquisition algorithms using machine learning and deep learning. Although UCA supply genuinely useful data about coronary capillary flow and coronary reserve using vasodilators, these contrast echocardiography studies are not included in such technical improvements. Another reason to keep contrast echocardiography as an artisan practice instead of a simple current study, the workflow advances to technician acquisition, automatic quantification, and offline delayed physician's interpretation.

The application of contrast echocardiography was reduced to endocardial border recognition, left cardiac chambers opacification, and cardiac masses identification. Thus, the circle of disruptive technology closed.

In conclusion, in my humble opinion, echocardiographers have great responsibility in the unexpected small developments of contrast echocardiography. Financial issues are another reason to explain the difficulties in its development. Time revealed that an expected disruptive technique was not used despite its demonstrated usefulness in echocardiography labs in Europe and Japan. Here in Latin America, if UCA were widely available, most labs would be using it now and in the future despite economic problems. Reimbursement should be ensured as with other disruptive technologies.

Author contributions

Ronderos R; manuscript writing: Ronderos R; critical review of the manuscript for important intellectual content.

Conflict of interest

The authors have declared that they have no conflict of interest.

Referências

Christensen Clayton**.** The Innovator's Dilemma: When New Technologies Cause Great Firms to Fail. Harvard Business Review Press; 1st edition May 1, 1997.

The World Health Organization Choosing Interventions That Are Cost-Effective (WHO-CHOICE) Update. [Cited 2021 Nov 10]. Available from: http://https://www.who.int/news-room/feature-stories/detail/new-cost-effectiveness-updates-from-who-choice.

Cosyns B, Helfen A, Leong-Poi H, Senior R. How to perform an ultrasound contrast myocardial perfusion examination? Eur Heart J Cardiovasc Imaging. 2022;23(6):727-729. doi: 10.1093/ehjci/jeac028.

Ronderos R. Contraste en Ecografía. Ecocardiografía e imágen cardiovascular en la práctica clínica. Ed Distribuna Colombia 2015. p. 117-153.

Ronderos R, Boskis M, Corneli D, Cuenca G, et al. Foro Latinoamericano de expertos en ecocardiografía de contraste. Guias y recomendaciones para el uso de ecocardiografía de contraste. Rev de la Fed Arg de cardiología. 2007; (36) Supl (1).

Ronderos R, Morcef F, Boskis M, Corneli D, Gutierrez Fajardo P, et al. Forum Latinoamericano de ecocardiografía com contraste. Guidelines and recommendations for the use of contrast Echocardiography. Arch Bras Cardiol 2007 (88) Suppl (2) 1-12. doi: https://doi.org/10.1590/S0066-782X2007000800001.

Ibanez B, James S, Agewall S, Antunes MJ, Bucciarelli-Ducci C, Bueno H, et al; ESC Scientific Document Group. 2017 ESC Guidelines for the management of acute myocardial infarction in patients presenting with ST-segment elevation: The Task Force for the management of acute myocardial infarction in patients presenting with ST-segment elevation of the European Society of Cardiology (ESC). Eur Heart J. 2018;39(2):119-177. doi: 10.1093/eurheartj/ehx393.

Ronderos RE, Boskis M, Chung N, Corneli DB, Escudero EM, Ha JW, et al.

Correlation between myocardial perfusion abnormalities detected with intermittent imaging using intravenous perfluorocarbon microbubbles and radioisotope imaging during high-dose dipyridamole stress echo. Clin Cardiol. 2002;25(3):103-11. doi: 10.1002/clc.4960250305.

Lindner JR, Belcik T, Main ML, Montanaro A, Mulvagh SL, Olson J, et al. Expert Consensus Statement from the American Society of Echocardiography on Hypersensitivity Reactions to Ultrasound Enhancing Agents in Patients with Allergy to Polyethylene Glycol. J Am Soc Echocardiogr. 2021;34(7):707-708. doi: 10.1016/j.echo.2021.05.002.

Dawson D, Kaul S, Peters D, Rinkevich D, Schnell G, Belcik JT, et al. Prognostic value of dipyridamole stress myocardial contrast echocardiography: comparison with single photon emission computed tomography. J Am Soc Echocardiogr. 2009;22(8):954-60. doi: 10.1016/j.echo.2009.04.034.

Song FX, Zhou J, Zhou JJ, Shi YX, Zeng MS, Zhang ZY, et al. The diagnosis of coronary plaque stability by multi-slice computed tomography coronary angiography. J Thorac Dis. 2018;10(4):2365-2376. doi: 10.21037/jtd.2018.04.43.

Original Article

Increased Wasted Myocardial Work as an Indicator of Significant Coronary Lesion

Aumento do Trabalho Miocárdico Desperdiçado como Indicador de Lesão Coronariana Significativa

Márcio Mendes Pereira[1], Amanda Castro Barroso[1], Marco Túlio Hercos Juliano[1], Márcio Mesquita Barbosa[1], Gustavo Travassos Gama[1], Rodrigo de Jesus Louzeiro Melo[1], José Bonifácio Barbosa[1], Carlos Alberto Vieira Gama[1], José Xavier de Melo Filho[1], Auridesio Cutrim de Araujo[1]

[1]UDI Hospital Rede D'Or São Luiz, São Luís, MA, Brazil.

Abstract

Introduction: The assessment of global myocardial work indices under baseline conditions may be useful for the clinical stratification of patients with suspected coronary obstruction.

Objective: To correlate the value of global myocardial work indices and the presence of significant obstructive coronary lesions.

Method: Cross-sectional study, with patients referred for elective coronary angiography. An echocardiogram was performed to obtain measurements to calculate the value of myocardial work and evaluated the presence or presence of significant obstructive coronary lesions at coronary angiography.

Results: The sample consisted of 30 patients, with a mean age of 64.2±12.8 years, the majority being male (63.3%), of which 68.4% had significant obstructive coronary lesions. The global myocardial work indices was 1,876mmHg%±253.8 in the group with significant obstructive coronary lesions and 2,054.2mmHg%±417.3 in those without significant lesions (p=0.089). Global constructive myocardial work in patients without significant obstructive coronary lesions was higher (2,329.3mmHg%±462.9) than in those with significant obstructive coronary lesions (2,109.5mmHg%±332.3; p=0.064). Global wasted myocardial work was higher in patients with significant obstructive coronary lesions (103.7mmHg%±47.1 versus 68.3mmHg%±33.8; p=0.038). The cutoff point of 115 mmHg% was the one with the best area under the curve (0.625), with a sensitivity of 83.3%.

Conclusion: The increase in global wasted myocardial work correlated with the presence of significant obstructive coronary lesions in our sample.

Keywords: Cardiac function; Echocardiography; Heart defects, congenital; Coronary stenosis.

Resumo

Introdução: *A avaliação dos índices de trabalho miocárdico global em condições basais pode ser útil para a estratificação clínica de pacientes com suspeita de obstrução coronariana.*

Objetivo: *Correlacionar o valor do índice de trabalho miocárdico global e a presença de lesões obstrutivas coronarianas significativas.*

Método: *Estudo transversal, com pacientes encaminhados para cinecoronarioangiografia eletiva. Foi realizado ecocardiograma com obtenção das medidas para cálculo do valor do trabalho miocárdico, sendo avaliada a presença de lesões obstrutivas coronarianas significativas à cinecoronarioangiografia.*

Resultados: *A amostra foi composta de 30 pacientes, com a idade média de 64,2±12,8 anos, sendo a maioria do sexo masculino (63,3%), dos quais 68,4% apresentaram lesões obstrutivas coronarianas significativas. O índice de trabalho miocárdico global foi de 1.876mmHg%±253,8 no grupo com lesões obstrutivas coronarianas significativas e de 2.054,2mmHg%±417,3 naqueles sem lesões significativas (p=0,089). O trabalho miocárdio construtivo global nos pacientes sem lesões obstrutivas coronarianas significativas foi maior (2.329,3mmHg%±462,9) do que naqueles com lesões obstrutivas coronarianas significativas (2.109,5mmHg%±332,3; p=0,064). O trabalho miocárdio desperdiçado global foi maior nos pacientes com lesões obstrutivas coronarianas significativas (103,7mmHg%±47,1 versus 68,3mmHg%±33,8; p=0,038). O ponto*

Mailing Address: Márcio Mendes Pereira •
Av. Prof. Carlos Cunha, 2000, Jaracaty, São Luís, MA, Brazil.
E-mail: marciomp50@hotmail.com
Manuscript received 9/20/2022; revised 10/28/2022; accepted 11/3/2022

Editor responsible for the review: Daniela do Carmo Rassi Frota

DOI: 10.47593/2675-312X/20223504eabc346i

de corte de 115mmHg% foi aquele com a melhor área sob a curva (0,625), com sensibilidade de 83,3%.

Conclusão: *O aumento do trabalho miocárdio desperdiçado global se correlacionou com a presença de lesões obstrutivas coronarianas significativas em nossa amostra.*

Palavras-chave: *Função cardíaca; Ecocardiografia; Cardiopatias congênitas; Estenose coronária.*

Introduction

The early detection of coronary artery disease (CAD) is crucial for its proper treatment. However, it remains challenging in echocardiography since the left ventricular ejection fraction (LVEF) is usually normal in the early disease stages. Stress echocardiography is a widely accepted method for such investigations, but it features the disadvantages of subjectivity and the need to achieve the target heart rate.[1]

Ventricular systolic function evaluation is an essential part of the echocardiogram, with LVEF being the most often used parameter.[2] LV global longitudinal strain (GLS) has gained attention, as it can detect subclinical abnormalities in patients with a normal LVEF.[3] However, it is afterload-dependent, which can reduce the GLS, causing regional and global contractile function interpretation errors.[4]

Myocardial work is a proposed new tool used to study LV performance,[5] surpassing LVEF and GLS when used alone.[6] Myocardial work incorporates LV pressure and adds information to LVEF and strain,[7] integrating the afterload to the LV function parameter.

Myocardial work is obtained by multiplying the GLS by the wall stress since work is the multiplication of force by distance.[6] Noninvasive myocardial work measurements showed a strong correlation with invasive measurements both experimentally and clinically.[8] Russell *et al.* reported that the LV strain curve pressure area was significantly reduced in areas supplied by an occluded coronary artery compared to those with normal perfusion assessed by angiography.[8]

This study aimed to assess the correlation between the noninvasive myocardial work value assessed by echocardiography and the presence of severe CAD assessed by cineangiography (CAG).

Methods

Echocardiographic assessment

This single-center cross-sectional study included prospectively recruited patients electively referred for CAG for CAD assessment. The exclusion criteria were chest pain at the time of the echocardiogram, previous history of acute myocardial infarction, LVEF < 50%, LV segmental contraction changes, moderate or more severe valvular heart disease, aortic stenosis, hypertrophic cardiomyopathy, biological or metallic aortic prosthesis, a pacemaker rhythm, or an irregular rhythm (frequent extrasystole or atrial fibrillation or flutter). As it is a pilot study, we arbitrated the sample in 30 patients.

The patients signed an Informed Consent Form upon arriving at the hemodynamics laboratory for elective CAG and subsequently underwent transthoracic echocardiography with electrocardiographic monitoring. The tests were performed using a Vivid E95 cardiovascular ultrasound device (GE Medical Systems, Horten, Norway) equipped with 3.5-MHz MS5 phased-array sector probes.

Echocardiographic measurements and assessments were obtained according to American Society of Echocardiography recommendations.[9] Two-dimensional standard images were obtained with three cycles trigged by the QRS complex and digitally recorded for offline analysis using EchoPAC software version 202 (GE Vingmed Ultrasound). LVEF was calculated using the three-dimensional method.

The myocardial global work index (GWI) was quantified by calculating the rate of regional shortening by the differentiation of the global longitudinal tracing and multiplying by the instantaneous LV pressure. This instantaneous measurement was integrated over time to measure myocardial work as a function of time during systole (time interval from mitral valve closure to mitral valve opening). The segments were analyzed during LV ejection for myocardial global wasted work (GWW) and/or myocardial global constructive work (GCW), with global values determined as the means of all segmental values and displayed on the pressure-LV deformation circuit diagram. The following parameters were generated by the software: GWI (mmHg%), area within the LV global pressure curve; GCW (mmHg%), estimated work performed by the LV segments consisting of shortening during systole plus stretching in isovolumetric relaxation; GWW (mmHg%), estimated negative work done by the LV segments consisting of myocardial stretching during systole plus any shortening during isovolumetric relaxation; myocardial global work efficiency (GWE; %), GCW divided by the sum of GCW and GWW expressed as a percentage (not affected by peak LV pressure).[1,10,11]

Functional ischemia area (FIA) was defined as established by Boe *et al.*,[7] who considered adjacent segments as ischemic when the absolute GLS value was < 14% and the GWI was < 1,700 mmHg%. According to these values, we defined and correlated the FIA with the significantly obstructed coronary artery.

Cineangiography assessment

CAG was performed using a Philips FD10 catheterization device according to Brazilian Society of Hemodynamics and Interventional Cardiology techniques.[12] Significant CAD was defined as luminal narrowing ≥ 50% in the left main coronary artery (LMCA) and/or ≥70% in the anterior descending (AD), diagonal (DG), circumflex (CX), marginal (MG), or right coronary (RC) arteries through visual assessment by the hemodynamic cardiologist.

Statistical analysis

The data were tabulated and analyzed using Stata® Intercooled software version 12.0.

Categorical variables are presented as absolute (n) and relative (%) frequency. Continuous variables are presented as mean and SD or as median and interquartile range according to the skewness and kurtosis normality tests.

The significance of any intergroup differences was assessed using Student's t-test for normally distributed data. The Mann-Whitney U or Kruskal-Wallis test was used to examine non-normally distributed variables.

The chi-square or the Fisher's exact test was used to examine categorical variables when appropriate.

Receiver operating characteristic analysis was used to identify the optimal cutoff point for each parameter.

A logistic regression model was performed to determine independent variables capable of identifying patients with significant coronary disease. The FIA determined by strain and myocardial work was analyzed in separate models.

P values < 0.05 indicated statistical significance.

Results

Clinical characteristics

A total of 30 patients with a mean age of 64.2 ± 12.8 years were included in the study; most were men (63.3%), of whom 68.4% had significant obstructive coronary lesions (SOCL) (Table 1).

Most patients were hypertensive and dyslipidemic (19 [63.3%] in each group), 36.6% were diabetic, 30% were obese, and none had a previous history of stroke. Significant lesions were present on CAG in 63.2% of hypertensive, 73.7% of dyslipidemic, 63.6% of diabetic, and 77.8% of obese patients.

Characteristics of cineangiography

Of the total number of patients in the sample, six (20%) had no lesions on CAG and 24 (80%) had coronary obstructions greater than 50%. Of the patients with coronary lesions, 19 (63.3%) had SOCL. In this group, 68.4% were men, with a mean age of 65.4 ± 10.6 years.

Regarding coronary lesion location, 18 patients (60%) had lesions in the AD, one (3.3%) in the LMCA, seven (23.3%) in the DG, five (16.7%) in the CX, four (13.3%) in the MG, and six (20%) in the RC artery.

Echocardiographic characteristics

The echocardiographic characteristics of the sample are described in Table 2. Grade 1 diastolic dysfunction was present in 50% of the sample. No patients had grade 3 diastolic dysfunction, while all had preserved systolic function. The mean LVEF calculated using the three-dimensional method was 65.2 ± 3.3% in patients with SOCL versus 63.6 ± 4.6% in those without SOCL.

According to Table 2, the mean GLS was 18.3 ± 2% in the sample with SOCL and 19.1 ± 2.9% without SOCL on CAG (p = 0.313).

Mean MGWI was 1,876 ± 253.8 mmHg% in patients with SOCL versus 2,054.2 ± 417.3 mmHg% in those without SOCL (p = 0.089).

The GCW was higher in patients without versus with SOCL on CAG, being 2,329.3 ± 462.9 mmHg% and 2,109.5 ± 332.3 mmHg%, respectively (p = 0.064).

The mean GWW values were higher in patients with versus without SOCL (103.7 ± 47.1 mmHg% vs. 68.3 ± 33.8 mmHg%, p = 0.038).

Figure 1 shows an image from a sample patient with an AD lesion in which the wasted myocardial work of the basal segment of the anterior septum is greater than the GWW. There was no difference in GWE between patients with or without significant lesions (95.6 ± 2.0 vs. 94.7 ± 2.2, p = 0.296).

GLS presented no statistically significant difference between patients with or without SOCL, the same occurring when analyzed by arterial territory (Table 3).

Table 1 – Clinical characteristics.

Variables	Total (n=30)
Age (years)	64.2 ± 12.8*
Weight (kg)	69.2 ± 16.9*
SBP (mmHg)	127.4 ± 16.6*
DBP (mmHg)	73 ± 9.1*
HR (bpm)	69.4 ± 11.8*
Comorbidities	
Hypertension	19 (63.3%)
DM 2	11 (36.7%)
Previous CAD	15 (50%)
Stroke	0 (0%)
Dyslipidemia	19 (63.3%)
Obesity	9 (30%)
Smoking	2 (6.7%)

*CAD: coronary artery disease; DBP: diastolic; blood pressure; DM 2: type 2 diabetes mellitus; HR: heart rate; SBP: systolic blood pressure; *mean ± standard deviation;*

Table 2 – Echocardiographic characteristics.

Variables	Total (n=30)	SOCL on CAG (=11)	No SOCL on CAG (=19)	P value
Diastolic dysfunction				0,167
Absent	7 (23.3)	2 (28.6)	5 (71.4)	
Grade 1	15 (50)	4 (26.7)	11 (73.3)	
Inconclusive	7 (23.3)	5 (71.4)	2 (28.6)	
Grade 2	1 (3.3)	0 (0)	1 (100)	
3D LVEF (%)	64.6 ± 3.8	63.3 ± 4.6	65.2 ± 3.3	0.313
GLS,%	18.3 ± 2.7	18.3 ± 2.4	19.1 ± 2.9	0.377
GWI (mmHg%)	1989 ± 371.2	1876 ± 253.8	2054.2 ± 417.3	0.089
GWE (%)	95 ± 2.2	95.6 ± 2.0	94.7 ± 2.2	0.296
GCW (mmHg%)	2248 ± 427.4	2109.5 ± 332.3	2329.3 ± 462.9	0.064
GWW (mmHg%)	90.7 ± 427.4	68.3 ± 33.8	103.7 ± 47.1	0.039

3D: three-dimensional; CAG: cineangiography; GCW: global constructive work; GLS: global longitudinal strain; GWE: global work efficiency; GWI: global work index; GWW: global wasted work; LVEF: left ventricular ejection fraction; SOCL: significant obstructive coronary lesions.

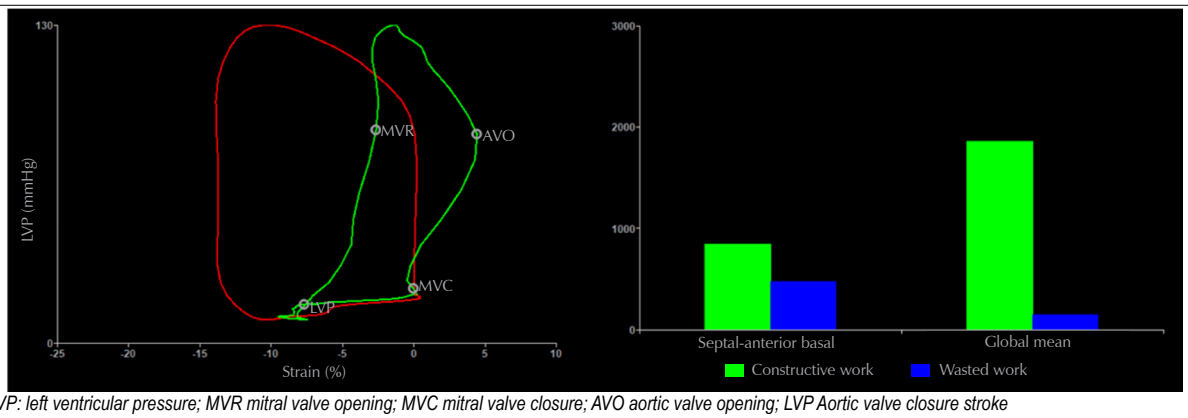

LVP: left ventricular pressure; MVR mitral valve opening; MVC mitral valve closure; AVO aortic valve opening; LVP Aortic valve closure stroke

Figure 1 – *Left ventricular pressure-strain curve diagram. (A) The global myocardial work is represented in red and the regional work of the basal segment of the anterior septum is represented in green. (B) There is decreased constructive work and increased wasted work of the septal-anterior basal segment in relation to the global mean.*

Table 3 – Relationship between coronary lesions and global longitudinal strain for each coronary territory.

	SOCL on CAG (=11)	No SOCL on CAG (=19)	P value
GLS (%)	18.3 ± 2.4	19.1 ± 2.9	0.377
AD strain (%)	19.5 ± 2.6	19.4 ± 3.2	0.900
CX strain (%)	17.8 ± 3.1	19.4 ± 3.5	0.359
RC strain (%)	18.2 ± 3.1	21.5 ± 3.0	0.103

AD: anterior descending artery; CX: circumflex artery; GLS: global longitudinal strain; RC: right coronary artery.

The presence of a GWW lower than 115 mmHg% demonstrated a sensitivity of 83.3% and a specificity of 41.7% for identifying patients with SOCL, with an area under the curve (AUC) of 0.625 (Table 4).

The separations of patients by arterial territory showed that the GWW presented a better AUC for identifying significant lesions in the AD (0.643) than in the RC (0.432) and CX (0.405) arteries (Figure 2).

The GLS was ≤16.5% in eight patients, of whom five had SOCL on catheterization with a sensitivity of 62.5% for obstructive CAD on CAG (Table 4).

Discussion

This study showed that GWW was higher in patients with SOCL on CAG than in those without SOCL.

Noninvasive myocardial work is a new tool for assessing LV systolic function as demonstrated in several studies, being superior to isolated LVEF and LV GLS.[8,13] Myocardial work parameters can assess LV performance and segmental function.

Wasted work is energy expenditure measured as work consumed during segmental lengthening (negative work) as a percentage of work during segmental shortening (positive work)[14]. Therefore, wasted work measurement can quantify the work done by the ventricle that does not contribute to ejecting blood from the LV.[15]

In the present study, a GWW > 115 mmHg% showed a sensitivity of 83.3% for identifying significant coronary obstructions, suggesting that it can be used to identify anatomically important lesions. Edwards *et al*. stated that a cutoff point of 80 mmHg% for GWW was associated with a sensitivity of 89.3% for SOCL detection similar to our study but with a lower cutoff point.[1]

A structurally normal heart presents few differences between the contraction times of the different LV segments.[16] All segments contract almost simultaneously against similar LV pressure, with only small physiological differences in segmental contraction timing.[15,14] When segmental contraction changes, some segments initiate relaxation at the end of systole under high ventricular pressure. This shows that some of the work done by the contracting segments is wasted during stretching of the relaxing segments.[15]

This study showed that the GWW in patients with significant AD artery lesions was greater than that in those without significant lesions in this artery compared to the global value when separated by arterial territory affected. Conversely, GCW was higher in patients without versus with significant lesions on CAG.

GWI can be defined as the total work accounted for by the LV strain curve pressure area from mitral valve closing to opening.[17] GWI can aid misinterpretations of reduced LV systolic function based only on decreased LV strain in patients with high afterload but no coronary obstruction.[7] In this study, the GWI was constant with the GLS. We also observed that GWI was lower in patients with SOCL on CAG, although the difference was not statistically significant.

A decreased LV GLS has been demonstrated as a predictor of CAD even in cases without significant obstruction[18] in addition to being superior to LVEF and LV segmental dysfunction as a predictor of cardiovascular events.[19] In our study, the assessment of LV GLS demonstrated a sensitivity of 62.5% for SOCL.

If confirmed by other studies, due to the good sensitivity

Table 4 – Echocardiographic parameters and detection of significant coronary artery obstruction.

	GLS	GWI	GWE	GCW	GWW
AUC	0,494	0,444	0,625	0,444	0,625
AUC CI95%	0,312-0,687	0,254-0,625	0,438-0,801	0,255-0,626	0,438-0,801
Cutoff value	<16,5%	<1700mmHg%	<95%	<2000mmHg%	>115mmHg%
Sensitivity (%)	62,5	55,6	75	55,5	83,3
Specificity (%)	36,4	33,3	50	33,3	41,7

AUC: area under the curve; CI: confidence interval; GLS: global longitudinal strain; GCW: global constructive work; GWE: global work efficiency; GWI: global work index; GWW: global wasted work.

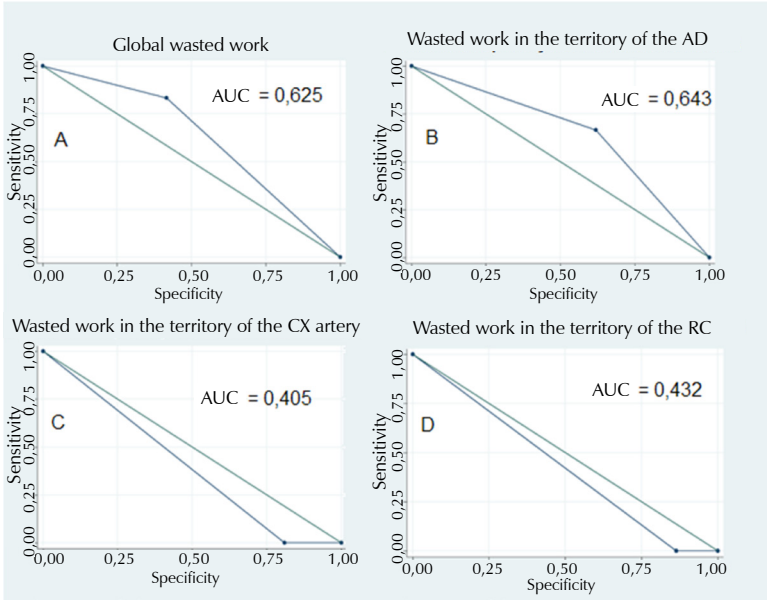

AUC, area under the curve; AD, anterior descending artery; CX, circumflex artery; RC, right coronary artery.

Figure 2 – *Area under the curve of the global wasted work and each arterial territory. (A) Global wasted work. (B) Work wasted in the territory of the anterior descending artery. (C) Wasted work in the circumflex artery territory. (D) Work wasted in the territory of the right coronary artery.*

of GWW, this method may be a screening tool for CAD with significant lesion (stenosis > 70%), selecting patients for further investigation.

Study limitations

The small sample of patients in this study may have contributed to its lack of statistical significance. In addition, an invasive stratification was performed in patients with a high probability of CAD, as coronary lesions were previously diagnosed by coronary computed tomography angiography or an ischemic functional test, thus restricting the number of patients who were young or lacking risk factors in our sample.

Conclusion

GWW correlated with the identification of significant coronary obstructions with a sensitivity of 83.3%. This myocardial work information can be used to detect significant obstructive lesions. Further studies are necessary to confirm the value of these promising data.

Authors' contributions

Research conception and design, manuscript writing, data analysis and interpretation, statistical analysis: Pereira MM; manuscript writing, data analysis and interpretation: Barroso AC; critical review of the manuscript for important intellectual content: Juliano MTH, Melo RJL, Gama CAV, Barbosa JB, and de Melo Filho JX; data collection: Barbosa MM, Araujo AC, and Gama GT.

Conflict of interest

The authors have declared that they have no conflict of interest.

References

1. Edwards NFA, Scalia GM, Shiino K, Sabapathy S, Anderson B, Chamberlain R, et al. Global Myocardial Work Is Superior to Global Longitudinal Strain to Predict Significant Coronary Artery Disease in Patients With Normal Left Ventricular Function and Wall Motion. J Am Soc Echocardiogr. 2019;32(8):947-57. doi: 10.1016/j.echo.2019.02.014. Erratum in: J Am Soc Echocardiogr. 2020;33(2):257.
2. Konstam MA, Abboud FM. Ejection Fraction: Misunderstood and Overrated (Changing the Paradigm in Categorizing Heart Failure). Circulation. 2017;135(8):717-9. doi: 10.1161/CIRCULATIONAHA.116.025795
3. Mor-Avi V, Lang RM, Badano LP, Belohlavek M, Cardim NM, Derumeaux G, et al. Current and evolving echocardiographic techniques for the quantitative evaluation of cardiac mechanics: ASE/EAE consensus statement on methodology and indications endorsed by the Japanese Society of Echocardiography. J Am Soc Echocardiogr. 2011;24(3):277-313. doi: 10.1016/j.echo.2011.01.015
4. Addetia K, Miyoshi T, Amuthan V, Citro R, Daimon M, Gutierrez Fajardo P, et al.; WASE Investigators. Normal Values of Left Ventricular Size and Function on Three-Dimensional Echocardiography: Results of the World Alliance Societies of Echocardiography Study. J Am Soc Echocardiogr. 2022;35(5):449-59. doi: 10.1016/j.echo.2021.12.004
5. Manganaro R, Marchetta S, Dulgheru R, Sugimoto T, Tsugu T, Ilardi F, et al. Correlation between non-invasive myocardial work indices and main parameters of systolic and diastolic function: results from the EACVI NORRE study. Eur Heart J Cardiovasc Imaging. 2020;21(5):533-41. doi: 10.1093/ehjci/jez203
6. van der Bijl P, Kostyukevich M, El Mahdiui M, Hansen G, Samset E, Ajmone Marsan N, et al. A Roadmap to Assess Myocardial Work: From Theory to Clinical Practice. JACC Cardiovasc Imaging. 2019;12(12):2549-54. doi: 10.1016/j.jcmg.2019.05.028
7. Boe E, Russell K, Eek C, Eriksen M, Remme EW, Smiseth OA, et al. Non-invasive myocardial work index identifies acute coronary occlusion in patients with non-ST-segment elevation-acute coronary syndrome. Eur Heart J Cardiovasc Imaging. 2015;16(11):1247-55. doi: 10.1093/ehjci/jev078
8. Russell K, Eriksen M, Aaberge L, Wilhelmsen N, Skulstad H, Remme EW, et al. A novel clinical method for quantification of regional left ventricular pressure-strain loop area: a non-invasive index of myocardial work. Eur Heart J. 2012;33(6):724-33. doi: 10.1093/eurheartj/ehs016
9. Lang RM, Badano LP, Mor-Avi V, Afilalo J, Armstrong A, Ernande L, et al. Recommendations for cardiac chamber quantification by echocardiography in adults: an update from the American Society of Echocardiography and the European Association of Cardiovascular Imaging. J Am Soc Echocardiogr. 2015;28(1):1-39.e14. doi: 10.1016/j.echo.2014.10.003
10. Boe E, Skulstad H, Smiseth OA. Myocardial work by echocardiography: a novel method ready for clinical testing. Eur Heart J Cardiovasc Imaging. 2019;20(1):18-20. doi: 10.1093/ehjci/jey156
11. Russell K, Eriksen M, Aaberge L, Wilhelmsen N, Skulstad H, Remme EW, et al. A novel clinical method for quantification of regional left ventricular pressure-strain loop area: a non-invasive index of myocardial work. Eur Heart J. 2012;33(6):724-33. doi: 10.1093/eurheartj/ehs016
12. Feres F, Costa RA, Siqueira D, Costa Júnior JR, Staico R, Chaves AJ, Abizaid A, et al. Diretriz da sociedade brasileira de cardiologia e da sociedade brasileira de hemodinâmica e cardiologia intervencionista sobre intervenção coronária percutânea. Arq Bras Cardiol. 2017;109;2541-619.
13. El Mahdiui M, van der Bijl P, Abou R, Ajmone Marsan N, Delgado V, Bax JJ. Global Left Ventricular Myocardial Work Efficiency in Healthy Individuals and Patients with Cardiovascular Disease. J Am Soc Echocardiogr. 2019;32(9):1120-7. doi: 10.1016/j.echo.2019.05.002
14. Vecera J, Penicka M, Eriksen M, Russell K, Bartunek J, Vanderheyden M, et al. Wasted septal work in left ventricular dyssynchrony: a novel principle to predict response to cardiac resynchronization therapy. Eur Heart J Cardiovasc Imaging. 2016;17(6):624-32. doi: 10.1093/ehjci/jew019
15. Russell K, Eriksen M, Aaberge L, Wilhelmsen N, Skulstad H, Gjesdal O, et al. Assessment of wasted myocardial work: a novel method to quantify energy loss due to uncoordinated left ventricular contractions. Am J Physiol Heart Circ Physiol. 2013;305(7):H996-1003. doi: 10.1152/ajpheart.00191.2013
16. Edwards NFA, Scalia GM, Shiino K, Sabapathy S, Anderson B, Chamberlain R, et al. Global Myocardial Work Is Superior to Global Longitudinal Strain to Predict Significant Coronary Artery Disease in Patients With Normal Left Ventricular Function and Wall Motion. J Am Soc Echocardiogr. 2019;32(8):947-57. doi: 10.1016/j.echo.2019.02.014. Erratum in: J Am Soc Echocardiogr. 2020;33(2):257.
17. Galli E, John-Matthwes B, Rousseau C, Schnell F, Leclercq C, Donal E. Echocardiographic reference ranges for myocardial work in healthy subjects: A preliminary study. Echocardiography. 2019;36(10):1814-24. doi: 10.1111/echo.14494
18. Montgomery DE, Puthumana JJ, Fox JM, Ogunyankin KO. Global longitudinal strain aids the detection of non-obstructive coronary artery disease in the resting echocardiogram. Eur Heart J Cardiovasc Imaging. 2012;13(7):579-87. doi: 10.1093/ejechocard/jer282
19. Stanton T, Leano R, Marwick TH. Prediction of all-cause mortality from global longitudinal speckle strain: comparison with ejection fraction and wall motion scoring. Circ Cardiovasc Imaging. 2009;2(5):356-64. doi: 10.1161/CIRCIMAGING.109.862334.

Global Longitudinal Strain as Predictor of Chemotherapy-Induced Cardiotoxicity

Strain Longitudinal Global como Preditor de Cardiotoxicidade Induzida por Quimioterapia

Monica Samuel Avila[2], Marco Stephan Lofrano Alves[2], Silvia Moreira Ayub-Ferreira[1], Mauro Rogerio de Barros Wanderley Junior[1], Fatima das Dores Cruz[1], Sara Michelly Gonçalves Brandão[1], Ludhmila Abrahão Hajjar[2,3], Roberto Kalil Filho[2,3], Cecilia Beatriz Bittencourt Viana Cruz[2,3], Maria Cristina Abduch[2], Danilo Bora Moleta, Edimar Alcides Bocchi[1]

[1]Universidade de São Paulo, Faculdade de Medicina, Heart Institute (InCor), Department of Heart Failure, São Paulo, SP, Brazil. [2]Universidade de São Paulo, Faculdade de Medicina, Heart Institute (InCor) do Hospital das Clínicas, São Paulo, SP, Brazil, [3]Cancer Institute do Estado de São Paulo (USP), São Paulo, SP, Brazil.

Abstract

Background: Chemotherapy-induced cardiotoxicity (ChC) is an important complication among patients receiving anthracyclines. Biomarkers and imaging parameters have been studied for their ability to identify patients at risk of developing ChC. Left ventricular global longitudinal strain (LV-GLS) is a sensitive parameter for detecting systolic dysfunction despite the presence of preserved left ventricular ejection fraction (LVEF).

Objective: To evaluate the role of the LV-GLS as a predictor of ChC.

Methods: This was a post-hoc analysis of the Carvedilol for Prevention of Chemotherapy-Related Cardiotoxicity trial, which evaluated the primary prevention of cardiotoxicity with carvedilol during doxorubicin chemotherapy in a population of patients with breast cancer. Cardiotoxicity was defined as a reduction ≥10% in LVEF. LV-GLS was determined before chemotherapy in patients with no prior cardiovascular disease or echocardiogram abnormalities.

Results: Thirty-one patients for whom a complete echocardiography study including measurement of LV-GLS was performed before chemotherapy were included in this analysis. An absolute LV-GLS<16.9% before chemotherapy showed 100% sensitivity and 73% specificity for predicting cardiotoxicity (area under the curve [AUC], 0.85; 95% confidence interval [CI], 0.680–0.959; p<0.001). In this population, LVEF values before chemotherapy did not predict ChC (95% CI, 0.478 to -0.842; p=0.17). The association of low LV-GLS (<17%) and brain-type natriuretic peptide serum levels (>17 pg/mL) at 2 months after chemotherapy increased the accuracy for detecting early-onset ChC (100% sensitivity, 88% specificity; AUC, 0.94; 95% CI, 0.781–0.995; p<0.0001).

Conclusions: Our data suggest that LV-GLS is a potential predictor of ChC. Larger studies are needed to confirm its clinical relevance in this clinical setting.

Keywords: Cardiotoxicity; Chemotherapy; Prevention; β-blockers; Echocardiogram; *Strain*.

Resumo

Fundamento: *A cardiotoxicidade induzida por quimioterapia (CiC) é uma complicação importante entre os pacientes que recebem antraciclinas. Biomarcadores e parâmetros de imagem têm sido estudados por sua capacidade de identificar pacientes com risco de desenvolver essa complicação. O strain longitudinal global do ventrículo esquerdo (SLG-VE) tem sido descrito como um parâmetro sensível para detectar disfunção sistólica, mesmo na presença de fração de ejeção do ventrículo esquerdo (FEVE) preservada.*

Objetivo: avaliar o papel do SLG-VE como preditor de CiC.

Métodos: *O presente estudo consiste em uma análise post-hoc do estudo CECCY (Carvedilol for Prevention of Chemotherapy-Related Cardiotoxicity [Carvedilol para Prevenção da Cardiotoxicidade Relacionada à Quimioterapia]), que avaliou a prevenção primária de cardiotoxicidade com carvedilol durante quimioterapia com doxorrubicina em uma população com câncer de mama. Definiu-se cardiotoxicidade como uma redução ≥10% na FEVE. O SLG-VE foi obtido antes da quimioterapia em pacientes sem doença cardiovascular prévia ou anormalidades no ecocardiograma.*

Mailing Address: Monica Samuel Avila •
R. Dr. Eneas de Carvalho Aguiar 44, São Paulo, Brazil, Postal Code: 05403900.
E-mail: mo_avila@hotmail.com
Manuscript received 08/25/2022; revised 10/04/2022; accepted 10/13/2022

Editor responsible for the review: Daniela do Carmo Rassi Frota

DOI: 10.47593/2675-312X/20223504eabc340i

Resultados: *Trinta e um pacientes submetidos a estudo ecocardiográfico completo incluindo avaliação de SLG-VE antes da quimioterapia foram incluídos nesta análise. Um SLG-VE absoluto <16,9% antes da quimioterapia mostrou 100% de sensibilidade e 73% de especificidade para predizer cardiotoxicidade (AUC=0,85; IC 95% 0,680–0,959, p<0,001). Nesta população, os valores de FEVE antes da quimioterapia não foram preditores de CiC (IC 95% 0,478 a -0,842, p=0,17). A associação de baixos níveis séricos de SLG-VE (<17%) e BNP (>17 pg/mL) dois meses após a quimioterapia aumentou a precisão para detectar CiC de início precoce (100% de sensibilidade, 88% de especificidade, AUC=0,94; IC 95% 0,781–0,995, p<0,0001).*

Conclusões: *Nossos dados sugerem que o SLG-VE é um possível preditor de cardiotoxicidade induzida por quimioterapia. São necessários estudos maiores para confirmar a relevância clínica desse parâmetro ecocardiográfico nesse cenário clínico.*

Palavras-chave: *Cardiotoxicidade; Quimioterapia; Prevenção; Betabloqueadores; Ecocardiograma; Strain.*

Introduction

The cardiovascular effects of chemotherapeutic agents are responsible for a significant proportion of severe complications, particularly among female patients with breast cancer.[1] There is evidence of increasing cardiovascular disease among hospitalized patients with cancer.[2] One of the most widely used agents,[3,4] anthracyclines (ANT), is responsible for early and late dose-related cardiotoxicity, particularly heart failure (HF).[5-7]

The detection of cardiotoxicity is routinely performed by left ventricular ejection fraction (LVEF). Although LVEF predicts the occurrence of HF, it has limited sensitivity.[8] Failure to detect subtle changes in LV systolic function occurs for many reasons: the need for geometrical assumptions for calculations, possible inadequate visualization of the LV apex, impossibility of identifying marginal regional wall motion abnormalities, and intrinsic measurement variability.[9] A decreased LVEF after chemotherapy is often a sign of already extensive myocardial damage and HF.[10]

Due to increased morbidity and mortality among patients with chemotherapy-related HF, higher-sensitivity markers of subclinical cardiac dysfunction and myocardial injury have been investigated to detect chemotherapy-induced cardiotoxicity (ChC). For this purpose, the evaluation of two-dimensional speckle-tracking imaging has emerged. This technique allows for the study of global and regional myocardial deformation. Several studies have already emphasized the role of LV global longitudinal strain (LV-GLS) to detect subtle alterations in systolic function particularly related to ANT chemotherapy.[11] The evaluation of GLS for the detection of subclinical LV dysfunction induced by chemotherapy is recommended by expert consensus.[12]

Considering this new field assessing ANT-induced cardiotoxicity using LV-GLS, we conducted a *post-hoc* analysis of the randomized double-blind placebo-controlled Carvedilol Effect in Preventing Chemotherapy Induced CardiotoxicitY (CECCY) trial, which aimed to evaluate the LV-GLS before ANT chemotherapy as a predictor of cardiotoxicity.

Methods

Study design

This *post-hoc* analysis of the CECCY trial evaluated the primary prevention of cardiotoxicity with carvedilol during doxorubicin chemotherapy in women with breast cancer. Cardiotoxicity was defined as a ≥10% reduction in LVEF. Patients were recruited and followed up at two different institutions, the Heart Institute and the Cancer Institute from the University of Sao Paulo, Sao Paulo, Brazil. The Ethics Committee of the Heart Institute and Cancer Institute from the University of Sao Paulo, Sao Paulo, Brazil, review board of both institutions approved the trial protocol. All methods were performed in accordance with the relevant guidelines and regulations. All participants were informed of the research objectives, research protocol, and treatment alternatives, and all participants provided written informed consent to participate. The trial was registered at ClinicalTrials.gov (NCT01724450) before study initiation.

Study patients

The CECCY trial included patients with *HER2*-negative breast cancer tumor status and therapy that included ANT, cyclophosphamide, and taxane from April 2013 to January 2017. The standard chemotherapy protocol comprised four cycles of cyclophosphamide 600 mg/m^2 and doxorubicin 60 mg/m^2 every 21 days (with a total cumulative dose of 240 mg/m^2), followed by paclitaxel 80 mg/m^2 weekly for 8 weeks. The trial design and results were described elsewhere.[13]

Study procedures

The present *post-hoc* analysis included only patients who underwent echocardiography studies and accomplished follow-up at the Heart Institute from the University of Sao Paulo, where the institutional protocol included speckle tracking echocardiography. Eligible patients underwent comprehensive transthoracic echocardiography before starting chemotherapy including proper imaging acquired to perform the strain analysis. Patients with an unsatisfactory acoustic window for the speckle tracking analysis due to artifacts caused by breast reconstruction techniques were excluded from the study. Echocardiographic studies were performed using a commercially available system (Vivid E9; General Electric, GE Vingmad Ultrasound AS, Norway) equipped with a 2–5-MHz transducer. All measurements were performed and reported according to American Society of Echocardiography recommendations (Lang 2015, Recommendations for cardiac chamber quantification by echocardiography in adults: an update from the American Society of Echocardiography and the European Association of Cardiovascular Imaging). LVEF was measured by Simpson's rule.

For the speckle tracking analysis, images were acquired

with an adjusted device to record three cardiac cycles within a period of 100 msec before and after the cycle. The second harmonic image, in grayscale, with a frame rate of 40–80 frames/s was used. To measure LV-GLS, cardiac images were obtained through the apical windows (APLAX, A4C and A2C). After the acquisition, the studies were stored for offline analysis with the EchoPAC software (v30 12; GE Vingmad Ultrasound AS). The analysis was performed of the sixteen LV segments, and the quantitative peak systolic longitudinal strain was quantified for each segment as well as the whole LV during a cycle cardiac. All scans were read by experienced board certified echocardiographers who were blinded to the patients' clinical information.

Statistical analysis

The data are expressed as median and 95% confidence interval. We tested the normality of a variable distribution using the D'Agostino-Pearson test. For comparisons between two independent samples, an unpaired *t*-test was used for variables with Gaussian distribution, while the Mann-Whitney rank sum test was applied for variables with non-Gaussian distributions. For comparison between paired samples with Gaussian distribution, the paired t-test was used, while the Wilcoxon matched pairs ranked test was used for pairs with a non-Gaussian distribution. We used receiver operating characteristic (ROC) curve analysis to determine the accuracy and optimal cutoff. The best cutoff for each variable was chosen through the shortest distance from the upper left angle to the curve obtained in the graph of the ROC curve by the method of DeLong et al.[14] P values <0.05 were considered significant.

Results

In this *post-hoc* analysis of the randomized double-blind placebo-controlled CECCY trial, we evaluated 53 patients who underwent echocardiography with the speckle tracking technique at the Heart Institute. Of these, six (11%) had an unsatisfactory acoustic window and were excluded from the analysis. Another 16 patients were excluded for attending subsequent echocardiographic follow-up at another institution. The population included in the analysis was at low risk of cardiovascular. The baseline characteristics of the remaining 31 patients are described in Table 1. Our population had low prevalence of cardiovascular comorbidities and risk factors for cardiotoxicity. In this group, 3 (9.7%) developed cardiotoxicity (LVEF decrease ≥10% from baseline). Considering the alternative and most accepted definition of cardiotoxicity as a decrease of 10 percentage points to a value below the low normal value of 50%,[15] only 1 patient fulfilled the criteria for cardiotoxicity and had a decrease of LVEF to 35% and a GLS of 13%. The 3 patients with cardiotoxicity were aged 51–63 years, only one had a diagnosis of arterial hypertension, and none had other risk factors for cardiovascular disease such as diabetes mellitus, hypercholesterolemia under statin treatment, or current/past smoking status.

LV-GLS predicted the development of cardiotoxicity (cutoff value, ≤16.9%), with 100% sensitivity and 73.1% specificity (area under the curve [AUC], 0.859; p<0.001). A serum brain-type natriuretic peptide (BNP) level >16 pg/mL measured 2 weeks after starting chemotherapy was also associated with cardiotoxicity with 100% sensitivity and 69.2% specificity (AUC, 0.878; p<0.001) (Figure 1, Central Illustration). On the other hand, baseline LVEF (AUC, 0.680; p=0.17) and serum troponin (AUC, 0.577; p=0.69) were not associated with the incidence of cardiotoxicity.

Table 2 shows the median and 95% CI values for serum LVEF, BNP, and troponin before and 2, 4, and 24 weeks after starting chemotherapy stratified according to baseline LV-GLS. Baseline LVEF was not significantly different in patients with an LV-GLS ≤16.9% versus >16.9%. Similarly, there was no intergroup difference in baseline BNP or troponin

Table 1 - Baseline characteristics of the study population.

Characteristic	Population (N=31)	LV-GLS ≤16,9% (N=10)	LV-GLS >16,9% (N=21)	P value
Age, years	51±9.69	54.9±6.7	49±10.4	NS
Menopause, no. of patients (%)				
Pre-menopause	14 (45)	4 (40)	10 (47)	NS
Post-menopause	17 (55)	6 (60)	11 (53)	
Therapy, no. of patients (%)				
Neoadjuvant	17 (55)	6 (60)	11 (47)	NS
Adjuvant	14 (45)	4 (40)	10 (53)	
Drug carvedilol, no. of patients (%)	18 (48)	6 (60)	12 (57)	
Body mass index (kg/m2)	27.1±7.45	30.3± 6.9	25.6±7.3	0.09
Cardiovascular risk factors, no of patients (%)				
Hypertension	1 (3.2)	1 (10%)	0	NS
Diabetes mellitus	1 (3.2)	0	1 (4)	NS
Hypercholesterolemia	1 (3.2)	1 (10%)	0	NS
Current/past smoker	11 (35.4)	4 (40)	7 (33)	NS
Systolic blood pressure (mmHg)	121±12.46	121±10.9	121±13.8	NS
Diastolic blood pressure (mmHg)	79±8.1	81±7.2	77±8.5	NS
Heart rate, beats/min	79±11.5	85±12.2	77±10.2	0.06

Data are expressed as mean ± SD or number. LV-GLS: left ventricular global longitudinal strain; NS: not significant.

values. However, LVEF evaluated by echocardiography was significantly lower after 4 weeks of chemotherapy in the group with a baseline LV-GLS ≤16.9% (p=0.003). Furthermore, serum BNP measured after 4 weeks of chemotherapy treatment was higher in the group with an LV-GLS ≤16.9% (p=0.004). There was no significant intergroup difference for troponin values at any time point.

Figure 2 shows median and 95% CI values for LVEF and LV-GLS before and after 12 months after chemotherapy. We observed that LV-GLS decreased significantly from baseline values (p=0.005), whereas LVEF did not. In the follow-up period after chemotherapy, LV-GLS decreased more than 5%, 10%, and 15% from baseline in 77%, 66%, and 42% of patients, respectively, whereas LVEF decreased more than 10% in only 9.7% of patients.

Discussion

In this *post-hoc* analysis of the randomized double-blind placebo-controlled CECCY trial that evaluated the role of the speckle tracking echocardiography in ANT-induced cardiotoxicity, LV-GLS was a potential predictor of ChC in patients with a low prevalence of cardiovascular comorbidities and risk factors for cardiovascular disease. In this scenario, LV-GLS was a better predictor of cardiotoxicity than LVEF. In addition, the combination of LV-GLS and BNP during follow-up could be a predictor of cardiotoxicity.

There has been great interest in the early detection of cardiotoxicity to reverse and prevent associated cardiomyopathy.[16] LVEF is a strong predictor of cardiac events, but it lacks sensitivity for the detection of subclinical changes in cardiac function.[17] Strain is defined as change in the length of the myocardium divided by the original length of the myocardium and peak systolic deformation between systole and diastole.[18] LV-GLS has emerged as the main measurement of subclinical myocardial dysfunction and demonstrated utility in predicting subsequent reductions in LVEF in patients after cancer treatment.[8,19,20] Ali et al.[8] demonstrated that an absolute LV-GLS value of less than -17.5% was associated with an increase in HF among patients with hematologic cancer undergoing ANT chemotherapy. Charbonnel et al.[11] showed that an LV-GLS value of greater than -17.45% obtained after ANT 150 mg/m^2 is an independent predictor of future cardiotoxicity.

Our study findings are in concordance with other studies that showed that the strain measure before chemotherapy predicts the development of cardiotoxicity.[19]

The SOCCOUR trial recently compared cardioprotection guided by changes in LV-GLS versus LVEF among patients undergoing ANT chemotherapy. In the trial, 331 patients were randomized to receive angiotensin-converting enzyme inhibitors or angiotensin receptor blockers and beta-blockers guided by a ≥12% relative reduction in LV-GLS (GLS-guided arm) or 10% absolute reduction in LVEF (EF-guided arm). Patients were followed for LVEF and cancer

Table 2 - Evolution of LVEF, serum troponin, and BNP after 2, 4, and 24 weeks of chemotherapy divided by LV-GLS value before chemotherapy.

	LV-GLS ≤16,9% (N=10)	LV-GLS >16,9% (N=21)	P value
LVEF before ChT, %	61.5 (59.9–64.0)	63.5 (60.9–64.4)	NS
LVEF 2 weeks, %	61.0 (58.2–66.0)	65.0 (62.8–67.0)	NS
LVEF 4 weeks, %	58.0 (56.1–62.9)	61.2 (62.5–65.5)	0.003
LVEF 24 weeks, %	63.0 (53.0–68.9)	63.0 (61.0–64.9)	NS
BNP before ChT, pg/mL	18.0 (7.42–46.9)	12.0 (9.2–19.2)	NS
BNP 2 weeks, pg/mL	19.0 (1.24–46.9)	9.0 (6.2–16.5)	NS
BNP 4 weeks, pg/mL	16.0 (-11.2–88.3)	13.0 (8.8–21.8)	NS
BNP 24 weeks, pg/mL	18.5 (-39.9–167.7)	8.0 (5.7–10.7)	0.004
Troponin before ChT, mg/mL	0.005 (0.003–0.011)	0.005 (0.004–0.006)	NS
Troponin 2 weeks, mg/mL	0.008 (0.005–0.016)	0.005 (0.006–0.011)	NS
Troponin 4 weeks, mg/mL	0.029 (0.014–0.077)	0.028 (0.025–0.054)	NS
Troponin 24 weeks, mg/mL	0.024 (0.015–0.048)	0.016 (0.009–0.037)	NS

BNP: brain-type natriuretic peptide; ChT: chemotherapy; LVEF: left ventricular ejection fraction; LV-GLS: left ventricular global longitudinal strain; NS: not significant.

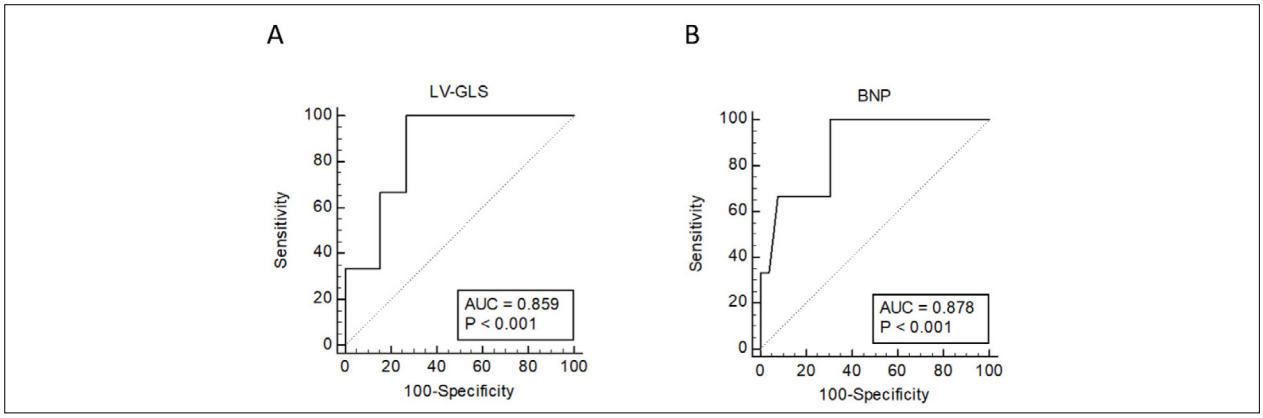

Figure 1 – *Receiver operating characteristic curve analyses of LV-GLS measured before the onset of chemotherapy (A) and BNP after 2 weeks of chemotherapy (B) and their association with cardiotoxicity. AUC: area under the curve; BNP: brain-type natriuretic peptide; LV-GLS: left ventricular global longitudinal strain (Central Illustration).*

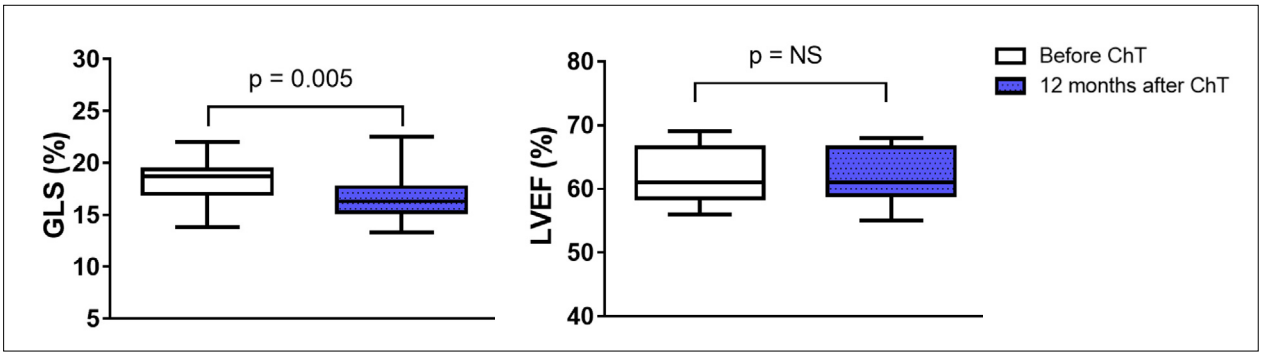

Figura 2 – *Mediana e IC de 95% para SLG-VE e FEVE antes e após 12 meses de quimioterapia. SLG-VE: strain longitudinal global do ventrículo esquerdo; FEVE: fração de ejeção do ventrículo esquerdo.*

therapy–related cardiac dysfunction (symptomatic drop of >5% or asymptomatic drop of >10% to <55%). At 1 year of follow-up, the LVEF did not change significantly in either group. However, in the GLS-guided arm, there was a greater use of cardioprotection and fewer patients met the cardiotoxicity criteria (5.8% vs. 13.7%; p=0.02). Patients who received cardioprotection in the EF-guided arm exhibited a greater reduction in LVEF at follow-up than those in the GLS-guided arm (9.1±10.9% *vs*. 2.9±7.4%; p=0.03) supporting the use of GLS for detecting cardiotoxicity.[21]

Oikonomou et al.[22] published a meta-analysis that evaluated the prognostic value of GLS for predicting cardiotoxicity and included 21 studies comprising 1782 patients with cancer treated with ANT with or without trastuzumab. The authors found an incidence of cardiotoxicity of 9.3–43.8%. Four studies evaluated the association of GLS before treatment initiation with subsequent cardiotoxicity: 2 found no association,[23,24] 1 reported a significant association (odds ratio per 1% decrease, 1.48; 95% CI, 1.15–1.89) and 1 reported an AUC of 0.76 (95% CI, 0.58–0.88), with an optimal cutoff value of -19.95% (sensitivity, 83%; specificity, 72%) for cardiotoxicity.[11]

Other biomarkers have been studied as a strategy for the early detection and monitoring of cardiotoxicity. The most studied biomarkers in cardiotoxicity include troponin and BNP. Regarding troponin, strong evidence favors its ability to predict cardiotoxicity and cardiac events.[15,25] However, the utility of BNP for chemotherapy-related cardiotoxicity remains controversial, with many studies reporting no prognostic value in this scenario.[26] Our study showed that the combination of the LV-GLS pre-chemotherapy with BNP during follow-up (until 24 weeks) could be a greater predictor of a >10% decrease in LVEF. However, the combination of LV-GLS with troponin showed no prognostic value regarding cardiotoxicity.

Limitations

This was a *post-hoc* analysis of the CECCY trial, so its findings were not pre-specified. We also included a small sample size due to difficulties obtaining speckle tracking images. We did not have a more robust modality for assessing EF such as planar equilibrium radionuclide angiocardiography or magnetic resonance imaging. Moreover, we noted a low incidence of cardiotoxicity that could have impaired the results.

Conclusion

LV-GLS is a potential predictor of ChC in patients with a low prevalence of cardiovascular comorbidities and risk factors for cardiovascular disease. LV-GLS was a better predictor of cardiotoxicity than LVEF, while the combination of LV-GLS and BNP during follow-up could be a predictor of cardiotoxicity. Overall, our findings confirm the ability of LV-GLS to detect subclinical cardiotoxicity and emphasize the need for early evaluations of LV-GLS to detect cardiotoxicity.

Authors' contributions

Plan Study, Conduct Study, Search Literature, Write Article: MS Avila, MSL Alves, and SMA Ferreira; Plan Study, Conduct Study, Search Literature, Review Article: MRB Wanderley: Conduct Study, Search Literature, Review Article: FD Cruz and SMG Brandão: Plan Study, Search Literature, Review Article: LA Hajjar and R Kalil Filho; Conduct Study, Review Article: CBBV Cruz, MC Abduch, and DB Moleta; Plan Study, Conduct Study, Search Literature, Review Article: EA Bocchi.

Conflict of interest

The authors have declared that they have no conflict of interest.

References

1. Patnaik JL, Byers T, DiGuiseppi C, Dabelea D, Denberg TD. Cardiovascular disease competes with breast cancer as the leading cause of death for older females diagnosed with breast cancer: a retrospective cohort study. Breast Cancer Res. 2011;13(3):R64. doi: 10.1186/bcr2901.
2. Agarwal MA, Aggarwal A, Rastogi S, Ventura HO, Lavie CJ. Cardiovascular disease burden in cancer patients from 2003 to 2014. Eur Heart J Qual Care Clin Outcomes. 2018;4(1):69-70. doi: 10.1093/ehjqcco/qcx033.
3. Ewer MS, Ewer SM. Cardiotoxicity of anticancer treatments. Nat Rev Cardiol. 2015;12(9):547-58. doi: 10.1038/nrcardio.2015.65.
4. Miller KD, Siegel RL, Lin CC, Mariotto AB, Kramer JL, Rowland JH, et al. Cancer treatment and survivorship statistics, 2016. CA Cancer J Clin. 2016;66(4):271-89. doi: 10.3322/caac.21349.

5. Suter TM, Ewer MS. Cancer drugs and the heart: importance and management. Eur Heart J. 2013;34(15):1102-11. doi: 10.1093/eurheartj/ehs181.

6. Valachis A, Nilsson C. Cardiac risk in the treatment of breast cancer: assessment and management. Breast Cancer (Dove Med Press). 2015;7:21-35. doi: 10.2147/BCTT.S47227.

7. Henriksen PA. Anthracycline cardiotoxicity: an update on mechanisms, monitoring and prevention. Heart. 2018;104(12):971-977. doi: 10.1136/heartjnl-2017-312103.

8. Ali MT, Yucel E, Bouras S, Wang L, Fei HW, Halpern EF, et al. Myocardial Strain Is Associated with Adverse Clinical Cardiac Events in Patients Treated with Anthracyclines. J Am Soc Echocardiogr. 2016;29(6):522-527.e3. doi: 10.1016/j.echo.2016.02.018.

9. Santoro C, Arpino G, Esposito R, Lembo M, Paciolla I, Cardalesi C, et al. 2D and 3D strain for detection of subclinical anthracycline cardiotoxicity in breast cancer patients: a balance with feasibility. Eur Heart J Cardiovasc Imaging. 2017;18(8):930-936. doi: 10.1093/ehjci/jex033.

10. Cardinale D, Colombo A, Lamantia G, Colombo N, Civelli M, De Giacomi G, Rubino M, Veglia F, Fiorentini C, Cipolla CM. Anthracycline-induced cardiomyopathy: clinical relevance and response to pharmacologic therapy. J Am Coll Cardiol. 2010;55(3):213-20. doi: 10.1016/j.jacc.2009.03.095.

11. Charbonnel C, Convers-Domart R, Rigaudeau S, Taksin AL, Baron N, et al. Assessment of global longitudinal strain at low-dose anthracycline-based chemotherapy, for the prediction of subsequent cardiotoxicity. Eur Heart J Cardiovasc Imaging. 2017;18(4):392-401. doi: 10.1093/ehjci/jew223.

12. Plana JC, Galderisi M, Barac A, Ewer MS, Ky B, Scherrer-Crosbie M, et al. Expert consensus for multimodality imaging evaluation of adult patients during and after cancer therapy: a report from the American Society of Echocardiography and the European Association of Cardiovascular Imaging. J Am Soc Echocardiogr. 2014;27(9):911-39. doi: 10.1016/j.echo.2014.07.012.

13. Avila MS, Ayub-Ferreira SM, de Barros Wanderley MR Jr, das Dores Cruz F, Gonçalves Brandão SM, et al. Carvedilol for Prevention of Chemotherapy-Related Cardiotoxicity: The CECCY Trial. J Am Coll Cardiol. 2018 May;71(20):2281-2290. doi: 10.1016/j.jacc.2018.02.049.

14. DeLong ER, DeLong DM, Clarke-Pearson DL. Comparing the areas under two or more correlated receiver operating characteristic curves: a nonparametric approach. Biometrics. 1988;44(3):837-45.

15. Zamorano JL, Lancellotti P, Rodriguez Muñoz D, Aboyans V, Asteggiano R, Galderisi M, et al; ESC Scientific Document Group. 2016 ESC Position Paper on cancer treatments and cardiovascular toxicity developed under the auspices of the ESC Committee for Practice Guidelines: The Task Force for cancer treatments and cardiovascular toxicity of the European Society of Cardiology (ESC). Eur Heart J. 2016;37(36):2768-2801. doi: 10.1093/eurheartj/ehw211.

16. Cardinale D, Colombo A, Bacchiani G, Tedeschi I, Meroni CA, Veglia F, et al. Early detection of anthracycline cardiotoxicity and improvement with heart failure therapy. Circulation. 2015;131(22):1981-8. doi: 10.1161/CIRCULATIONAHA.

17. Liu J, Banchs J, Mousavi N, Plana JC, Scherrer-Crosbie M, Thavendiranathan P, et al. Contemporary Role of Echocardiography for Clinical Decision Making in Patients During and After Cancer Therapy. JACC Cardiovasc Imaging. 2018;11(8):1122-1131. doi: 10.1016/j.jcmg.2018.03.025.

18. Lang RM, Badano LP, Mor-Avi V, Afilalo J, Armstrong A, Ernande L, et al. Recommendations for cardiac chamber quantification by echocardiography in adults: an update from the American Society of Echocardiography and the European Association of Cardiovascular Imaging. J Am Soc Echocardiogr. 2015;28(1):1-39.e14. doi: 10.1016/j.echo.2014.10.003.

19. Clasen SC, Scherrer-Crosbie M. Applications of left ventricular strain measurements to patients undergoing chemotherapy. Curr Opin Cardiol. 2018;33(5):493-497. doi: 10.1097/HCO.0000000000000541.

20. Thavendiranathan P, Amir E. Left Ventricular Dysfunction With Trastuzumab Therapy: Is Primary Prevention the Best Option? J Clin Oncol. 2017;35(8):820-825. doi: 10.1200/JCO.2016.71.0038.

21. Thavendiranathan P, Negishi T, Somerset E, Negishi K, Penicka M, Lemieux J, et al; SUCCOUR Investigators. Strain-Guided Management of Potentially Cardiotoxic Cancer Therapy. J Am Coll Cardiol. 2021;77(4):392-401. doi: 10.1016/j.jacc.2020.11.020.

22. Oikonomou EK, Kokkinidis DG, Kampaktsis PN, Amir EA, Marwick TH, Gupta D, Thavendiranathan P. Assessment of Prognostic Value of Left Ventricular Global Longitudinal Strain for Early Prediction of Chemotherapy-Induced Cardiotoxicity: A Systematic Review and Meta-analysis. JAMA Cardiol. 2019;4(10):1007-1018. doi: 10.1001/jamacardio.2019.2952.

23. Narayan HK, French B, Khan AM, Plappert T, Hyman D, Bajulaiye A, et al. Noninvasive Measures of Ventricular-Arterial Coupling and Circumferential Strain Predict Cancer Therapeutics-Related Cardiac Dysfunction. JACC Cardiovasc Imaging. 2016;9(10):1131-1141. doi: 10.1016/j.jcmg.2015.11.024.

24. Narayan HK, Wei W, Feng Z, Lenihan D, Plappert T, Englefield V, et al. Cardiac mechanics and dysfunction with anthracyclines in the community: results from the PREDICT study. Open Heart. 2017;4(1):e000524. doi: 10.1136/openhrt-2016-000524.

25. Cardinale D, Colombo A, Torrisi R, Sandri MT, Civelli M, Salvatici M, et al. Trastuzumab-induced cardiotoxicity: clinical and prognostic implications of troponin I evaluation. J Clin Oncol. 2010;28(25):3910-6. doi: 10.1200/JCO.2009.27.3615.

26. Chaudry M, Banchs J, Chavez-MacGregor M. Anthracycline or trastuzumab-related cardiotoxicity: do we have a predictive biomarker? Biomark Med. 2016;10(3):315-28. doi: 10.2217/bmm.15.124.

Review Article

Hypertrophic Cardiomyopathy: A Review Using Magnetic Resonance Imaging

Cardiomiopatia Hipertrófica: Uma Revisão pelo Olhar da Ressonância Magnética

Raul Serra Valério[1], *Marcio Sommer Bittencourt*[1,2], *Marly M. Uellendahl*,[1,3]

[1]*DASA, São Paulo, SP, Brazil.* [2]*Clinical and Epidemiological Research Center, University Hospital, University of São Paulo (USP), São Paulo, SP, Brazil.* [3]*Federal University of São Paulo (UNIFESP), São Paulo, SP, Brazil.*

Abstract

Hypertrophic cardiomyopathy, the most common genetic cardiopathy in the general population, is characterized by asymmetric left ventricular hypertrophy. However, the phenotypic changes in this cardiomyopathy extend beyond ventricular hypertrophy and include changes in the mitral valve apparatus, papillary muscles, and right ventricle. Due to the difficult differential diagnosis among multiple causes of hypertrophy, cardiac magnetic resonance has played a fundamental role in its diagnostic and prognostic evaluation; magnetic cine-resonance in defining the location and extent of hypertrophy; late enhancement, in the detection of areas of myocardial fibrosis; more recent techniques such as T1 mapping that assesses interstitial fibrosis and extracellular volume; and finally tissue tracking in the analysis of myocardial deformation.

Introduction

Hypertrophic cardiomyopathy (HCM) was first described by the English pathologist Robert Donald Teare, who reported the presence of asymmetric myocardial hypertrophy *postmortem* in a series of eight patients, of whom seven had died of sudden cardiac death (SCD).[1]

The prevalence of HCM is 1:500 in the general population, making it the most common genetic cardiac pathology. It affects the sexes at similar frequencies, although women are more often underdiagnosed, tending to be older with more advanced cardiomyopathy at the initial evaluation.[2-4]

HCM is defined as an unexplained increase in the thickness of the left ventricular (LV) wall with hypertrophy ≥15 mm in end diastole and in any ventricular segment, with involvement restricted to the heart and in the absence of other pathologies that may cause similar hypertrophy.[3,4] However, morphological changes in the mitral valve apparatus or papillary muscles and the presence of myocardial fibrosis and microvascular disease are also part of the spectrum of this disease.[5]

Keywords

Cardiomyopathy, Hypertrophic; Magnetic Resonance; Cardiac Imaging Techniques.

Mailing Address: Marly M. Uellendahl •
R. Joaquim Nabuco, 1560, Brooklyn Paulista, SP, Brazil, Postal Code: 04621-005.
E-mail: mauellendahl@gmail.com

Manuscript received 9/29/2022; revised 10/5/2022; accepted 10/20/2022

Editor responsible for the review: Daniela do Carmo Rassi Frota

DOI: 10.47593/2675-312X/20223504erer_15i

The LV hypertrophy (LVH) found in HCM has heterogeneous phenotypic patterns that can vary with LVH type (asymmetric, symmetric, focal, or diffuse) and ventricular wall location (ranging from the apex to the base). Other extremely important signs in the evaluation of HCM include LV outflow tract (LVOT) obstruction and LV ejection fraction (LVEF) changes.[6-10]

The myocardial hypertrophy in these patients is explained by characteristic histopathological findings, disorganized and hypertrophic myocardial fibers, and microvascular dysfunction with consequent silent ischemia and subsequent interstitial fibrosis.[11]

The life expectancy for most patients with HCM is similar to that of individuals without cardiomyopathy;[12,13] however, a small proportion is at higher risk of cardiovascular events such as SCD, heart failure (HF), and stroke.[13-15] Around 30–40% of patients with HCM are estimated to develop adverse events related to heart disease. Nonetheless, the current therapeutic arsenal, especially related to risk stratification and the use of implantable cardioverter-defibrillators (ICD), has reduced the mortality rate of these patients, even in the most severe cases, to less than 1% annually.[4]

Genetics

HCM is an autosomal dominant genetic disease caused by mutations of different genes that encode cardiac sarcomere proteins.[5,16]

More than 1,500 mutations have been identified in more than 13 different genes that interfere with the coding of sarcomere contractile proteins. Numerous mutations are known, with the most prevalent being located in the beta-myosin heavy chain (*MYH7*) and myosin-binding protein C (*MYBPC3*) genes.[4,5] Almost every patient with an HCM-related mutation will demonstrate phenotypic evidence until early adulthood, especially with increased myocardial thickness.[17-20]

Genetic testing can identify the mutation in up to 30–60% of patients with the HCM phenotype. However, a significant proportion of patients with phenotypic change resents no recognized genetic basis.[4,21-23] Notably, genetic changes are not correlated with the subject's phenotype, and similar genetic mutations may present as different cardiomyopathy phenotypes.[24]

The advantage of genetic confirmation is the opportunity to test first-degree relatives and, consequently, perform a cascade screening to enable early evaluation and follow-up, if indicated, for these patients.[6,19,22,25] Relatives in whom the gene mutation is identified have a high probability of developing phenotypic changes at some point in life; therefore, follow-up with imaging tests is

indicated. On the other hand, relatives not carrying the genetic mutation have no risk of developing the disease and require no clinical follow-up.[22,23]

Phenotypic presentations of LVH

Different patterns of hypertrophy comprise this phenotype within the spectrum of HCM. The most common segment of LVH, involved in up to 70% of cases, is the confluence of the basal anterior septum with the contiguous anterior free wall, often the thickest segment.[26-28] The second most common region of LVH is the posterior mid-apical LV septum.[8,29]

However, most phenotypes present hypertrophy in more than 50% of the total myocardium. On the other hand, some cases may present as focal hypertrophy, mainly in the basal anterior septum region or the basal anterior segment. These cases of focal hypertrophy may have a normal myocardial mass (up to 20%) despite a clinical diagnosis of HCM, constituting a greater diagnostic challenge, especially on echocardiography.[7,26,28,30]

Another extremely important but less frequent phenotype is midventricular hypertrophy, which, by causing dynamic LV obstruction, favors the onset of ventricular arrhythmias, myocardial necrosis, and apical aneurysms, causing thrombus and systemic embolic events.[27,31]

Apical ventricular hypertrophy, found in 5–25% of cases, is a heterogeneous HCM phenotype predominant in the apical segments that is often related to T-wave inversion on electrocardiography.[32]

Figure 1 shows the main hypertrophy patterns found in HCM cases.

Other phenotypic changes in HCM

HCM, in addition to typical LVH, has other cardiac presentations that, with the increased use of cardiac magnetic resonance (CMR), have become more evident and require consideration to reduce diagnostic failure.

Right ventricle

The use of CMR as a diagnostic method in cases of HCM demonstrated that up to one third of patients have right ventricular (RV) hypertrophy (considered if the thickness is ≥8 mm) associated with already known LVH. These patients may also progress with increased total RV mass.[33]

The main region of RV hypertrophy is at the insertion of the RV free wall in the anterior or posterior interventricular septum. In addition to ventricular hypertrophy, other phenotypic changes can be found in the RV, such as the presence of the supraventricular crest (muscle structure adjacent to the interventricular septum). This finding is important due to its location, as it may be erroneously included in the calculation of LV mass, leading to an overestimated total value.[33]

LV apical aneurysms

LV apical aneurysms are another phenotypic HCM change that has increasing diagnostic importance with the greater use of CMR. The use of gadolinium-based contrast and late enhancement (LE) showed that these aneurysms are composed of fibrotic tissue and these changes are associated with increased risks of arrhythmias and SCD, with an important impact on treatment and ICD implantation evaluation. Therefore, it is necessary to investigate these aneurysms to ensure better patient follow-up and diagnostic guidance.[34-36]

Mitral valve apparatus

Changes in the mitral valve apparatus are considered primary phenotypic presentations of HCM regardless of hypertrophy degree and other phenotypic findings, which suggests a more complex pathophysiology of this cardiomyopathy that extends beyond sarcomere-bound protein changes in the myocyte.[33,37,38]

Up to one third of patients with HCM may have elongated mitral leaflets, with an anterior mitral valve leaflet ≥ 30 mm and a posterior mitral valve leaflet ≥17 mm.[33,37,38]

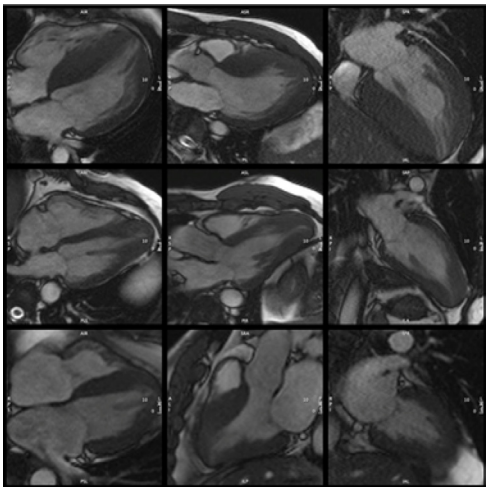

Figure 1 – *Cardiac magnetic resonance imaging scan showing a longitudinal section (4C, 3C, 2C) with major hypertrophic cardiomyopathy (HCM) patterns. (A) HCM with septal predominance; (B) HCM with apical predominance; and (C) HCM with midventricular predominance.*

This leaflet change plays an important role in the mechanisms responsible for LVOT obstruction, and, consequently, for the generated subaortic gradient, thereby also interfering with treatment options and strategies.[33]

Trabeculations

Hypertrabeculation can be defined as a network of prominent trabeculations, particularly those involving the mid-apical region of the inferior and lateral LV wall. Its assessment is visual on short-axis images of the distal two-thirds of the LV and when trabeculations occupy >50% of the myocardial cavity or >50% of the endocardial perimeter.[37]

LV noncompaction, characterized by increased LV trabeculations, shares a genetic basis with some HCM genetic mutations; thus, the two pathologies can coexist and are described as being associations of different sarcomere gene mutations. Therefore, this may be a finding in patients diagnosed with HCM.[39]

Papillary muscle

HCM can also present varied phenotypic disorders involving the papillary muscles. Up to 50% of cases present with a greater number of papillary muscles (three to four). Papillary muscle hypertrophy is also a disorder of HCM, including the presence of LE after the injection of gadolinium-based contrast.[40,41]

Another characteristic, especially on CMR, is anteriorization of the anterolateral papillary muscle. This change is identified on CMR in mid-basal sections of the LV short axis, where more than half of the anterolateral papillary muscle remains above an imaginary line dividing the left ventricular cavity into two equal parts starting from the RV junction in the posterior septum.[37]

Some HCM cases present with direct insertion of the papillary muscle into the mitral valve leaflets with complete or partial absence of the chordae tendineae.[37]

Apical-basal accessory muscle

The apical-basal accessory muscle configures another secondary HCM change and corresponds to a muscle band connected to the ventricular apex that runs longitudinally in the ventricular cavity and close to the anterior septum, reaching the basal septum of the anterior wall. Its presence is first analyzed in section 3C and then reviewed in LV short-axis images.[37]

Myocardial crypts

Congenital abnormalities are related to myocardial fibers and have been described in both healthy and HCM patients (<5%).[26,39,42] The crypts are perpendicular to the LV long axis and must penetrate more than 50% of the compacted myocardium in end diastole and collapse in end systole. Multiple crypts are commonly located mainly in the basal and inferior inferoseptal wall of the LV at the junction with the RV.[43,44]

The differential diagnosis between LV crypts and trabeculations becomes important, with the latter, unlike crypts, being parallel to the endocardial border and not penetrating the compacted myocardium.[43]

Left atrium

The left atrium (LA) is commonly enlarged in cases of HCM; its size is related to increased morbidity and mortality rates since it is a risk marker for cardiovascular events. The cause of atrial enlargement is multifactorial and not yet fully established; however, it may be related to increased ventricular filling pressures and mitral regurgitation as well as mitral valve systolic anterior motion (SAM).[45]

Figure 2 shows some phenotypical findings that can be seen in HCM cases.

Functional changes

Together with the reported heterogeneous phenotypic changes, HCM also involves extremely important functional changes that require evaluation in this population.

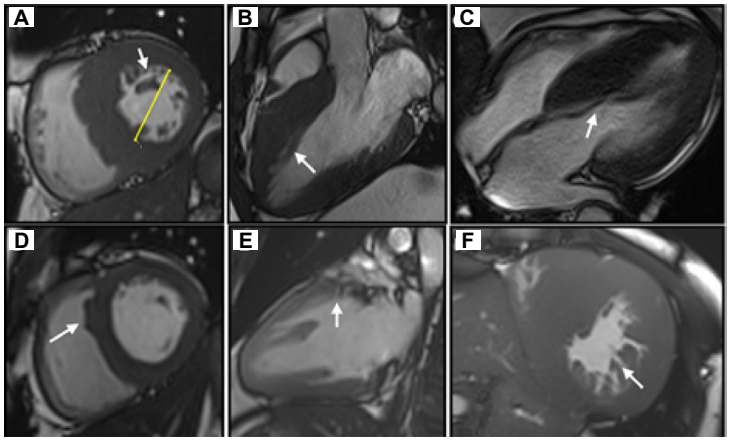

Figure 2 – *Secondary phenotypic findings in hypertrophic cardiomyopathy. (A) Anterior anterolateral papillary muscle; (B) Apical-basal muscle accessory band; (C) Direct insertion of the papillary muscle into the anterior leaflet of the mitral valve; (D) Supraventricular right ventricular crest; (E) Crypts in the left ventricular lower basal wall; and (F) Left ventricular hypertrabeculation.*

Systolic function

Ventricular volumes are often reduced in HCM; therefore, LVEF is often overestimated (hyperkinetic LV). Thus, LVEF is often inadequate for evaluating the disease course and guiding therapy.[5,26] However, advanced HCM (5–10% of cases) is characterized by ventricular remodeling and consequent ventricular wall thinning and cavity dilation. At this point, the LVEF decreases.[46] About 75–100% of end-stage HF patients have extensive LE (≥25% of ventricular mass). These patients are at high risk of HF-related complications of about 10% per year.[26,47]

LVOT obstruction

LVOT obstruction occurs due to a complex anatomical relationship of the cardiac structures involving the basal septum, LVOT, mitral valve apparatus, and papillary muscles.[26,48] This obstruction is present in 70% of the classic phenotypic presentations of HCM and associated with increased cardiovascular risk and worse prognosis.[5,26]

Cine magnetic resonance imaging (cine-MRI) can effectively identify the presence of mitral valve SAM in the long- and short-axis view and signs of increased blood flow velocity in the LVOT.[49] In these cases, an MRI flow velocity mapping sequence (phase-contrast) can be used to estimate the peak velocity and, therefore, the systolic gradient. However, this method has few studies and limited evaluations compared to Doppler echocardiography.[49,50] In addition, it is performed at rest, and up to one-third of patients with HCM show signs of LVOT obstruction only on exertion.[5]

Video 1 below shows a CMRI with SAM.

Diastolic dysfunction

Unlike systolic function, diastolic function is among the first markers of HCM and related to myocardial fiber disarray and fibrosis, even in the absence of hypertrophy, being useful for evaluating cardiomyopathy.[26,51]

This evaluation is well studied and consolidated in echocardiography using several parameters, including mitral transvalvular Doppler.[52]

Role of resonance in HCM

CMR is an important diagnostic method in cardiology practice, with a fundamental role in HCM. CMR provides a detailed characterization of different HCM phenotypes, being used as a diagnostic and prognostic tool.[29] This method allows the formation of tomographic images with high temporal and spatial resolution without the need for iodinated contrast.[53] Cine-MRI sequences (steady-state free precession imaging) enable a detailed analysis of the endocardial and myocardial contour with an accurate analysis of myocardial thickness and function.[29] Moreover, CMR has none of the image acquisition limitations found in echocardiography, such as limited echocardiographic windows and oblique ventricular measurements.[53]

Added to this, CMR allows the identification and quantification of myocardial fibrosis through LE with gadolinium-based contrast, thus identifying patients at high risk of experiencing cardiac events.[29] It also features promising techniques such as T1 mapping, a very useful tool in the differential diagnosis of ventricular hypertrophies and the identification of interstitial myocardial fibrosis and extracellular volume.

Consequently, CMR has garnered an important role in HCM, especially when echocardiographic images are inadequate or suboptimal, and has proven more sensitive than echocardiography for detecting some hypertrophy phenotypes such as apical predominance and secondary phenotypic changes. Therefore, CMR should be routinely used in such patients.[54,55]

Table 1 shows the main hypertrophy patterns found in HCM cases.

Late enhancement

Through a noninvasive evaluation, LE CMR has a unique ability to identify and quantify areas of fibrosis in the myocardium, thereby providing important diagnostic and prognostic information.[55]

The histopathology of HCM-related fibrosis is diffusely present in the myocardium and constitutes a substrate for tachyarrhythmias and SCD.[47,56]

LE pattern and distribution in HCM

The presence of LE in HCM has various distributions and location patterns. However, it is not commonly related to a specific coronary territory.[45] It frequently presents a multifocal, heterogeneous, and mesocardial enhancement pattern in about 30% of patients, but transmural LE can also be found.[55,57] The most common LE sites are the interventricular septum and the LV free wall, occurring in more than 30% of patients. However, focal enhancement can also be found in the free wall, RV insertion, interventricular septum, and apex.

Other structures outside the LV may also present LE areas, including the RV and papillary muscles.[58] There is a correlation between myocardial thickness and the presence of LE, according to which the greater the LV hypertrophy, the greater the chance of LE.[58-60]

The literature also shows a consistent relationship between LVEF and the presence of LE. An extensive LE area is observed in patients with an LVEF < 50%; on the other hand, patients with hyperdynamic systolic function have comparatively smaller LE areas.[58-60]

Patients with LVEF at the lower limit of normal present with LE and ventricular volumes closer to those of end-stage patients, suggesting the need for closer clinical follow-up and serial imaging.[56]

LE quantification

Different methods and protocols quantify the LE area in HCM. The most widely used technique is based on semiautomatic algorithms that identify areas with increased signal intensity corresponding to regions with LE. A region of interest is selected in the annular myocardium and a gray scale is applied, with a standard deviation (SD) above the signal intensity of the signaled region of interest and selecting the areas corresponding to the enhancement. In some studies, the correlation between LE quantification and 6SD showed a greater correlation with the visual analysis of the area of fibrosis presented, proven as more reproducible in practice.[33,61]

An important study published in 2014 by Chan et al. demonstrated that fibrosis ≥ 15% in relation to total LV mass is useful for identifying patients with a preserved LVEF at risk of progression to HF and SCD.[62,63]

Risk stratification for SCD by LE

Risk stratification for SCD in HCM patients has been studied for a long time and is extremely important. Today, several risk scores and guidelines aid the appropriate selection of patients who are indicated for ICD as primary prevention, a therapy that is the main determinant that reduces HCM-related mortality. Major factors in this stratification include a family history of SCD, unexplained syncope, non-sustained ventricular tachycardia, end-stage HCM (with systolic dysfunction), apical aneurysm on echocardiography or CMR, and the presence of LE in more than 15% of the ventricular mass. Therefore, as LE is considered a major risk factor for SCD, it must be detected and quantified in these patients (Figure 3).[29,63-65]

T1 mapping

Histologically, HCM fibrosis is diffuse and global and not fully recognized on LE. In this case, T1 mapping is a new and promising tool that can analyze the entire extracellular content and thus provide a better evaluation of this fibrosis pattern.[66,67]

The T1 mapping sequence, which measures T1 longitudinal relaxation time, is used to identify the extent of increased extracellular content in patients with HCM and may be superior to the consolidated LE technique due to its ability to achieve the early detection of fibrosis.[68,69]

The native T1 mapping and extracellular volume fraction, which are high at times in patients with HCM, can be used in the early stages of HCM for the early detection of interstitial fibrosis and aid in the differential diagnosis of hypertrophies.

Tissue tracking analysis (strain)

New CMR techniques have emerged for the evaluation of myocardial deformation, including tissue tracking (TT), a noninvasive post-processing technique used to evaluate myocardial strain.[70,71]

In HCM, fibrosis and hypertrophy contribute to mechanical abnormalities of the myocardium. Wall stress associated with relative endocardial ischemia and fibrosis help decrease strain values. Therefore, strain – mainly global longitudinal strain – may be useful in differentiating between hypertrophy

Table 1 - CMR indications in HCM defined by the American Heart Association/ American College of Cardiology, 2020.

Recommendation	Evidence level	Recommendation
I	B-NR	In patients with suspected HCM and inconclusive echocardiography findings, CMR is indicated for diagnostic clarification
I	B-NR	In patients with LVH, when alternative diagnoses such as infiltrative storage diseases and athlete's heart are considered, CMR is helpful
I	B-NR	In patients with HCM who are not identified as at high risk of cardiovascular events or when the decision for ICD remains uncertain after clinical evaluation (including personal assessment/family history/echocardiogram/electrocardiogram), CMR is beneficial to assess maximum ventricular thickness, LVEF, apical aneurysms, and extension of the area of myocardial fibrosis by LE
1	B-NR	In patients with obstructive HCM, when the anatomic mechanism of obstruction is inconclusive on echocardiography, CMR is indicated to assess septal reduction indication and planning
2b	C-EO	In patients with HCM, repeat CMR with periodic contrast (after 3–5 years) to re-stratify cardiovascular risk may be considered to evaluate LE and other morphologic changes, including LVEF, apical aneurysms, and LVH

Source: Ommen et al.[4] NR: nonrandomized; CMR: cardiac magnetic resonance; EO: expert opinion; HCM: hypertrophic cardiomyopathy; ICD: implantable cardioverter defibrillator; LE: late enhancement; LVEF: left ventricular ejection fraction; LVH: left ventricular hypertrophy.

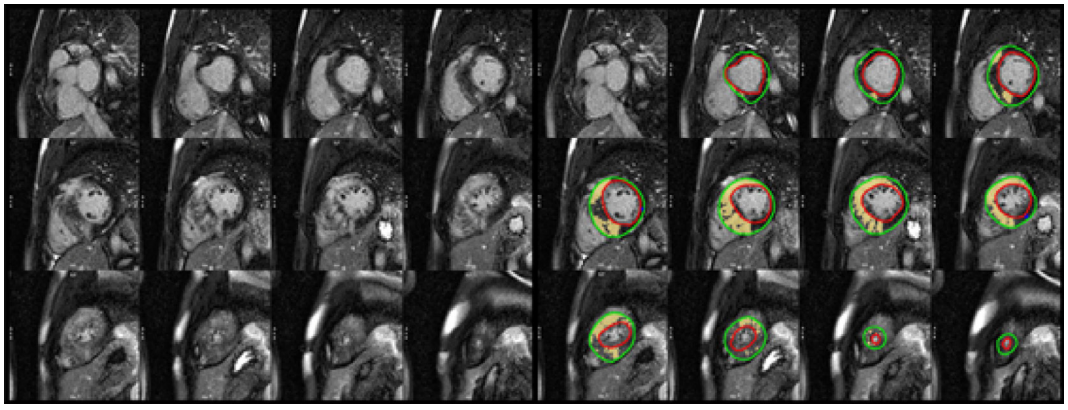

Figure 3 – *Late enhancement quantification in a patient with hypertrophic cardiomyopathy using a semiautomatic algorithm and showing extensive myocardial fibrosis (±30% of the myocardial mass).*

types (pathological or physiological). Global longitudinal strain was also indirectly proportional to the fibrosis values, being a possible predictor of arrhythmic events. The endocardial dysfunction noted in HCM leads to a reduced radial strain. The literature showed a TT analysis with reduced longitudinal, radial, and circumferential strain values in patients with HCM versus the control group (Figure 4).[70,71]

Videos 2 and 3 show a tissue-tracking analysis using CMRI and 3D reconstruction.

Differential diagnosis

LVH is a heterogeneous myocardial involvement with multifactorial causes related to several heart diseases that can be physiological as in athletes. Therefore, it is necessary to emphasize the importance of the differential diagnosis and diagnostic complexity of hypertrophy.

Infiltrative diseases

Although HCM is the main cause of unexplained LVH in adults, other infiltrative diseases such as amyloidosis, Fabry disease, and Danon disease have increased myocardial thickness as a phenotypic presentation[37] and enter the differential diagnosis of hypertrophic phenotypes. Although morphological findings on CMR may suggest the etiology of ventricular hypertrophy and allow the differential diagnosis between infiltrative diseases and HCM, the hypertrophy pattern is not pathognomonic.[23] On the other hand, although not definitive, LE may provide stronger differentiation data. Amyloidosis presents a characteristic LE pattern represented by subendocardial and subsequent transmural enhancement with difficult annulling due to extracellular glycoprotein deposits.[55] T1 mapping, as already mentioned, can be an extremely useful tool in this differentiation since it allows the quantification of native myocardial T1. Native T1 values are higher in amyloidosis than in HCM but reduced in Fabry disease.[55] Analysis of the data obtained by CMR associating morphological and functional criteria, RT, and T1 mapping are fundamental to a more accurate differentiation.

Noncompaction myocardium

The higher spatial resolution of CMR tests showed that cases with a previous diagnosis of apical HCM presented significantly increased ventricular trabeculations rather than hypertrophy and were reclassified to noncompaction myocardium. These pathologies have a common genetic basis and may be associated.[72,73]

Hypertensive heart disease

Patients exposed to arterial hypertension for the long term that is not adequately treated are reasonably likely to develop symmetrical LVH between the septum and the LV free wall (concentric hypertrophy). However, hypertensive heart disease is rarely associated with LVOT obstruction[8] or the phenotypic findings described herein.

Thus, CMR may be important for detecting myocardial thickness changes after antihypertensive drug treatment, when hypertrophy regression favors the diagnosis of hypertensive heart disease.[29]

Athlete's heart

In clinical practice, the distinction between athlete's physiological hypertrophy and pathological hypertrophy is a diagnostic challenge of important clinical relevance, with HCM causing one-third of SCD events in young competitive athletes.[74]

In this case, CMR can be useful for hypertrophy follow-up after physical deconditioning (16–18 months).[74] In the athlete's physiological hypertrophy, a regression of at least 2 mm in myocardial thickness is expected, while in HCM, the thickness is expected to remain the same. Another aspect is that LE is not expected to occur in patients with athlete's heart. LE is a factor that corroborates the diagnosis of HCM.[75]

The athlete's physiological hypertrophy does not usually progress with very increased thicknesses despite having similar ventricular mass values to those of other pathological hypertrophies (e.g., HCM, hypertensive heart disease) in addition to increased ventricular volumes and a decreased LVEF.[74]

Asymmetry is also a debatable differential diagnosis factor that affects up to 6% of patients with HCM and concentric hypertrophy.[74] Maron et al. showed that 43% of athletes with SCD due to HCM had a normal septum/free wall ratio on autopsy.[76]

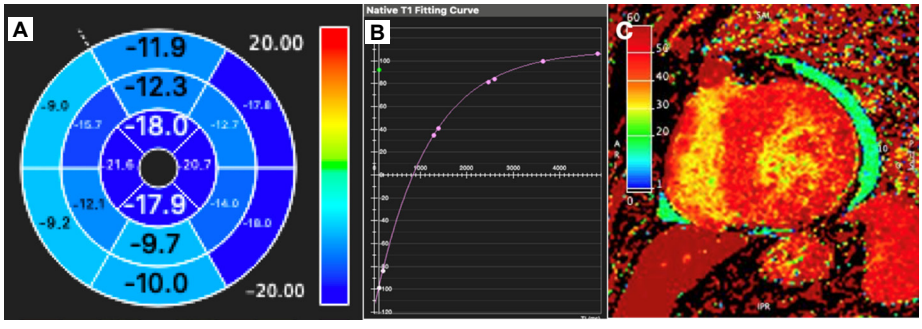

Figure 4 – *(A) Bull's eye analysis of global longitudinal strain by tissue tracking in a patient with hypertrophic cardiomyopathy; (B) Native T1 mapping analysis showing increased values in relation to normal; and (C) T1 parametric mapping.*

Outlook

CMR techniques have showed remarkable advancement and evolution in recent years in addition to a growing role in the diagnostic and prognostic evaluation of the most diverse cardiomyopathies.

However, techniques such as TT for analyzing the myocardial infarction strain have not yet been fully applied in clinical practice and are currently used mainly for scientific research. Another technique with promising prospects is the 4D-flow analysis. This innovative technique provides a visual analysis of the blood flow, velocity, and pattern, allowing the choice of the correct plane to analyze the appropriate measurements with advantages in relation to the two-dimensional analysis performed by the phase-contrast technique already consolidated in resonance testing.[77]

Authors' contributions

Review conception and design: Valério RS, Uellendahl, M.; manuscript writing: Valério RS, Uellendahl M.; critical review of the manuscript for intellectual content: Uellendahl M, Bittencourt M.

Conflict of interest

The authors have declared that they have no conflict of interest.

References

1. Teare D. Asymmetrical hypertrophy of the heart in young adults. Br Hear J. 1958;20:1-8. doi: https://doi.org/10.1136/hrt.20.1.1
2. Olivotto I, Maron MS, Adabag AS, Casey SA, Vargiu D, Link MS, et al. Gender-related differences in the clinical presentation and outcome of hypertrophic cardiomyopathy. J Am Coll Cardiol. 2005;46:480-7. doi: https://doi.org/10.1016/j.jacc.2005.04.043
3. Maron BJ, McKenna WJ, Danielson GK, Kappenberger LJ, Kuhn HJ, Seidman CE, et al.; Task Force on Clinical Expert Consensus Documents. American College of Cardiology; Committee for Practice Guidelines. European Society of Cardiology. American College of Cardiology/European Society of Cardiology clinical expert consensus document on hypertrophic cardiomyopathy. A report of the American College of Cardiology Foundation Task Force on Clinical Expert Consensus Documents and the European Society of Cardiology Committee for Practice Guidelines. J Am Coll Cardiol. 2003;42(9):1687-713. doi: https://doi.org/10.1016/s0735-1097(03)00941-0
4. Ommen SR, Mital S, Burke MA, Day SM, Deswal A, Elliott P, et al. 2020 AHA/ACC Guideline for the Diagnosis and Treatment of Patients With Hypertrophic Cardiomyopathy: A Report of the American College of Cardiology/American Heart Association Joint Committee on Clinical Practice Guidelines. J Am Coll Cardiol. 2020;76(25):e159-e240. doi: https://doi.org/10.1016/j.jacc.2020.08.045
5. Authors/Task Force members, Elliott PM, Anastasakis A, Borger MA, Borggrefe M, Cecchi F, Charron P, et al. 2014 ESC Guidelines on diagnosis and management of hypertrophic cardiomyopathy: the Task Force for the Diagnosis and Management of Hypertrophic Cardiomyopathy of the European Society of Cardiology (ESC). Eur Heart J. 2014;35(39):2733-79. doi: https://doi.org/10.1093/eurheartj/ehu284
6. Maron BJ, Ommen SR, Semsarian C, Spirito P, Olivotto I, Maron MS. Hypertrophic cardiomyopathy: present and future, with translation into contemporary cardiovascular medicine. J Am Coll Cardiol. 2014;64(1):83-99. doi: https://doi.org/10.1016/j.jacc.2014.05.003. Erratum in: J Am Coll Cardiol. 2014;64(11):1188.
7. Maron MS, Maron BJ. Clinical Impact of Contemporary Cardiovascular Magnetic Resonance Imaging in Hypertrophic Cardiomyopathy. Circulation. 2015;132(4):292-8. doi: https://doi.org/10.1161/CIRCULATIONAHA.114.014283
8. Maron MS, Maron BJ, Harrigan C, Buros J, Gibson CM, Olivotto I, et al. Hypertrophic cardiomyopathy phenotype revisited after 50 years with cardiovascular magnetic resonance. J Am Coll Cardiol. 2009;54(3):220-8. doi: https://doi.org/10.1016/j.jacc.2009.05.006
9. Maron BJ, Rowin EJ, Casey SA, Link MS, Lesser JR, Chan RH, et al. Hypertrophic Cardiomyopathy in Adulthood Associated With Low Cardiovascular Mortality With Contemporary Management Strategies. J Am Coll Cardiol. 2015;65(18):1915-28. doi: https://doi.org/10.1016/j.jacc.2015.02.061
10. Maron BJ, Maron MS, Wigle ED, Braunwald E. The 50-year history, controversy, and clinical implications of left ventricular outflow tract obstruction in hypertrophic cardiomyopathy from idiopathic hypertrophic subaortic stenosis to hypertrophic cardiomyopathy: from idiopathic hypertrophic subaortic stenosis to hypertrophic cardiomyopathy. J Am Coll Cardiol. 2009;54(3):191-200. doi: https://doi.org/10.1016/j.jacc.2008.11.069
11. Hughes SE. The pathology of hypertrophic cardiomyopathy. Histopathology. 2004;44(5):412-27. doi: https://doi.org/10.1111/j.1365-2559.2004.01835.x
12. Cecchi F, Olivotto I, Montereggi A, Santoro G, Dolara A, Maron BJ. Hypertrophic cardiomyopathy in Tuscany: clinical course and outcome in an unselected regional population. J Am Coll Cardiol. 1995;26(6):1529-36. doi: https://doi.org/10.1016/0735-1097(95)00353-3
13. Maron BJ, Casey SA, Poliac LC, Gohman TE, Almquist AK, Aeppli DM. Clinical course of hypertrophic cardiomyopathy in a regional United States cohort. JAMA. 1999;281(7):650-5. doi: https://doi.org/10.1001/jama.281.7.650. Erratum in: JAMA 1999;281(24):2288.
14. Olivotto I, Cecchi F, Casey SA, Dolara A, Traverse JH, Maron BJ. Impact of atrial fibrillation on the clinical course of hypertrophic cardiomyopathy. Circulation. 2001;104(21):2517-24. doi: https://doi.org/10.1161/hc4601.097997
15. Maron BJ. Hypertrophic cardiomyopathy: a systematic review. JAMA. 2002;287(10):1308-20. doi: https://doi.org/10.1001/jama.287.10.1308
16. Lopes LR, Zekavati A, Syrris P, Hubank M, Giambartolomei C, Dalageorgou C, et al.; Uk10k Consortium, Plagnol V, Elliott PM. Genetic complexity in hypertrophic cardiomyopathy revealed by high-throughput sequencing. J Med Genet. 2013;50(4):228-39. doi: https://doi.org/10.1136/jmedgenet-2012-101270
17. Seidman JG, Seidman C. The genetic basis for cardiomyopathy: from mutation identification to mechanistic paradigms. Cell. 2001;104(4):557-67. doi: https://doi.org/10.1016/s0092-8674(01)00242-2
18. Ackerman MJ, VanDriest SL, Ommen SR, Will ML, Nishimura RA, Tajik AJ, et al. Prevalence and age-dependence of malignant mutations in the beta-myosin heavy chain and troponin T genes in hypertrophic cardiomyopathy: a comprehensive outpatient perspective. J Am Coll Cardiol. 2002;39(12):2042-8. doi: https://doi.org/10.1016/s0735-1097(02)01900-9
19. Watkins H, Thierfelder L, Hwang DS, McKenna W, Seidman JG, Seidman CE. Sporadic hypertrophic cardiomyopathy due to de novo myosin mutations. J Clin Invest. 1992;90(5):1666-71. doi: https://doi.org/10.1172/JCI116038

20. Maron BJ, Niimura H, Casey SA, Soper MK, Wright GB, Seidman JG, et al. Development of left ventricular hypertrophy in adults in hypertrophic cardiomyopathy caused by cardiac myosin-binding protein C gene mutations. J Am Coll Cardiol. 2001;38(2):315-21. doi: https://doi.org/10.1016/s0735-1097(01)01386-9

21. Wheeler M, Pavlovic A, DeGoma E, Salisbury H, Brown C, Ashley EA. A new era in clinical genetic testing for hypertrophic cardiomyopathy. J Cardiovasc Transl Res. 2009;2(4):381-91. doi: https://doi.org/10.1007/s12265-009-9139-0

22. Bos JM, Towbin JA, Ackerman MJ. Diagnostic, prognostic, and therapeutic implications of genetic testing for hypertrophic cardiomyopathy. J Am Coll Cardiol. 2009;54(3):201-11. doi: https://doi.org/10.1016/j.jacc.2009.02.075

23. Ho CY. Genetics and clinical destiny: improving care in hypertrophic cardiomyopathy. Circulation. 2010;122(23):2430-40; discussion 2440. doi: https://doi.org/10.1161/CIRCULATIONAHA.110.978924

24. Binder J, Ommen SR, Gersh BJ, Van Driest SL, Tajik AJ, Nishimura RA, et al. Echocardiography-guided genetic testing in hypertrophic cardiomyopathy: septal morphological features predict the presence of myofilament mutations. Mayo Clin Proc. 2006;81(4):459-67. doi: https://doi.org/10.4065/81.4.459

25. Watkins H, Rosenzweig A, Hwang DS, Levi T, McKenna W, Seidman CE, et al. Characteristics and prognostic implications of myosin missense mutations in familial hypertrophic cardiomyopathy. N Engl J Med. 1992;326(17):1108-14. doi: https://doi.org/10.1056/NEJM199204233261703

26. Bogaert J, Olivotto I. MR Imaging in Hypertrophic Cardiomyopathy: From Magnet to Bedside. Radiology. 2014;273(2):329-48. doi: https://doi.org/10.1148/radiol.14131626

27. Baxi AJ, Restrepo CS, Vargas D, Marmol-Velez A, Ocazionez D, Murillo H. Hypertrophic Cardiomyopathy from A to Z: Genetics, Pathophysiology, Imaging, and Management. Radiographics. 2016;36(2):335-54. doi: https://doi.org/10.1148/rg.2016150137

28. Maron BJ, Roberts WC, Arad M, Haas TS, Spirito P, Wright GB, et al. Clinical outcome and phenotypic expression in LAMP2 cardiomyopathy. JAMA. 2009;301(12):1253-9. doi: https://doi.org/10.1001/jama.2009.371

29. Maron MS. Clinical utility of cardiovascular magnetic resonance in hypertrophic cardiomyopathy. J Cardiovasc Magn Reson. 2012;14(1):13. doi: https://doi.org/10.1186/1532-429X-14-13

30. Olivotto I, Maron MS, Autore C, Lesser JR, Rega L, Casolo G, et al. Assessment and significance of left ventricular mass by cardiovascular magnetic resonance in hypertrophic cardiomyopathy. J Am Coll Cardiol. 2008;52(7):559-66. doi: https://doi.org/10.1016/j.jacc.2008.04.047

31. Maron MS, Finley JJ, Bos JM, Hauser TH, Manning WJ, Haas TS, et al. Prevalence, clinical significance, and natural history of left ventricular apical aneurysms in hypertrophic cardiomyopathy. Circulation. 2008;118(15):1541-9. doi: https://doi.org/10.1161/CIRCULATIONAHA.108.781401

32. Moon JC, Fisher NG, McKenna WJ, Pennell DJ. Detection of apical hypertrophic cardiomyopathy by cardiovascular magnetic resonance in patients with non-diagnostic echocardiography. Heart. 2004;90(6):645-9. doi: https://doi.org/10.1136/hrt.2003.014969

33. Maron MS. Clinical utility of cardiovascular magnetic resonance in hypertrophic cardiomyopathy. J Cardiovasc Magn Reson. 2012;14(1):13. doi: https://doi.org/10.1186/1532-429X-14-13

34. Shenoy C, Maron MS. Hypertrophic cardiomyopathy with left ventricular apical aneurysm in brothers. Am J Cardiol. 2011;108(4):612-3. doi: https://doi.org/10.1016/j.amjcard.2011.03.094

35. Lim KK, Maron BJ, Knight BP. Successful catheter ablation of hemodynamically unstable monomorphic ventricular tachycardia in a patient with hypertrophic cardiomyopathy and apical aneurysm. J Cardiovasc Electrophysiol. 2009;20(4):445-7. doi: https://doi.org/10.1111/j.1540-8167.2008.01366.x

36. Maron MS, Olivotto I, Harrigan C, Appelbaum E, Gibson CM, Lesser JR, et al. Mitral valve abnormalities identified by cardiovascular magnetic resonance represent a primary phenotypic expression of hypertrophic cardiomyopathy. Circulation. 2011;124(1):40-7. doi: https://doi.org/10.1161/CIRCULATIONAHA.110.985812

37. Urbano-Moral JA, Gutierrez-Garcia-Moreno L, Rodriguez-Palomares JF, Matabuena-Gomez-Limon J, Niella N, Maldonado G, et al. Structural abnormalities in hypertrophic cardiomyopathy beyond left ventricular hypertrophy by multimodality imaging evaluation. Echocardiography. 2019;36(7):1241-52. doi: https://doi.org/10.1111/echo.14393

38. Maron MS, Olivotto I, Harrigan C, Appelbaum E, Gibson CM, Lesser JR, et al. Mitral valve abnormalities identified by cardiovascular magnetic resonance represent a primary phenotypic expression of hypertrophic cardiomyopathy. Circulation. 2011;124(1):40-7. doi: https://doi.org/10.1161/CIRCULATIONAHA.110.985812

39. Germans T, Wilde AA, Dijkmans PA, Chai W, Kamp O, Pinto YM, et al. Structural abnormalities of the inferoseptal left ventricular wall detected by cardiac magnetic resonance imaging in carriers of hypertrophic cardiomyopathy mutations. J Am Coll Cardiol. 2006;48(12):2518-23. doi: https://doi.org/10.1016/j.jacc.2006.08.036

40. Harrigan CJ, Appelbaum E, Maron BJ, Buros JL, Gibson CM, Lesser JR, et al. Significance of papillary muscle abnormalities identified by cardiovascular magnetic resonance in hypertrophic cardiomyopathy. Am J Cardiol. 2008;101(5):668-73. doi: https://doi.org/10.1016/j.amjcard.2007.10.032

41. Kwon DH, Setser RM, Thamilarasan M, Popovic ZV, Smedira NG, Schoenhagen P, et al. Abnormal papillary muscle morphology is independently associated with increased left ventricular outflow tract obstruction in hypertrophic cardiomyopathy. Heart. 2008;94(10):1295-301. doi: https://doi.org/10.1136/hrt.2007.118018

42. Deva DP, Williams LK, Care M, Siminovitch KA, Moshonov H, Wintersperger BJ, et al. Deep basal inferoseptal crypts occur more commonly in patients with hypertrophic cardiomyopathy due to disease-causing myofilament mutations. Radiology. 2013;269(1):68-76. doi: https://doi.org/10.1148/radiol.13122344

43. Maron MS, Rowin EJ, Lin D, Appelbaum E, Chan RH, Gibson CM, et al. Prevalence and clinical profile of myocardial crypts in hypertrophic cardiomyopathy. Circ Cardiovasc Imaging. 2012;5(4):441-7. doi: https://doi.org/10.1161/CIRCIMAGING.112.972760

44. Efthimiadis GK, Pagourelias ED, Hadjimiltiades S, Meditskou S, Karvounis H, et al. Feasibility and significance of preclinical diagnosis in hypertrophic cardiomyopathy. Cardiol Rev. 2015;23(6):297-302. doi: https://doi.org/10.1097/CRD.0000000000000076

45. Soler R, Méndez C, Rodríguez E, Barriales R, Ochoa JP, Monserrat L. Phenotypes of hypertrophic cardiomyopathy. An illustrative review of MRI findings. Insights Imaging. 2018;9(6):1007-20. doi: https://doi.org/10.1007/s13244-018-0656-8

46. Yamada T, Kay GN. Anatomical Consideration in Catheter Ablation of Idiopathic Ventricular Arrhythmias. Arrhythm Electrophysiol Rev. 2016;5(3):203-9. doi: https://doi.org/10.15420/aer.2016:31:2

47. Olivotto I, Cecchi F, Poggesi C, Yacoub MH. Patterns of disease progression in hypertrophic cardiomyopathy: an individualized approach to clinical staging. Circ Heart Fail. 2012;5(4):535-46. doi: https://doi.org/10.1161/CIRCHEARTFAILURE.112.967026

48. Patel P, Dhillon A, Popovic ZB, Smedira NG, Rizzo J, Thamilarasan M, et al. Left Ventricular Outflow Tract Obstruction in Hypertrophic Cardiomyopathy Patients Without Severe Septal Hypertrophy: Implications of Mitral Valve and Papillary Muscle Abnormalities Assessed Using Cardiac Magnetic Resonance and Echocardiography. Circ

Cardiovasc Imaging. 2015;8(7):e003132. doi: https://doi.org/10.1161/CIRCIMAGING.115.003132

49. Schulz-Menger J, Abdel-Aty H, Busjahn A, Wassmuth R, Pilz B, Dietz R, et al. Left ventricular outflow tract planimetry by cardiovascular magnetic resonance differentiates obstructive from non-obstructive hypertrophic cardiomyopathy. J Cardiovasc Magn Reson. 2006;8(5):741-6. doi: https://doi.org/10.1080/10976640600737383

50. Nagueh SF, Bierig SM, Budoff MJ, Desai M, Dilsizian V, Eidem B, et al; American Society of Echocardiography; American Society of Nuclear Cardiology; Society for Cardiovascular Magnetic Resonance; Society of Cardiovascular Computed Tomography. American Society of Echocardiography clinical recommendations for multimodality cardiovascular imaging of patients with hypertrophic cardiomyopathy: Endorsed by the American Society of Nuclear Cardiology, Society for Cardiovascular Magnetic Resonance, and Society of Cardiovascular Computed Tomography. J Am Soc Echocardiogr. 2011;24(5):473-98. doi: https://doi.org/10.1016/j.echo.2011.03.006

51. Tsang TS, Barnes ME, Gersh BJ, Bailey KR, Seward JB. Left atrial volume as a morphophysiologic expression of left ventricular diastolic dysfunction and relation to cardiovascular risk burden. Am J Cardiol. 2002;90(12):1284-9. doi: https://doi.org/10.1016/s0002-9149(02)02864-3

52. Wu V, Chyou JY, Chung S, Bhagavatula S, Axel L. Evaluation of diastolic function by three-dimensional volume tracking of the mitral annulus with cardiovascular magnetic resonance: comparison with tissue Doppler imaging. J Cardiovasc Magn Reson. 2014;16(1):71. doi: https://doi.org/10.1186/s12968-014-0071-3

53. Pennell DJ. Cardiovascular magnetic resonance. Circulation. 2010;121(5):692-705. doi: https://doi.org/10.1161/CIRCULATIONAHA.108.811547

54. Oliveira DC, Assunção FB, Santos AA, Nacif MS. Cardiac Magnetic Resonance and Computed Tomography in Hypertrophic Cardiomyopathy: an Update. Arq Bras Cardiol. 2016;107(2):163-72. doi: https://doi.org/10.5935/abc.20160081

55. Brenes JC, Doltra A, Prat S. Cardiac magnetic resonance imaging in the evaluation of patients with hypertrophic cardiomyopathy. Glob Cardiol Sci Pract. 2018;2018(3):22. doi: https://doi.org/10.21542/gcsp.2018.22

56. Olivotto I, Maron BJ, Appelbaum E, Harrigan CJ, Salton C, Gibson CM, et al. Spectrum and clinical significance of systolic function and myocardial fibrosis assessed by cardiovascular magnetic resonance in hypertrophic cardiomyopathy. Am J Cardiol. 2010;106(2):261-7. doi: https://doi.org/10.1016/j.amjcard.2010.03.020

57. Maron MS, Appelbaum E, Harrigan CJ, Buros J, Gibson CM, Hanna C, et al. Clinical profile and significance of delayed enhancement in hypertrophic cardiomyopathy. Circ Heart Fail. 2008;1(3):184-91. doi: https://doi.org/10.1161/CIRCHEARTFAILURE.108.768119

58. Maron MS, Olivotto I, Maron BJ, Prasad SK, Cecchi F, Udelson JE, et al. The case for myocardial ischemia in hypertrophic cardiomyopathy. J Am Coll Cardiol. 2009;54(9):866-75. doi: https://doi.org/10.1016/j.jacc.2009.04.072

59. Moon JC, McKenna WJ, McCrohon JA, Elliott PM, Smith GC, Pennell DJ. Toward clinical risk assessment in hypertrophic cardiomyopathy with gadolinium cardiovascular magnetic resonance. J Am Coll Cardiol. 2003;41(9):1561-7. doi: https://doi.org/10.1016/s0735-1097(03)00189-x

60. Choudhury L, Mahrholdt H, Wagner A, Choi KM, Elliott MD, Klocke FJ, et al. Myocardial scarring in asymptomatic or mildly symptomatic patients with hypertrophic cardiomyopathy. J Am Coll Cardiol. 2002;40(12):2156-64. doi: https://doi.org/10.1016/s0735-1097(02)02602-5

61. Maron MS, Appelbaum E, Harrigan CJ, Buros J, Gibson CM, Hanna C, et al. Clinical profile and significance of delayed enhancement in hypertrophic cardiomyopathy. Circ Heart Fail. 2008;1(3):184-91. doi: https://doi.org/10.1161/CIRCHEARTFAILURE.108.768119

62. Weng Z, Yao J, Chan RH, He J, Yang X, Zhou Y, et al. Prognostic Value of LGE-CMR in HCM: A Meta-Analysis. JACC Cardiovasc Imaging. 2016;9(12):1392-402. doi: https://doi.org/10.1016/j.jcmg.2016.02.031

63. Chan RH, Maron BJ, Olivotto I, Pencina MJ, Assenza GE, Haas T, et al. Prognostic value of quantitative contrast-enhanced cardiovascular magnetic resonance for the evaluation of sudden death risk in patients with hypertrophic cardiomyopathy. Circulation. 2014;130(6):484-95. doi: https://doi.org/10.1161/CIRCULATIONAHA.113.007094

64. Maron MS, Rowin EJ, Wessler BS, Mooney PJ, Fatima A, Patel P, et al. Enhanced American College of Cardiology/American Heart Association Strategy for Prevention of Sudden Cardiac Death in High-Risk Patients With Hypertrophic Cardiomyopathy. JAMA Cardiol. 2019;4(7):644-57. doi: https://doi.org/10.1001/jamacardio.2019.1391

65. Maron BJ, Rowin EJ, Maron MS. Paradigm of Sudden Death Prevention in Hypertrophic Cardiomyopathy. Circ Res. 2019;125(4):370-8. doi: https://doi.org/10.1161/CIRCRESAHA.119.315159

66. Puntmann VO, Voigt T, Chen Z, Mayr M, Karim R, Rhode K, et al. Native T1 mapping in differentiation of normal myocardium from diffuse disease in hypertrophic and dilated cardiomyopathy. JACC Cardiovasc Imaging. 2013;6(4):475-84. doi: https://doi.org/10.1016/j.jcmg.2012.08.019

67. Dass S, Suttie JJ, Piechnik SK, Ferreira VM, Holloway CJ, Banerjee R, et al. Myocardial tissue characterization using magnetic resonance noncontrast t1 mapping in hypertrophic and dilated cardiomyopathy. Circ Cardiovasc Imaging. 2012;5(6):726-33. doi: https://doi.org/10.1161/CIRCIMAGING.112.976738

68. Sado DM, White SK, Piechnik SK, Banypersad SM, Treibel T, Captur G, et al. Identification and assessment of Anderson-Fabry disease by cardiovascular magnetic resonance noncontrast myocardial T1 mapping. Circ Cardiovasc Imaging. 2013;6(3):392-8. doi: https://doi.org/10.1161/CIRCIMAGING.112.000070

69. Sado DM, Flett AS, Banypersad SM, White SK, Maestrini V, Quarta G, et al. Cardiovascular magnetic resonance measurement of myocardial extracellular volume in health and disease. Heart. 2012;98(19):1436-41. doi: https://doi.org/10.1136/heartjnl-2012-302346

70. Jung HN, Kim SM, Lee JH, Kim Y, Lee SC, Jeon ES, et al. Comparison of tissue tracking assessment by cardiovascular magnetic resonance for cardiac amyloidosis and hypertrophic cardiomyopathy. Acta Radiol. 2020;61(7):885-93. doi: https://doi.org/10.1177/0284185119883714

71. Neisius U, Myerson L, Fahmy AS, Nakamori S, El-Rewaidy H, Joshi G, et al. Cardiovascular magnetic resonance feature tracking strain analysis for discrimination between hypertensive heart disease and hypertrophic cardiomyopathy. PLoS One. 2019;14(8):e0221061. doi: https://doi.org/10.1371/journal.pone.0221061

72. Kelley-Hedgepeth A, Towbin JA, Maron MS. Images in cardiovascular medicine. Overlapping phenotypes: left ventricular noncompaction and hypertrophic cardiomyopathy. Circulation. 2009;119(23):e588-9. doi: https://doi.org/10.1161/CIRCULATIONAHA.108.829564

73. Spirito P, Autore C. Apical hypertrophic cardiomyopathy or left ventricular non-compaction? A difficult differential diagnosis. Eur Heart J. 2007;28(16):1923-4. doi: https://doi.org/10.1093/eurheartj/ehm266

74. Petersen SE, Selvanayagam JB, Francis JM, Myerson SG, Wiesmann F, Robson MD, et al. Differentiation of athlete's heart from pathological forms of cardiac hypertrophy by means of geometric indices derived from cardiovascular magnetic resonance. J Cardiovasc Magn Reson. 2005;7(3):551-8. doi: https://doi.org/10.1081/jcmr-200060631

75. Maron BJ. Distinguishing hypertrophic cardiomyopathy from athlete's heart physiological remodelling: clinical significance, diagnostic strategies and implications for preparticipation screening. Br J Sports Med. 2009;43(9):649-56. doi: https://doi.org/10.1136/bjsm.2008.054726

76. Maron BJ, Roberts WC, McAllister HA, Rosing DR, Epstein SE. Sudden death in young athletes. Circulation. 1980;62(2):218-29. doi: https://doi.org/10.1161/01.cir.62.2.218

77. Nordmeyer S, Riesenkampff E, Messroghli D, Kropf S, Nordmeyer J, Berger F, et al. Four-dimensional velocity-encoded magnetic resonance imaging improves blood flow quantification in patients with complex accelerated flow. J Magn Reson Imaging. 2013;37(1):208-16. doi: https://doi.org/10.1002/jmri.23793

Review Article

My Approach to Assess Diastolic Function in the Presence of Atrial Fibrillation?

Como eu Faço a Análise da Função Diastólica na Presença de Fibrilação Atrial

Antonio Amador Calvilho Júnior[1,2], João Moron Saes Braga[3], Jorge Eduardo Assef[1], Andrea de Andrade Vilela[1,4]

[1]Dante Pazzanese Institute of Cardiology, São Paulo, SP, Brazil. [2]Sorocaba Hospital Complex, São Paulo, SP, Brazil. [3]Marília School of Medicine, São Paulo, SP, Brazil. [4]Fleury Group, São Paulo, SP, Brazil.

Introduction

Atrial fibrillation (AF) is a prevalent arrhythmia that can occur alone or in combination with other clinical conditions. Its onset interferes both in common diagnostic algorithms and in their respective protocol procedures. In diastolic function assessments by echocardiography, it drastically changes the analysis sequence.[1] This relationship becomes even more complex because diastolic dysfunction is onc cause of non-valvular AF.[2]

A group of conditions called "special populations" or "situations" in diastology also modify study algorithms, especially but not exclusively sinus tachycardia, hypertrophic cardiomyopathy, restrictive cardiomyopathy, non-cardiac pulmonary hypertension, mitral stenosis, mitral regurgitation, greater than mild mitral annulus calcification, heart transplantation, and constrictive pericarditis.[3–12]

Special populations are so important in diastology that the presence of these conditions must be ruled out before any analysis may be performed and the common algorithm can be applied. Therefore, despite being groups of different clinical conditions that can be wrongly relegated to a category of secondary importance and seemingly underrepresented in guidelines and reviews, knowing them is essential to a reliable and comprehensive diastolic function assessment.

Determination and graduation of diastolic dysfunction with af

Chronic atrial fibrillation (CAF) is the most prominent of these special situations due to both its high prevalence and the correlation of AF with the same etiologies classically associated with diastolic dysfunction.[13] For this reason, the presence of CAF is indicative of diastolic dysfunction in the same way as when determining myocardial disease (e.g., left ventricular ejection fraction < 50%, left ventricular hypertrophy, changes in myocardial segmental contractility, and signs of longitudinal systolic dysfunction).[1] Despite not being explicitly stated in current guidelines, reviews on the subject, or original articles, FAC represents a diseased heart for which this rationale makes sense.

In the presence of sinus rhythm without other special situations, diastolic dysfunction is classified into three categories: grade I, normal filling pressure; grade II, increased filling pressure; and grade III, increased filling pressure and filling restriction signs. This restrictive pattern (grade III) is defined as left ventricular (LV) filling restrictions during atrial contraction, translated by a relatively small A wave measured by transmitral Doppler, which obviously ceases to occur as a result of AF. For this reason, diastolic dysfunction grading in the presence of AF is limited to the first two categories (Figure 1).

Assessment sequence

Several echocardiographic variables indicate increased filling pressures in the presence of AF. However, the cutoff values used in these determinants do not always correspond to the same values used in sinus rhythm.

The first rule for determining filling pressures in the presence of CAF is not to use atrial dimensions, i.e., regardless of measurement type, volume, or anteroposterior dimension, indexed or not, its increase does not correlate with increased filling pressures. This is due to the well-known mechanical remodeling induced by AF, which increases atrial dimensions regardless of the filling pressure.[13]

The second rule is to start by measuring the maximum tricuspid regurgitation jet velocity, a good determinant of the filling pressure increase when ≥2.8 m/s (the same cutoff line recommended for the study in sinus rhythm). However, this measure cannot be used in two situations: the absence of a measurable jet; and the presence of concomitant diseases affecting the pulmonary vascular resistance, such as primary arterial hypertension, chronic obstructive pulmonary disease, and pulmonary thromboembolism.

Even respecting these two rules, the data will be insufficient, as it is recommended to use more than one determinant. Therefore, other Doppler variables well studied in this scenario and with good accuracy are used, each with its own limitation (Table 1).

The first choice is to measure the mitral inflow E-wave deceleration time (DT) by pulsed Doppler for being an easy and highly accurate measurement. However, this is only valid for subjects with reduced left ventricular ejection fraction (LVEF) (<50%), as E-wave DT is not a good determinant of filling pressure increase in subjects with preserved LVEF.[14,15]

Keywords

Echocardiography; Diastole; Atrial fibrillation.

Mailing Address: Antonio Amador Calvilho Júnior •
Av. Dr. Dante Pazzanese, 500 - Vila Mariana São Paulo - SP - CEP: 04012-909
E-mail: dr.calvilho@gmail.com
Manuscript received 6/24/2022; revised 7/11/2022; accepted 8/9/2022

Editor responsible for the review: Daniela do Carmo Rassi Frota

DOI: 10.47593/2675-312X/20223504eabc344i

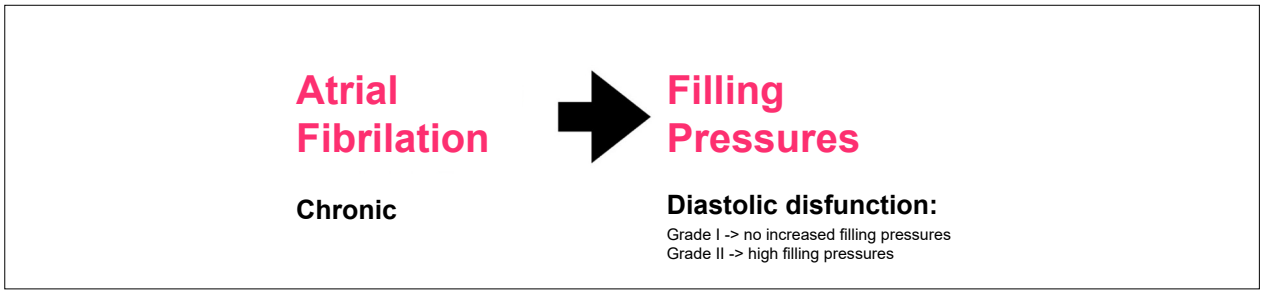

Figure 1 – *Graduation of diastolic dysfunction in atrial fibrillation.*

Tabela 1 – Variáveis complementares para diastologia em casos de fibrilação atrial.

Variável	Correlação	Sensibilidade (%)	Especificidade(%)	Autores
E/e' septal	0,79	75	93	Sohn DW et al (1999) [16]
TD onda E mitral	-0,95	100	96	Temporelli PL et al (1999) [14]
TD onda D pulmonar	-0,91	100	100	Chirillo F et al (1997) [17]
Pico de aceleração da onda E mitral	0,84	77	94	Nagueh SF et al (1996) [15]
TRIV	-0,76	72	88	Nagueh SF et al (1996) [15]
E/VPF	0,88	72	100	Nagueh SF et al (1996) [15]
TD onda E mitral (FEVE <45%)	-0,78	76	100	Nagueh SF et al (1996) [15]

E = pico de velocidade da onda E do fluxo transmitral, e' = pico de velocidade da onda e' do anel mitral, FEVE = Fração de ejeção do ventrículo esquerdo, TRIV = tempo de relaxamento isovolumétrico, TD = tempo de desaceleração, VPF = velocidade de propagação de fluxo

Therefore, in cases with reduced LVEF, an E-wave DT ≤ 160 ms indicates high filling pressure.[1]

A set of variables can be used in cases with preserved LVEF:

- Peak E-wave acceleration rate (PEAR) - cutoff value ≥ 1,900 cm/s²
- Isovolumetric relaxation time (IVRT) - cutoff value ≤ 65 ms
- Pulmonary venous diastolic velocity DT - cutoff value ≤ 220 ms
- Peak E-wave velocity/LV flow propagation velocity ratio (E/FPV) - cutoff value ≥ 1.4
- Septal E/e' ratio - cutoff ≥ 11

All measurements have good accuracy; thus, choosing which one to use depends on other characteristics, such as tool availability in the software (PEAR), which may not be available on the equipment used. In addition, reproducibility issues should also be considered, such as variables using pulmonary venous flow pulsed Doppler and flow propagation velocity, which are particularly limited in this regard. Therefore, IVRT and septal E/e' ratio continue to be strongly recommended, the first for being simple and practical and the second for being commonly used in basic protocols.

Regardless of the method chosen, the standard recommendation is to measure 10 consecutive cardiac cycles, but this extends the testing time. Alternatively, three non-consecutive cycles can be evaluated, provided that their rate is 10–20% of the mean heart rate.[1,15]

A last and simple resource to complement the assessment of filling pressures in patients with CAF is the variable maximum mitral inflow velocity between beats (E-wave), a consequence of typical rhythm irregularity in AF. This variability is reduced in patients with increased filling pressures, making it a possible determinant, although it is qualitative (Figure 2).[15] However, as it has no cutoff value or any form of quantification, this type of evaluation is subjective, which justifies its use as a last option.

Finally, the resources presented here can be listed as a logical four-step sequence (Figure 3). This proposition corroborates the 2016 guidelines of the American Society of Echocardiography and the European Society of Cardiovascular Imaging for the assessment of diastolic function, and it respects the balance between assessment accuracy, practicality, and availability. It is important to note that, regardless of the variable chosen and/or available at each stage, the use of more than one determinant is recommended.[1]

Final considerations

Although the concepts chosen to justify our assessment of diastolic function are quite clear, some points are debatable, as is the case of attributing the presence of diastolic dysfunction to the mere occurrence of AF, a flawed concept not explicitly clear in the literature. However, considering these logical aspects, it makes no sense to grade diastolic dysfunction in the absence of a diagnosis. Therefore, while there is no more specific proposal in this regard, this is the recommended rationale.

The assessment described here is aimed at non-valvular CAF, i.e., in case of significant mitral valve diseases or other conditions, the physician should use specific algorithms and common sense.

New technologies were not mentioned, as they are not the purpose of this article, which focused on what we actually use in current practice. Some technologies can help and considerably

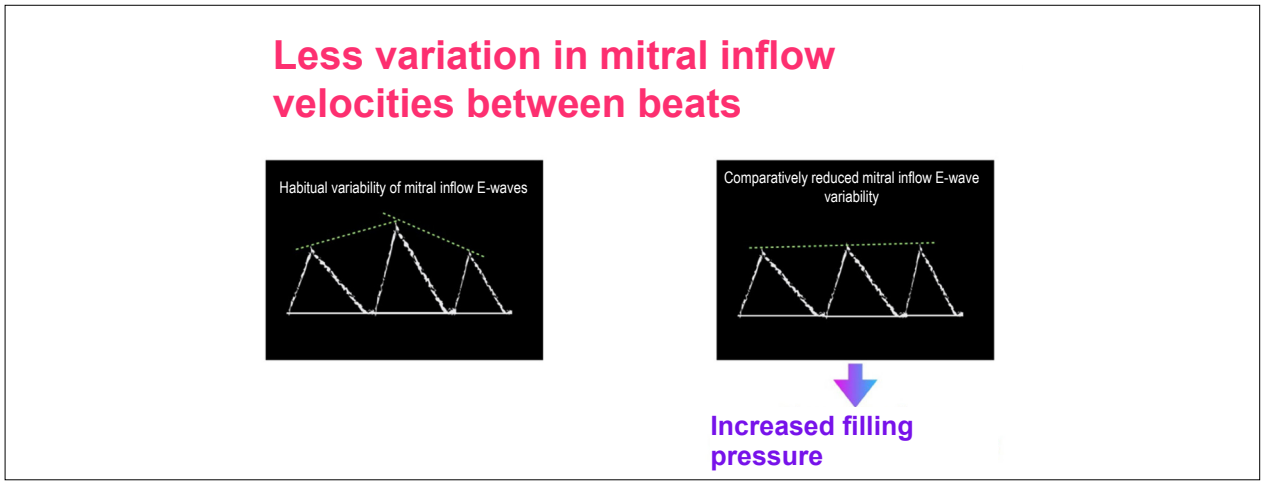

Figure 2 – *Qualitative assessment of E-wave variability in atrial fibrillation.*

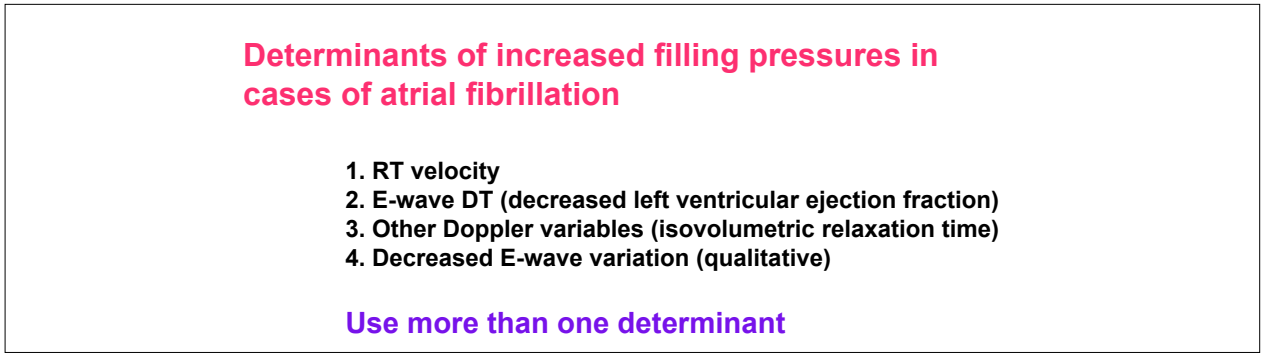

Figure 3 – *Sequence for assessing diastolic dysfunction in atrial fibrillation.*

simplify the assessment of diastolic function in patients with AF, such as special transducers capable of simultaneously recording mitral annulus and transmitral flow tissue Doppler.[18-20] However, such tools are not used in current practice.

Authors' contributions

Manuscript Writing: Calvilho Júnior AA and Assef JE: Bibliographic Research, review of the Manuscript and intellectual concept of its structure: Braga JMS and Vilela AA.

Conflict of interest

The authors have declared that they have no conflict of interest.

References

1. Nagueh SF, Smiseth OA, Appleton CP, Byrd BF 3rd, Dokainish H, Edvardsen T, et al. Recommendations for the Evaluation of Left Ventricular Diastolic Function by Echocardiography: An Update from the American Society of Echocardiography and the European Association of Cardiovascular Imaging. J Am Soc Echocardiogr. 2016;29(4):277-314. doi: https://doi.org/10.1016/j.echo.2016.01.011
2. Tsang TS, Gersh BJ, Appleton CP, Tajik AJ, Barnes ME, Bailey KR, et al. Left ventricular diastolic dysfunction as a predictor of the first diagnosed nonvalvular atrial fibrillation in 840 elderly men and women. J Am Coll Cardiol. 2002;40(9):1636-44. doi: https://doi.org/10.1016/s0735-1097(02)02373-2
3. Nagueh SF, Mikati I, Kopelen HA, Middleton KJ, Quiñones MA, Zoghbi WA. Doppler estimation of left ventricular filling pressure in sinus tachycardia. A new application of tissue doppler imaging. Circulation. 1998;98(16):1644-50. doi: https://doi.org/10.1161/01.cir.98.16.1644
4. Geske JB, Sorajja P, Nishimura RA, Ommen SR. Evaluation of left ventricular filling pressures by Doppler echocardiography in patients with hypertrophic cardiomyopathy: correlation with direct left atrial pressure measurement at cardiac catheterization. Circulation. 2007;116(23):2702-8. doi: https://doi.org/10.1161/CIRCULATIONAHA.107.698985
5. Nagueh SF, Lakkis NM, Middleton KJ, Spencer WH 3rd, Zoghbi WA, Quiñones MA. Doppler estimation of left ventricular filling pressures in patients with hypertrophic cardiomyopathy. Circulation. 1999;99(2):254-61. doi: https://doi.org/10.1161/01.cir.99.2.254
6. Nishimura RA, Appleton CP, Redfield MM, Ilstrup DM, Holmes DR Jr, Tajik AJ. Noninvasive doppler echocardiographic evaluation of left ventricular filling pressures in patients with cardiomyopathies: a simultaneous

Doppler echocardiographic and cardiac catheterization study. J Am Coll Cardiol. 1996;28(5):1226-33. doi: https://doi.org/10.1016/S0735-1097(96)00315-4

7. Ruan Q, Nagueh SF. Clinical application of tissue Doppler imaging in patients with idiopathic pulmonary hypertension. Chest. 2007;131(2):395-401. doi: https://doi.org/10.1378/chest.06-1556

8. Diwan A, McCulloch M, Lawrie GM, Reardon MJ, Nagueh SF. Doppler estimation of left ventricular filling pressures in patients with mitral valve disease. Circulation. 2005;111(24):3281-9. doi: https://doi.org/10.1161/CIRCULATIONAHA.104.508812. Erratum in: Circulation. 2005;112(4):e76. Diwan, Abhvinav [corrected to Diwan, Abhinav].

9. Bruch C, Stypmann J, Gradaus R, Breithardt G, Wichter T. Usefulness of tissue Doppler imaging for estimation of filling pressures in patients with primary or secondary pure mitral regurgitation. Am J Cardiol. 2004;93(3):324-8. doi: https://doi.org/10.1016/j.amjcard.2003.10.012

10. Abudiab MM, Chebrolu LH, Schutt RC, Nagueh SF, Zoghbi WA. Doppler Echocardiography for the Estimation of LV Filling Pressure in Patients With Mitral Annular Calcification. JACC Cardiovasc Imaging. 2017;10(12):1411-20. doi: https://doi.org/10.1016/j.jcmg.2016.10.017

11. Valantine HA, Appleton CP, Hatle LK, Hunt SA, Billingham ME, Shumway NE, et al. A hemodynamic and Doppler echocardiographic study of ventricular function in long-term cardiac allograft recipients. Etiology and prognosis of restrictive-constrictive physiology. Circulation. 1989;79(1):66-75. doi: https://doi.org/10.1161/01.cir.79.1.66

12. Reuss CS, Wilansky SM, Lester SJ, Lusk JL, Grill DE, Oh JK, et al. Using mitral 'annulus reversus' to diagnose constrictive pericarditis. Eur J Echocardiogr. 2009;10(3):372-5. doi: https://doi.org/10.1093/ejechocard/jen258

13. Bisbal F, Baranchuk A, Braunwald E, Bayés de Luna A, Bayés-Genís A. Atrial Failure as a Clinical Entity: JACC Review Topic of the Week. J Am Coll Cardiol. 2020;75(2):222-32. doi: https://doi.org/10.1016/j.jacc.2019.11.013

14. Temporelli PL, Scapellato F, Corrà U, Eleuteri E, Imparato A, Giannuzzi P. Estimation of pulmonary wedge pressure by transmitral Doppler in patients with chronic heart failure and atrial fibrillation. Am J Cardiol. 1999;83(5):724-7. doi: https://doi.org/10.1016/s0002-9149(98)00978-3

15. Nagueh SF, Kopelen HA, Quiñones MA. Assessment of left ventricular filling pressures by Doppler in the presence of atrial fibrillation. Circulation. 1996;94(9):2138-45. doi: https://doi.org/10.1161/01.cir.94.9.2138

16. Sohn DW, Song JM, Zo JH, Chai IH, Kim HS, Chun HG, et al. Mitral annulus velocity in the evaluation of left ventricular diastolic function in atrial fibrillation. J Am Soc Echocardiogr. 1999;12(11):927-31. doi: https://doi.org/10.1016/s0894-7317(99)70145-8

17. Chirillo F, Brunazzi MC, Barbiero M, Giavarina D, Pasqualini M, Franceschini-Grisolia E, et al. Estimating mean pulmonary wedge pressure in patients with chronic atrial fibrillation from transthoracic Doppler indexes of mitral and pulmonary venous flow velocity. J Am Coll Cardiol. 1997;30(1):19-26. doi: https://doi.org/10.1016/s0735-1097(97)00130-7

18. Kusunose K, Yamada H, Nishio S, Tomita N, Niki T, Yamaguchi K, et al. Clinical utility of single-beat E/e' obtained by simultaneous recording of flow and tissue Doppler velocities in atrial fibrillation with preserved systolic function. JACC Cardiovasc Imaging. 2009;2(10):1147-56. doi: https://doi.org/10.1016/j.jcmg.2009.05.013

19. Wada Y, Murata K, Tanaka T, Nose Y, Kihara C, Uchida K, et al. Simultaneous Doppler tracing of transmitral inflow and mitral annular velocity as an estimate of elevated left ventricular filling pressure in patients with atrial fibrillation. Circ J. 2012;76(3):675-81. doi: https://doi.org/10.1253/circj.cj-11-0703

20. Li C, Zhang J, Zhou C, Huang L, Tang H, Rao L. Will simultaneous measurement of E/e' index facilitate the non-invasive assessment of left ventricular filling pressure in patients with non-valvular atrial fibrillation? Eur J Echocardiogr. 2010;11(3):296-301. doi: https://doi.org/10.1093/ejechocard/jep218

Review Article

My Approach to the Echocardiographic Assessment of a Pediatric Patient with Cancer

Como eu faço Avaliação Ecocardiográfica do Paciente Oncológico Pediátrico

Claudia Cosentino Gallafrio[1,2,3], Ricardo H. Pignatelli[4]

[1]GRAACC Hospital, São Paulo, SP, Brazil; [2]Hospital Israelita Albert Einstein, São Paulo, SP, Brazil; [3]DASA Group-Alta Diagnósticos, São Paulo, SP, Brasil; [4]Texas Children's Hospital, Baylor College of Medicine Houston, TX, USA.

What is the importance of cardiovascular assessments in pediatric patients with cancer?

Pediatric oncology has greatly progressed in recent decades due to the development of more effective treatment protocols; in fact, 5-year disease-free survival rates now exceed 80%. However, despite improved survival rates, the cardiovascular risks arising from these therapies are 5- to 6-fold greater in long-term surviving oncology patients than the general pediatric population.[1,2] Thus, cardiovascular events, such as myocardial infarction, heart failure, and stroke, are the major cause of non-cancer death in these patients.[1]

Cardiotoxicity is defined as any structural or functional damage incurred by the heart and circulation during or after cancer treatment. These changes may be caused by chemotherapeutic agents, radiotherapy, or even the disease itself (Table 1). Cardiotoxicity may present as symptomatic or asymptomatic heart failure, pericardial changes, arrhythmias, thromboembolic events, arterial hypertension, or valve and coronary diseases[3,4] and can be classified by time of onset as follows:[5]

- Acute cardiotoxicity: occurs soon after treatment initiation but is rare; may be reversible; most commonly presents as arrhythmias and ventricular dysfunction (Figure 1).
- Early-onset cardiotoxicity: occurs in the first year after the end of cancer treatment; usually progressive, featuring ventricular dilation and dysfunction.
- Late-onset cardiotoxicity: diagnosed after the first year of the end of treatment and is more common; characterized by dilated or restrictive cardiomyopathy (Figure 2).

What are the main risk factors for cardiotoxicity?

- Age, especially in children younger than 5 years of age, and a high risk of cardiotoxicity in children younger than 1 year of age;
- Female sex;
- Accumulated anthracycline doses greater than 240 mg/m^2, but it depends on individual susceptibility, with reports of cardiotoxicity at doses lower than 100 mg/m^2, and THERE IS NO SAFE DOSE;
- Thoracic radiotherapy at doses above 30 Gy greatly increases the risk of cardiotoxicity, as does associated use of anthracyclines;
- Combined therapies, such as cyclophosphamide, vincristine, mitoxantrone, among others, can potentiate toxic effects on the cardiovascular system. Special attention should be directed to new-generation drugs (tyrosinase inhibitors, chimeric antigen receptor T-cell therapy, immune checkpoint inhibitors, etc.) and its impact on the myocardial units;
- Pre-existing risk factors include arterial hypertension, valvular heart disease, cardiomyopathy, congenital heart disease, and previous high-risk treatment for cardiotoxicity;
- Alcohol, tobacco, and illicit drug use;
- Comorbidities including diabetes, obesity, kidney disease, endocrinopathy, infection, and previous thrombosis; and
- Others include trisomy 21, African descent, and genetic predisposition.[6]

How to proceed with echocardiographic follow-up?

These patients should be followed up using multimodal imaging methods, electrocardiography, metabolic screening, and specific biomarkers whenever available. The patient should always be assessed before (initial tests), during, and after treatment (long-term follow-up). The objective is the early detection of cardiovascular changes. Thus, echocardiography is a useful tool due to its high accessibility, noninvasive nature, and low cost in addition to diagnosis of any subclinical dysfunction.

Cardiotoxicity is traditionally diagnosed by echocardiography as a 10-point drop in left ventricular (LV) ejection fraction (LVEF) compared to the initial assessment test (<55% is reference for pediatric patients).[10] However, this diagnosis by LVEF or shortening fraction alone is suboptimal, as it does not include preclinical myocardial injury changes but is affected by common conditions such as sepsis, pulmonary hypertension, and hyperhydration. Thus, volumetric LVEF (two- or three-dimensional), myocardial deformation, and diastolic analyses are fundamental to better follow-up.

Keywords

Cadio-Oncology, Echocardiography, Pediatrics.

Mailing Address: Claudia Cosentino Gallafrio •
Rua Pedro de Toledo, 572 - Vila Clementino, São Paulo - SP, 04039-001.
E-mail: claudia.mcosentino@gmail.com
Manuscript received 8/8/2022; revised 8/29/2022; accepted 9/16/2022

Editor responsible for the review: Karen Saori Shiraishi Sawamura

DOI: 10.47593/2675-312X/20223504ecom33i

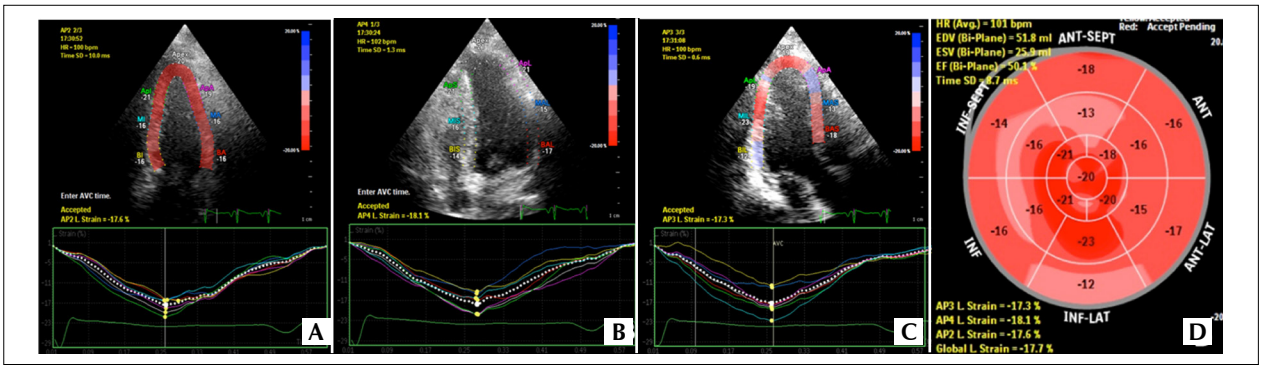

Figure 1 – *Acute cardiotoxicity. Images of a 10-year-old female patient diagnosed with acute lymphocytic leukemia. Left ventricular global longitudinal strain (GLS) was obtained from four- (A), two- (B), and three-chamber (C) images. Bullseye plot (D) showing discreet ventricular dysfunction. Left ventricular ejection fraction (LVEF) = 50%. Reduced GLS = -17.7% with changed segmental contractility.*

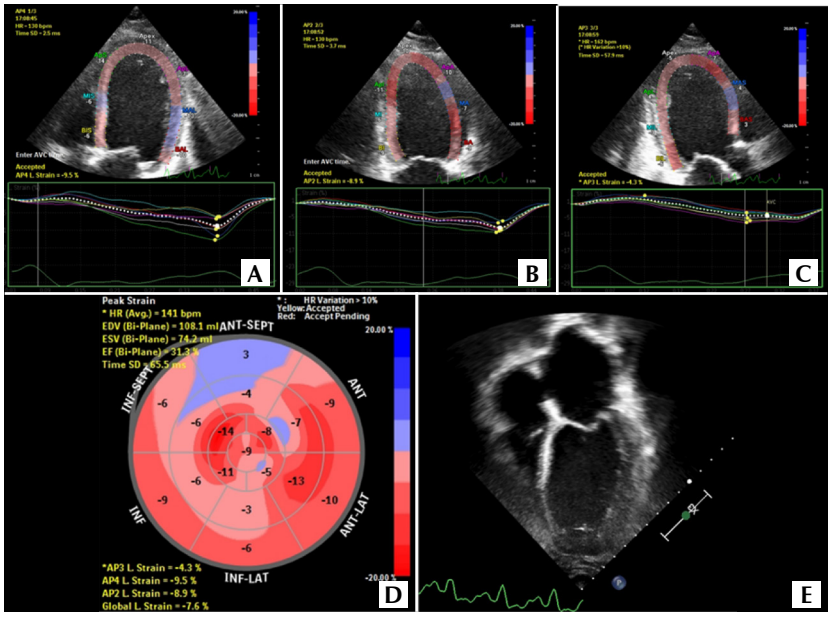

Figure 2 – *Late-onset cardiotoxicity. Images of a 22-year-old woman with a history of acute lymphoblastic leukemia taken 18 years after the end of cancer treatment. Left ventricular global longitudinal strain (GLS) obtained from four- (A), two- (B), and three-chamber (C) images. Bullseye plot (D) showing ventricular dysfunction. Left ventricular ejection fraction = 31%. Very reduced GLS = -7.6% with changed segmental contractility and areas of dyskinesia (blue). (E) Left heart chamber dilation.*

Echocardiographic assessment:

LV systolic function

Volumetric LVEF analysis

The biplane Simpson's method (Figures 3A, 3B) for estimating myocardial function from LV volumes overcomes the limitations of shortening methods and the Teichholz formula derived from linear M-mode or two-dimensional measurements. It should be the test of choice for myocardial function analyses in patients with cancer. Most popular volumetric techniques to obtain LVEF are Simpson's method. In younger patients, this could be shortened in the two-chamber apical view and the area-length or bullseye method using the formula V = 5/6 of the short-axis basal area × LV length (Figure 3C) as an alternative.

Three-dimensional LVEF analysis (Figure 3D) is a promising method. The software currently performs semi-automated calculations to estimate the three-dimensional volume with improved image acquisition and data processing. However, this remains challenging to perform in the pediatric population.

LV global longitudinal strain

Myocardial strain analysis derived from two-dimensional speckle tracking is growing in popularity that is less dependent

Table 1 - Cardiovascular system damage caused by main oncological treatments used in pediatric oncology patients.[7,8]

Agent	Examples	Cardiovascular damage
Anthracyclines	Doxorubicin Daunorubicin *Mitoxantrone	Arrhythmia Ventricular dysfunction Myocardial fibrosis Endothelial dysfunction
Alkylating agents	Cyclophosphamide Busulfan	Arrhythmia Endothelial dysfunction Pericardial effusion Thrombosis
Antimetabolites	Cytarabine (Ara-C) Cisplatin Methotrexate 5-Fluorouracil	Arrhythmia Myocardial ischemia
Tyrosine kinase inhibitors	Imatinib Dasatinib Pazopanib	Arterial hypertension Endothelial dysfunction Prolonged QTc Thrombosis Ventricular dysfunction Pericardial effusion
Vinca alkaloids	Vincristine	Myocardial ischemia
Radiotherapy		Pericarditis Valve disease Coronary artery disease Systemic arterial hypertension Ventricular dysfunction
Immunotherapy	Immune checkpoint inhibitors CAR T-cell therapy	Arterial hypertension Endothelial dysfunction Prolonged QTc Thrombosis Ventricular dysfunction Pericardial effusion

**Mitoxantrone is usually allocated to the anthracycline class, but studies show a different cardiotoxicity mechanism. It is 10× more cardiotoxic than doxorubicin.[9]*

on angle and easier to calculate than that from tissue Doppler. It also has low intra- and interobserver variability.[11] A global longitudinal strain (GLS) reduction of 15% compared to the initial baseline test appears to be a good cutoff value for the early detection of anthracycline-induced cardiotoxicity.[10] In the absence of an initial assessment for comparison, GLS values lower than -17% increase the sensitivity for diagnosing cardiotoxicity when associated with biomarkers, mainly high-sensitivity troponin.[12]

Strain to detect subclinical ventricular dysfunction in patients with preserved global myocardial function (EF%) can be an excellent method for the early diagnosis of cardiac compromise by oncological treatment.

LV diastolic function

Diastolic function changes in the adult population with cancer may precede systolic dysfunction; therefore, it represents an early sign of LV functional changes. However, further studies of this topic are needed in the pediatric population in clinical practice using Doppler indices such as mitral valve E/A ratio, deceleration time, E/e' ratio (Figures 4A, 4C, 4D), and indexed left atrial volume (Figure 4B).

The left atrium (LA) plays an important role in LV filling pressures and LV diastolic function. Although the focus of myocardial function is the LV, currently studies suggest that the LA assessment may be related to the early detection of LV dysfunction. Furthermore, LA function is associated with prognosis in heart failure. Adults treated with anthracycline showed a significant change in LA strain (LAS). A small study of children showed that changes in LA function demonstrated by LVEF, strain, and strain rate were mild in children and young

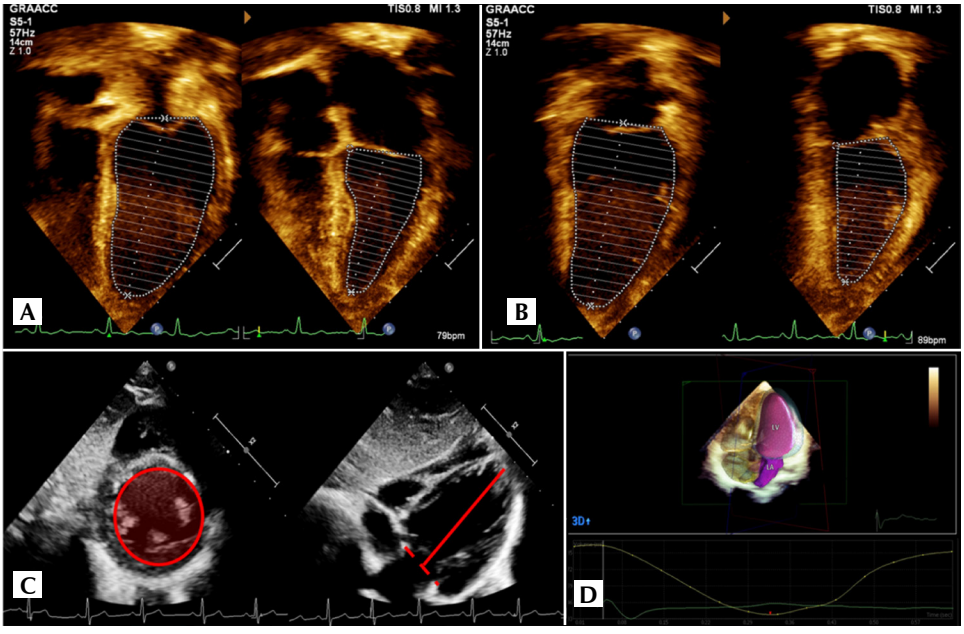

Figure 3 – *(A, B) Biplane Simpson's method. Apical four- (A) and two-chamber (B) left ventricular volumetric analysis. (C) Area-length or bullseye method used to determine left ventricular ejection fraction (LVEF). (D) LVEF analysis performed using the three-dimensional method.*

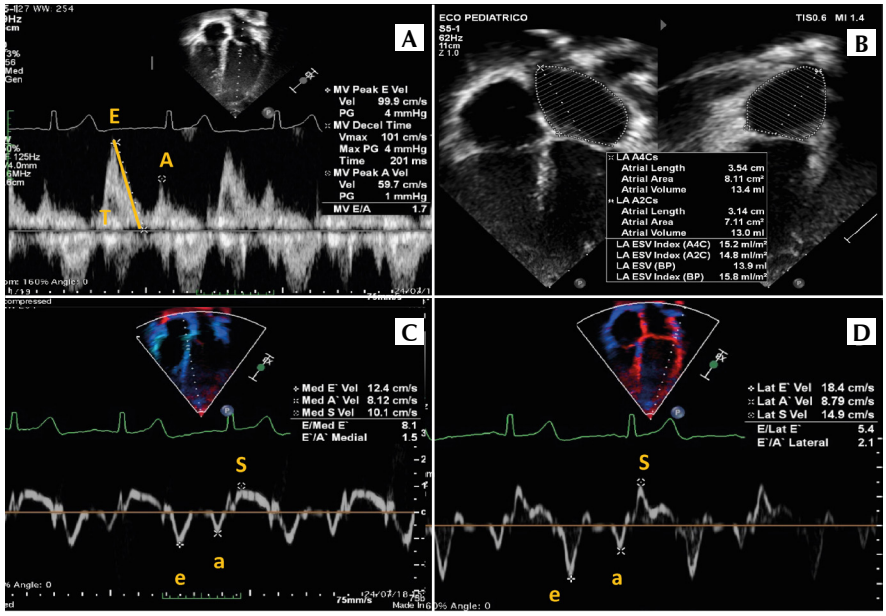

Figure 4 – *ALeft ventricular (LV) diastolic assessment. (A) Pulsed Doppler of mitral valve flow showing peak velocities during early ventricular diastole (E), atrial contraction (A), and deceleration time. (B) Left atrial volume assessment performed at the end of systole in the apical four- and two-chamber planes. (C) Tissue Doppler with septal mitral annulus velocities. (D) Tissue Doppler with mitral annulus velocities on the lateral wall of the LV.*

adults exposed to anthracyclines. In pre-adolescence, the effects of anthracyclines were more significant in this population.[13,14] Another study compared survivors of childhood cancer exposed to anthracyclines who were ≥1 year out from completing chemotherapy with controls. Those exposed to higher anthracycline doses had worse peak LAS (reservoir phase). The authors suggested that further studies of LAS as a potential marker of cancer therapy–related cardiac dysfunction are indicated and may provide insight into the prompt detection, treatment, and recovery of myocardial function.[15]

This new echocardiographic option such LAS is encouraging but still under investigation; for the time being, there is no evidence in the pediatric population of its predictive value of clinical outcomes.

Right ventricular function

The American Society of Echocardiography recommends the use of fraction area change (FAC), tricuspid annular plane systolic excursion (TAPSE), and Doppler analysis for the assessment of right ventricular (RV) systolic function in children.[16]

FAC assesses the RV area in end-diastole and systole on apical four-chamber view of the modified RV (Figure 5A). Values < 35% indicate RV systolic dysfunction.[17] TAPSE measures RV longitudinal shortening on an apical four-chamber view by M-mode in the tricuspid valve annulus (Figure 5B).[17]

On tissue Doppler imaging, the RV lateral wall S' wave velocity is easy to measure, reliable, and reproducible; moreover, it is highly correlated with other RV systolic function measurements (Figure 5C). Velocities < 10 cm/s indicate right systolic dysfunction.[17]

New techniques such as three-dimensional echocardiography (Figure 5D) have been useful for obtaining more accurate volume and LVEF measurements that have excellent correlation with magnetic resonance imaging (MRI), the gold standard for evaluating RV EF and volume.[18] RV strain was also validated to assess RV function (Figure 5E).[19]

Further studies in the pediatric population with cancer are needed to define the usefulness of RV strain for the early diagnosis of cardiotoxicity.

Guidelines are lacking regarding how often imaging screening should be performed at each stage of pediatric cancer treatment; thus, further studies are needed to enable standardization. The Children's Oncology Group[20] published long-term follow-up guidelines for standardization. However, individualizing follow-up based on treatment history is the best strategy in cases of early diagnosis.

Role of multimodality

Cardiac MRI, an important diagnostic tool in the follow-up of pediatric cancer patients, features excellent reproducibility and is unaffected by a limited acoustic window or complex ventricular geometry.

Cardiac MRI, which plays an important role in preclinical lesion detection, allows the diagnosis of early interstitial edema on a T2-weighted view and of the subsequent myocardial fibrosis by T1 mapping and late gadolinium enhancement.

The disadvantages of routine use of this method are its low availability in national medical services, high cost, and need for sedation in young children.[3]

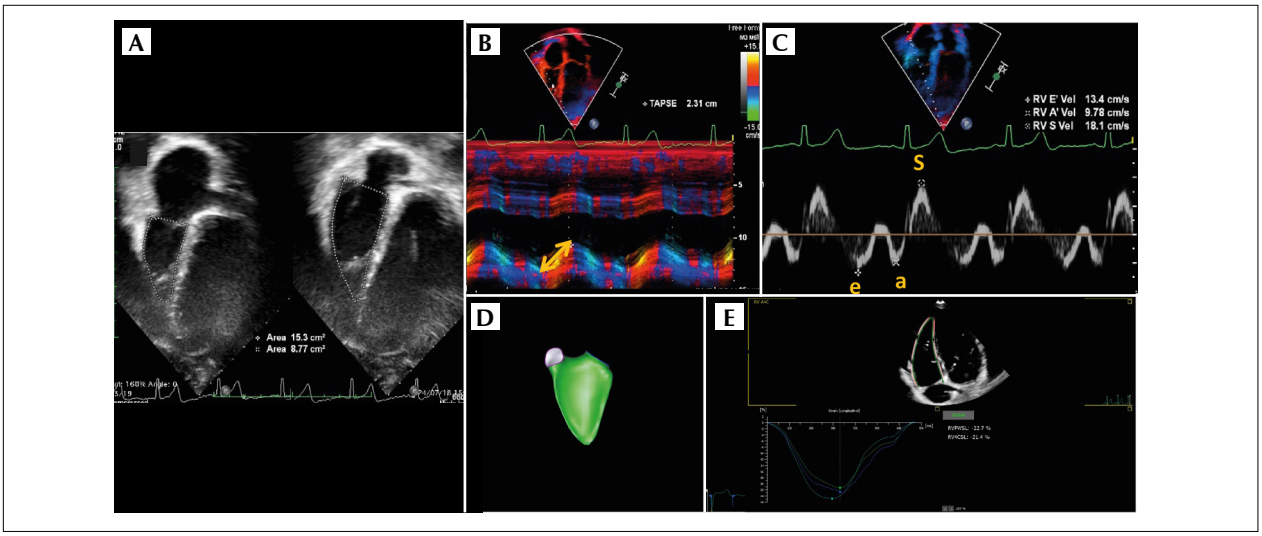

Figure 5 – *Right ventricular (RV) systolic function assessment. (A) RV fraction area change. (B) Tricuspid annular plane systolic excursion. (C) Tissue Doppler showing tricuspid annulus velocities on the lateral wall of the left ventricle. (D) Three-dimensional analysis of RV volumes and ejection fraction. (E) Apical four-chamber plane focusing on the RV for calculation of the RV global longitudinal strain.*

Conclusion

Despite the growing number of cardio-oncology studies, imaging guidelines and robust longitudinal scientific studies of pediatric populations are lacking. Echocardiography has become an important imaging method for diagnosing cardiotoxicity.

We strongly recommend volumetric EF% as the primary tool for following these patients. Independent of which method is being used to obtain EF%, a quality control program should be instituted to avoid a variability higher than 10% in each echocardiology laboratory. We also strongly support LV GLS measurements as an early sign of subclinical manifestation of cardiotoxicity.

We encourage left atrial strain analysis, but it should be recognized that it remains an early phase of research requiring more data.

Cardiac MRI is a solid technique that is underused mostly due to economic reasons and scarce availability to requesting physicians. Cardiac MRI should be considered when echocardiographic evaluation results are questionable or conflicting values are obtained. MRI tissue evaluations offer a promising aspect of this technique.

Authors' contributions

Research conception and design: Gallafrio CG, Pignatelli RH; data collection: Gallafrio CG, Pignatelli RH; data analysis and interpretation: Gallafrio CG, Pignatelli RH; manuscript writing: Gallafrio CG; critical review of the manuscript for important intellectual content: Pignatelli RH.

Conflict of interest

The authors have declared that they have no conflict of interest.

References

1. Brickler M, Raskin A, Ryan TD. Current state of pediatric cardio-oncology: a review. Children. 2022;9(2):1-16. doi: https://doi.org/10.3390/children9020127
2. Chow EJ, Leger KJ, Bhatt NS, Mulrooney DA, Ross CJ, Aggarwal S, et al. Paediatric cardio-oncology: Epidemiology, screening, prevention, and treatment. Cardiovasc Res. 2019;115(5):922-34. doi: https://doi.org/10.1093/cvr/cvz031
3. Loar RW, Noel C V., Tunuguntla H, Colquitt JL, Pignatelli RH. State of the art review: Chemotherapy-induced cardiotoxicity in children. Congenit Heart Dis. 2018;13(1):5-15. doi: https://doi.org/10.1111/chd.12564
4. Zamorano JL, Lancellotti P, Rodriguez Muñoz D, Aboyans V, Asteggiano R, Galderisi M, et al.; ESC Scientific Document Group. 2016 ESC Position Paper on cancer treatments and cardiovascular toxicity developed under the auspices of the ESC Committee for Practice Guidelines. Eur Heart J. 2016;37(36):2768-801. doi: https://doi.org/10.1093/eurheartj/ehw211. Erratum in: Eur Heart J. 2016 Dec 24;: PMID: 27567406
5. Lipshultz SE, Adams MJ, Colan SD, Constine LS, Herman EH, Hsu DT, et al.; American Heart Association Congenital Heart Defects Committee of the Council on Cardiovascular Disease in the Young, Council on Basic Cardiovascular Sciences, Council on Cardiovascular and Stroke Nursing, Council on Cardiovascular Radiolo. Long-term cardiovascular toxicity in children, adolescents, and young adults who receive cancer therapy: pathophysiology, course, monitoring, management, prevention, and research directions: a scientific statement from the American Heart Association. Circulation. 2013;128(17):1927-95. doi: https://doi.org/10.1161/CIR.0b013e3182a88099. Erratum in: Circulation. 2013;128(19):e394.
6. Hutchins KK, Siddeek H, Franco VI, Lipshultz SE. Prevention of cardiotoxicity among survivors of childhood cancer. Br J Clin Pharmacol. 2017;83(3):455-65. doi: https://doi.org/10.1111/bcp.13120
7. Sociedade Brasileira de Cardiologia (SBC). I Diretriz Brasileira de Cardio-Oncologia Pediátrica Sociedade Brasileira de Cardiologia. 2013;100. doi: 10.5935/abc.2013S005.

8. Martinez HR, Beasley GS, Goldberg JF, Absi M, Ryan KA, Guerrier K, et al. Pediatric cardio-oncology medicine: A new approach in cardiovascular care. Children. 2021;8(12):1200. doi: https://doi.org/10.3390/children8121200

9. Leerink JM, de Baat EC, Feijen EA, Bellersen L, van Dalen EC, Grotenhuis HB, et al. Cardiac Disease in Childhood Cancer Survivors: Risk Prediction, Prevention, and Surveillance. JACC CardioOncology. 2020;2(3):363-78. doi: https://doi.org/10.1016/j.jaccao.2020.08.006

10. Plana JC, Galderisi M, Barac A, Ewer MS, Ky B, Scherrer-Crosbie M, et al. Expert consensus for multimodality imaging evaluation of adult patients during and after cancer therapy: A report from the American society of echocardiography and the European association of cardiovascular imaging. J Am Soc Echocardiogr. 2014;27(9):911-39. doi: https://doi.org/10.1016/j.echo.2014.07.012

11. Thavendiranathan P, Poulin F, Lim KD, Plana JC, Woo A, Marwick TH. Use of myocardial strain imaging by echocardiography for the early detection of cardiotoxicity in patients during and after cancer chemotherapy: A systematic review. J Am Coll Cardiol. 2014;63(25 PART A):2751-68. doi: http://dx.doi.org/10.1016/j.jacc.2014.01.073

12. Melo MD, Paiva MG, Santos MV, Rochitte CE, Moreira VM, Saleh MH, et al. Posicionamento Brasileiro sobre o Uso da Multimodalidade de Imagens na Cardio-Oncologia – 2021. Arq Bras Cardiol. 2021 [citado 2022 Out. 13];1-64. Disponível em: https://medicinanuclearnh.com.br/materiais/posicionamento-brasileiro-sobre-o-uso-da-multimodadlidade-de-imgens-na-cardio-oncologia_port.pdf

13. Patel NR, Chyu CK, Satou GM, Halnon NJ, Nguyen KL. Left atrial function in children and young adult cancer survivors treated with anthracyclines. Echocardiography. 2018;35(10):1649-56. doi: https://doi.org/10.1111/echo.14100

14. Laufer-Perl M, Gilon D, Kapusta L, Iakobishvili Z. The role of speckle strain echocardiography in the diagnosis of early subclinical cardiac injury in cancer patients—is there more than just left ventricle global longitudinal strain? J Clin Med. 2021;10(1):154. doi: https://doi.org/10.3390/jcm10010154

15. Loar RW, Colquitt JL, Rainusso NC, Gramatges MM, Liu AM, Noel CV., et al. Assessing the left atrium of childhood cancer survivors. Int J Cardiovasc Imaging. 2021;37(1):155-62. doi: https://doi.org/10.1007/s10554-020-01970-x

16. Lopez L, Colan SD, Frommelt PC, Ensing GJ, Kendall K, Younoszai AK, et al. Recommendations for Quantification Methods During the Performance of a Pediatric Echocardiogram: A Report From the Pediatric Measurements Writing Group of the American Society of Echocardiography Pediatric and Congenital Heart Disease Council. J Am Soc Echocardiogr. 2010;23(5):465-95; quiz 576-7. doi: https://doi.org/10.1016/j.echo.2010.03.019

17. Rudski LG, Lai WW, Afilalo J, Hua L, Handschumacher MD, Chandrasekaran K, et al. Guidelines for the echocardiographic assessment of the right heart in adults: a report from the American Society of Echocardiography endorsed by the European Association of Echocardiography, a registered branch of the European Society of Cardiology, and the Canadian Society of Echocardiography. J Am Soc Echocardiogr. 2010;23(7):685-713; quiz 786-8. doi: https://doi.org/10.1016/j.echo.2010.05.010

18. Lang RM, Badano LP, Tsang W, Adams DH, Agricola E, Buck T, et al.; American Society of Echocardiography; European Association of Echocardiography. EAE/ASE recommendations for image acquisition and display using three-dimensional echocardiography. J Am Soc Echocardiogr. 2012;25(1):3-46. doi: https://doi.org/10.1016/j.echo.2011.11.010

19. Badano LP, Kolias TJ, Muraru D, Abraham TP, Aurigemma G, Edvardsen T, et al.; Industry representatives; Reviewers: This document was reviewed by members of the 2016–2018 EACVI Scientific Documents Committee. Standardization of left atrial, right ventricular, and right atrial deformation imaging using two-dimensional speckle tracking echocardiography: a consensus document of the EACVI/ASE/Industry Task Force to standardize deformation imaging. Eur Heart J Cardiovasc Imaging. 2018;19(6):591-600. doi: https://doi.org/10.1093/ehjci/jey042. Erratum in: Eur Heart J Cardiovasc Imaging. 2018;19(7):830-3.

20. Children's Oncology Group. Long-Term Follow-Up Guidelines for Survivors of Childhood, Adolescent and Young Adult Cancers. Child Oncol Gr. 2018. [Outubro 2018]. Available from: chrome-extension://efaidnbmnnnibpcajpcglclefindmkaj/http://www.survivorshipguidelines.org/pdf/2018/cog_ltfu_guidelines_v5.pdf

Review Article

My Approach to Contrast Echocardiography

Como eu faço Contraste Ecocardiográfico

Miguel Osman Dias Aguiar[1,2], Alessandra Joslin Oliveira[1,3], Carolina Stangenhaus[1,3], Wilson Mathias Junior[3,4]

[1]Hospital Israelita Albert Einstein, São Paulo, SP, Brazil. [2]Hospital São Camilo, SP, Brazil. [3]University of São Paulo (FMUSP), School of Medicine, Heart Institute (InCor), São Paulo, SP, Brazil. [4]Grupo Fleury, São Paulo, SP, Brazil.

Introduction

Contrast echocardiography (CE) uses ultrasound enhancing agents (UEA) that, when introduced into the bloodstream and subjected to ultrasound (US), contrast the blood due to the great reflective capacity of microbubbles. It completely opacifies the left ventricle (LV), with better definition of endocardial borders, Doppler signal enhancement, and myocardial perfusion (MP).

Commercially available second-generation UEA are composed of high molecular weight gases surrounded by an outer shell of albumin, phospholipid, or polymer. These inert structures aggregate and remain within the intravascular space, presenting kinetics similar to those of red blood cells but at less than half their size (1.0–4.5 μm), which allows them to pass the pulmonary capillary barrier and reach the left chambers. They are predominantly excreted through the lungs, have a high metabolism (half-life, 10–12 min), do not deposit in the tissues, and, unlike iodinated contrast agents, present no known risk factors of nephrotoxicity.[1,2]

Adverse events and safety of UEA

Adverse events related to UEA use are rare, being mostly transient and self-limiting. In a meta-analysis of 110,500 patients, the incidence of severe allergic and anaphylactoid reactions immediately after UEA administration was estimated in 0.009% and 0.004%, respectively.[3] Aggeli et al. evaluated 5,250 patients and found supraventricular arrhythmias (0.1–0.5%), ventricular arrhythmias (0.02–0.20%), headache (5.3%), back pain (0.5%), dizziness (7.4%), and hypersensitivity reactions (0.44%) as the most frequent adverse events related to contrast echocardiography. That study reported no cases of death or acute myocardial infarction (AMI) related to UEA use.[4]

According to the latest American Society of Echocardiography guideline, UEA use is safe in adolescents and children over 5 years of age for Doppler signal enhancement and regional parietal motility (RPM) assessments as well as in children and adults with patent foramen ovale and a small right-to-left shunt. Furthermore, its use is safe in patients with pulmonary hypertension. UEA is contraindicated in patients with a known allergy to its components; moreover, data are lacking on its safety in pregnant women and children under five years of age. As with other advanced echocardiographic modalities, the unit must be properly equipped to manage possible serious complications.[5]

Keywords

Echocardiography; Contrast Echocardiography; Perfusion Imaging.

Mailing Address: Miguel Osman Dias Aguiar •
Av. Pompéia, 1178, Pompeia, São Paulo, SP, Brazil, Postal Code: 05022-001.
E-mail: miguel@wavesmed.com.br
Manuscript received 10/24/2022; revised 10/31/2022; accepted 11/5/2022

Editor responsible for the review: Daniela do Carmo Rassi Frota

DOI: 10.47593/2675-312X/20223504ecom36i

Cost-effectiveness of UEA

A prospective cohort of 632 consecutive studies of patients with technically limited windows showed a significantly increased number of LV segments visualized after UEA administration versus no UEA in different settings and scenarios (inpatient, intensive care unit, operating room, and elective patients).

The analysis of RPM abnormality detection also showed an increased number of segments visualized with versus UEA in the same scenarios.

The same study evaluated the impact of the association of UEA with echocardiography on the clinical management of these patients. An influence of the contrast-enhanced technique was demonstrated in 35% of cases considering the drug treatment change and the reduced performance of invasive tests such as transesophageal echocardiography or those involving radiation exposure. These results were associated with a cost reduction of USD 122 per patient.[6]

Image generation techniques

The interaction between US and microbubbles is crucial for blood contrast. The use of low-energy US pulses, i.e., with a mechanical index (MI) < 0.2, makes the microbubbles resonate, producing harmonic frequencies that enable the assessment of LV opacification and the study of MP. The use of an ultrasonic pulse with a high MI (>0.8) makes the gas microbubbles expand, retract, and eventually break, thus losing their reflective capacity.

LV opacification images must be acquired with respect to some technical aspects. In addition to the low MI, the focus should be positioned at the level of the mitral valve to reduce microbubble destruction. The ventricular cavity should be homogeneously filled by UEA, with an acoustic shadow on the left atrium and no swirls in the apical region.

Most current devices have presets for UEA use.

UEA administration techniques

UEA infusion amount and rate affect imaging quality. High doses attenuate (cause a shadow) the image, while low

doses shorten the enhancement duration. A rapid infusion rate can lead to high UEA concentrations at the ventricular apex, causing attenuation artifacts in the LV basal region by generating a shadow on the ventricular cavity, while a slow infusion rate can lead to swirl formation and incomplete opacification (Figure 1 e Video 1).

Initially, peripheral venous access should be punctured in one of the upper limbs (preferably antecubital) with a larger caliber catheter (18–22) to preserve microbubble integrity. Connectors and intermediate tubes should be avoided, as should the use of a 3-way tap with the syringe containing the UEA in the straight position and the saline solution in the transverse line (T) since the microbubbles can be destroyed in the tap "curve." After UEA infusion, the subsequent saline solution flush should be delivered smoothly and slowly.

In Brazil, the available UEA is the SonoVue® (Bracco, Italy), which is used in a bolus infusion of 1.0 mL of pure agent followed by a bolus of 10 mL of 0.9% saline solution for each group of images to be acquired. It is also possible to optimize this bolus by lifting the injected arm 90 degrees (usually the right upper arm). The volume should be adjusted in subsequent injections according to obtained image quality.

Clinical applications

The only formal recommendation approved for UEA use in the assessment of cardiovascular disease is aimed at LV opacification when at least two contiguous myocardial segments are not well visualized during the conventional echocardiographic study. However, current guidelines supported by recent scientific evidence consider other applications such as MP and intracardiac mass assessment, spectral Doppler signal enhancement, and stress echocardiography.[5]

Quantification of volumes, EF, and regional LV parietal motility

Echocardiographic windows with suboptimal images and the presence of myocardial trabeculations hinder the correct identification of the blood interface with the compacted myocardium. After UEA injection, the contrasted blood fills the intra-trabecular spaces up to the compacted myocardium, allowing a more accurate assessment and making ventricular volume measurements more reproducible. These images should be acquired when the LV is completely opacified and the volumes quantified by the two-dimensional biplanar method performed by tracing the interface of the compacted myocardium and the ventricular cavity, excluding the trabeculae (Figure 2).[7] Ventricular volumes obtained by CE are greater than those found in non-contrast two- and three-dimensional echocardiograms with good correlation with the ventricular volumes found in cardiac magnetic resonance imaging.[8]

RPM analysis is a subjective assessment that depends on image quality. Thus, UEA should be used to assess ventricular volumes, quantify ejection fraction, and in situations in which volume analysis and RPM require diagnostic accuracy, such as in coronary heart disease, cardiomyopathies, and the follow-up of patients using cardiotoxic drugs.[9]

Echocardiography with myocardial perfusion

Since it presents behavior similar to that of red blood cells, UEA works as a marker of myocardial blood flow. Thus, myocardial perfusion echocardiography (MPE) can be used to assess risk area during AMI, viability after AMI (no-reflow identification), reperfusion therapy efficacy, and in the context of chronic coronary artery disease (Videos 2A, 2B, 2C).

MPE is performed after the infusion of small UEA bolus in low MI images, followed by the application of a high MI ultrasonic pulse – called a flash – to destroy the microbubbles and allow the subsequent analysis of their refilling in the myocardium (Figure 3).[9,10]

MP can be quantitatively evaluated through software post-processing (not yet commercially available for clinical use) or qualitatively evaluated through visual analysis. Qualitative analysis uses a semi-quantitative score with the following graduations: 1 = normal MP (with intense enhancement within 4 s after the flash); 2 = hypoperfusion (normal or

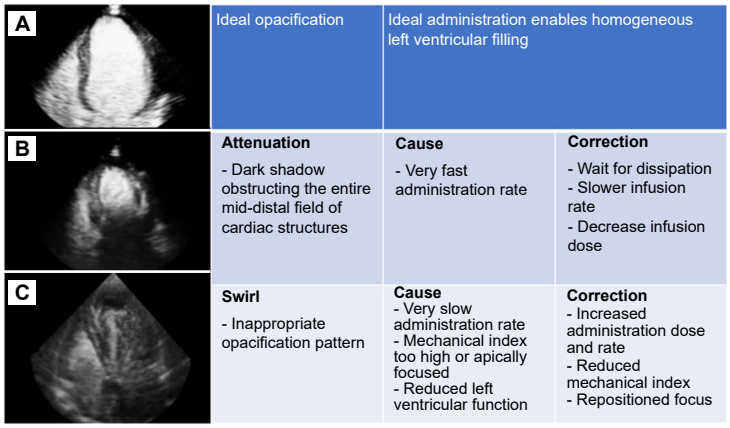

LV: left ventricle; MI: mechanical index.

Figure 1 – *Technical aspects of ventricular opacification. (a) Apical four-chamber plane focused on the right ventricle. Ideal opacification. (B) Apical four-chamber plane. Attenuation. (a) Apical four-chamber plane. Swirling. Video 1.*

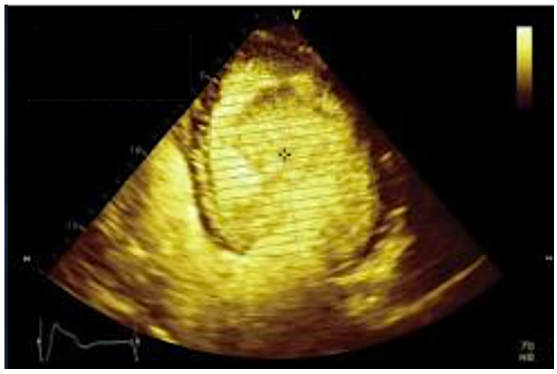

Figure 2 – *Apical four-chamber plane on contrast echocardiography showing sample ejection fraction calculation.*

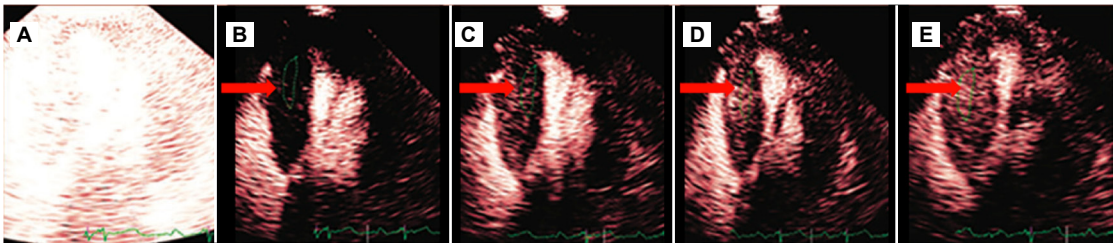

Figure 3 – *Apical four-chamber plane on sample myocardial perfusion echocardiography demonstrating myocardial refilling with an ultrasound enhancing agent after a flash (A) illustrated as a bright frame. After the high mechanical index pulse, microbubbles are destroyed (B), followed by myocardial refilling in subsequent images (C, D, E).*

rarefied enhancement 4–10 s after the flash); and 3 = no MP (little or no enhancement more than 10 s after the flash). Thus, normal myocardial refilling should occur in up to 4 s at rest and in up to 2 s during stress. The presence of normal MP in a given segment is considered a sign of myocardial viability.

Intracardiac abnormalities

Masses can correspond to innocent structures such as a false tendon, accessory papillary muscle, and prominent trabeculation; or pathological structures such as a thrombus or tumor. Thus, UEA can be used to confirm or exclude a suspected finding in this context.

Intracardiac thrombi

Despite advances in other imaging modalities, echocardiography is the most commonly. used initial diagnosis and risk stratification tool for patients predisposed to developing intracardiac thrombi.

LV thrombi are commonly located in the apical region. Their identification by conventional echocardiography can be challenging; however, using CE, the thrombus is visualized as a "filling defect" since the UEA does not penetrate its interior since it is an avascular structure (Figure 4A).[11]

Intracardiac masses

MPE characterizes the vascularization of cardiac masses, helping differentiate between malignant and benign tumors. This evaluation is qualitative and based on the visual analysis of the UEA refill time after a flash.

Benign tumors such as myxomas are poorly vascularized and have a perfusion similar to that of the myocardium (Figure 4B).

Malignant tumors are hypervascularized. Thus, increased tumor mass perfusion suggests malignancy (Figure 4C).[12]

Hypertrophic cardiomyopathy

CE can be performed in suspected cases of hypertrophic cardiomyopathy (HCM), especially the apical variant in which cardiac apex visualization is challenging.

Complete opacification of the LV by the UEA allows the identification of apical segment hypertrophy and the typical spade-like shape of the ventricular cavity in diastole (Figure 5A). Complications associated with HCM such as apical aneurysm and thrombus can also be identified.[13]

Noncompaction myocardium

Complete opacification of the LV cavity facilitates the recognition of deep trabecular recesses characteristic of noncompaction myocardium, increasing differentiation between compacted and non-compacted portions of the myocardium.[14]

Complications after myocardial infarction

In limited echocardiographic windows, CE may be essential

for visualizing LV aneurysm and associated complications such as thrombus (Figure 5C). Pseudoaneurysms, free wall rupture, and interventricular septum communications can also be identified using UEA.[15]

Stress echocardiogram

CE can increase the sensitivity, specificity, and diagnostic accuracy of tests under physical or pharmacological stress due to the adequate visualization of endocardial borders and RPM (Figure 6).[16]

The UEA should be administered with the patient at rest and later at peak stress 5–10 s before the end of the exercise or during the infusion of the pharmacological agent using the same route to compare the two moments. Additionally, an MP analysis helps assess subtle contractility abnormalities due to subendocardial ischemia since perfusion abnormalities occur before parietal motility abnormalities in the progression of the ischemic cascade.[17]

Therefore, the use of UEA during stress echocardiography is recommended whenever at least one myocardial segment is not well visualized.[18]

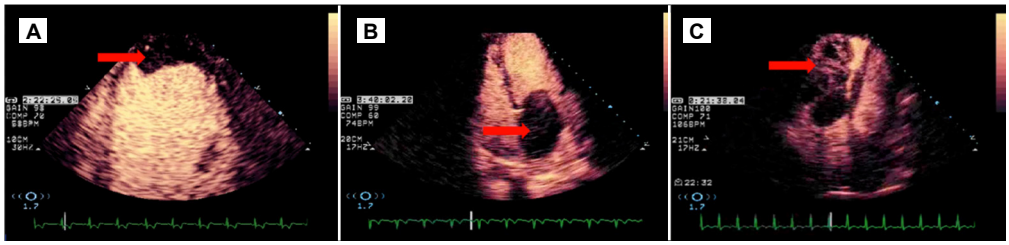

Figure 4 – *(A) Apical four-chamber plane on sample myocardial perfusion echocardiography focused on the right ventricle showing an unenhanced mass consistent with a thrombus. Video 3A. (B) Apical four-chamber plane of a left atrial myxoma mass with almost no enhancement.Video 3B. (C) Apical four-chamber plane of a right ventricle metastasis. The hypervascular mass demonstrates increased perfusion and areas of necrosis. Video 3C.*

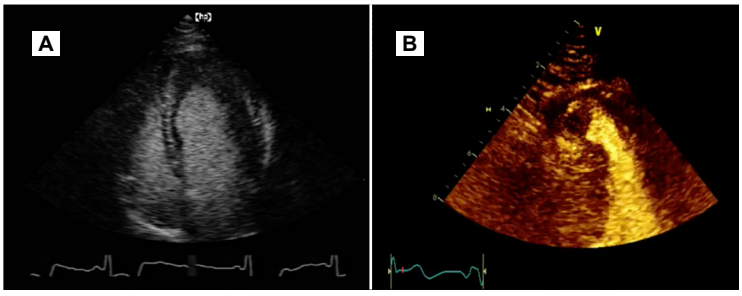

Figure 5 – *(A) Apical four-chamber plane on cardiac echocardiography demonstrating apical myocardial hypertrophy. Video 4A. (B) Apical two-chamber plane on cardiac echocardiography focused on the left ventricle showing an apical aneurysm with a thrombus. Video 4B.*

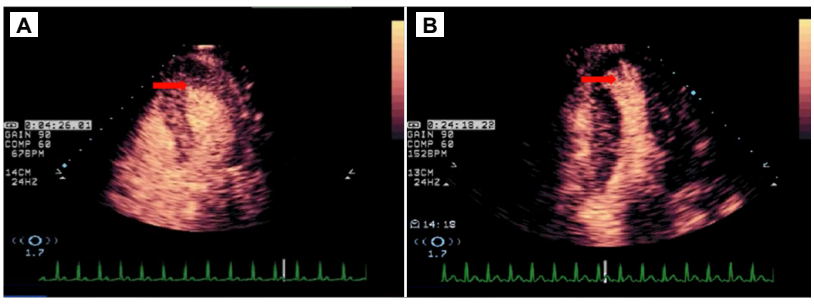

Figure 6 – *Sample contrast echocardiography under pharmacological stress with dobutamine and atropine. (A) Apical four-chamber plane at rest showing normal regional parietal motility and myocardial perfusion (red arrow). Video 5A. (B) Apical four-chamber plane at peak stress showing akinesia and a myocardial perfusion defect in the apical region (red arrow). Video 5B.*

Conclusion

CE is considered an essential component of a modern echocardiography laboratory due to its ability to provide unique information that improves the diagnosis of cardiovascular disease. Implementing UEA requires knowledge on agent-specific imaging protocols, a process that identifies patients likely to benefit from its use, and sound laboratory policies that ensure quality, efficiency, and safety.

Authors' contributions

Conception and writing of the manuscript: Aguiar, MOD; Oliveira, AJ; Stangenhaus, C; Critical revision of the manuscript important intellectual content: Mathias, W.

Conflict of interest

The authors have declared that they have no conflict of interest.

References

1. Elder SA. Cavitation microstreaming. The Journal of the Acoustical Society of America. 1959;31(1);54-64. doi: https://doi.org/10.1121/1.1907611
2. Blinc A, Francis CW, Trudnowski JL, Carstensen EL. Characterization of ultrasound-potentiated fibrinolysis in vitro. Blood. 1993;81(10):2636-43. PMID: 8490172.
3. Khawaja OA, Shaikh KA, Al-Mallah MH. Meta-analysis of adverse cardiovascular events associated with echocardiographic contrast agents. Am J Cardiol. 2010;106:742-7. doi: https://doi.org/10.1016/j.amjcard.2010.04.034
4. Aggeli C, Giannopoulos G, Roussakis G, Christoforatou E, Marinos G, Toli C, et al. Safety of myocardial flash-contrast echocardiography in combination with dobutamine stress testing for the detection of ischaemia in 5250 studies. Heart. 2008;94(12):1571-7. doi: https://doi.org/10.1136/hrt.2007.135145
5. Porter TR, Mulvagh SL, Abdelmoneim SS, Becher H, Belcik JT, Bierig M, et al. Clinical Applications of Ultrasonic Enhancing Agents in Echocardiography: 2018 American Society of Echocardiography Guidelines Update. J Am Soc Echocardiogr. 2018;31(3):241-74. doi: https://doi.org/10.1016/j.echo.2017.11.013
6. Kurt M, Shaikh KA, Peterson L, Kurrelmeyer KM, Shah G, Nagueh SF, et al. Impact of contrast echocardiography on evaluation of ventricular function and clinical management in a large prospective cohort. J Am Coll Cardiol. 2009;53(9):802-10. doi: https://doi.org/10.1016/j.jacc.2009.01.005
7. Lang RM, Badano LP, Mor-Avi V, Afilalo J, Armstrong A, Ernande L, et al. Recommendations for cardiac chamber quantification by echocardiography in adults: an update from the American Society of Echocardiography and the European Association of Cardiovascular Imaging. J Am Soc Echocardiogr. 2015;28(1):1-39.e14. doi: https://doi.org/10.1016/j.echo.2014.10.003
8. Hoffmann R, Barletta G, von Bardeleben S, Vanoverschelde JL, Kasprzak J, Greis C, et al. Analysis of left ventricular volumes and function: a multicenter comparison of cardiac magnetic resonance imaging, cine ventriculography, and unenhanced and contrast-enhanced two-dimensional and three-dimensional echocardiography. J Am Soc Echocardiogr. 2014;27(3):292-301. doi: https://doi.org/10.1016/j.echo.2013.12.005
9. Porter TR, Abdelmoneim S, Belcik JT, McCulloch ML, Mulvagh SL, Olson JJ, et al. Guidelines for the cardiac sonographer in the performance of contrast echocardiography: a focused update from the American Society of Echocardiography. J Am Soc Echocardiogr. 2014;27(8):797-810. doi: https://doi.org/10.1016/j.echo.2014.05.011
10. Mulvagh SL, Rakowski H, Vannan MA, Abdelmoneim SS, Becher H, Bierig SM, et al.; American Society of Echocardiography. American Society of Echocardiography Consensus Statement on the Clinical Applications of Ultrasonic Contrast Agents in Echocardiography. J Am Soc Echocardiogr. 2008;21(11):1179-201; quiz 1281. doi: https://doi.org/10.1016/j.echo.2008.09.009
11. Weinsaft JW, Kim RJ, Ross M, Krauser D, Manoushagian S, LaBounty TM, et al. Contrast-enhanced anatomic imaging as compared to contrast-enhanced tissue characterization for detection of left ventricular thrombus. JACC Cardiovasc Imaging. 2009;2(8):969-79. doi: https://doi.org/10.1016/j.jcmg.2009.03.017
12. Kirkpatrick JN, Wong T, Bednarz JE, Spencer KT, Sugeng L, Ward RP, et al. Differential diagnosis of cardiac masses using contrast echocardiographic perfusion imaging. J Am Coll Cardiol. 2004;43(8):1412-9. doi: https://doi.org/10.1016/j.jacc.2003.09.065
13. Thanigaraj S, Pérez JE. Apical hypertrophic cardiomyopathy: echocardiographic diagnosis with the use of intravenous contrast image enhancement. J Am Soc Echocardiogr. 2000;13(2):146-9. doi: https://doi.org/10.1016/s0894-7317(00)90026-9
14. Chow CM, Lim KD, Wu L, Leong-Poi H. Images in cardiovascular medicine. Isolated left ventricular noncompaction enhanced by echocontrast agent. Circulation. 2007;116(4):e90-1. doi: https://doi.org/10.1161/CIRCULATIONAHA.107.699314
15. Moreno R, Zamorano JL, Almería C, Rodrigo JL, Villate A, Serra V, et al. Usefulness of contrast agents in the diagnosis of left ventricular pseudoaneurysm after acute myocardial infarction. Eur J Echocardiogr. 2002;3(2):111-6. doi: https://doi.org/10.1053/euje.2001.0130
16. Mathias W Jr, Arruda AL, Andrade JL, Filho OC, Porter TR. Endocardial border delineation during dobutamine infusion using contrast echocardiography. Echocardiography. 2002;19(2):109-14. doi: https://doi.org/10.1046/j.1540-8175.2002.00109.x
17. Tsutsui JM, Xie F, O'Leary EL, Elhendy A, Anderson JR, McGrain AC, et al. Diagnostic accuracy and prognostic value of dobutamine stress myocardial contrast echocardiography in patients with suspected acute coronary syndromes. Echocardiography. 2005;22(6):487-95. doi: https://doi.org/10.1111/j.1540-8175.2005.40037.x
18. Pellikka PA, Arruda-Olson A, Chaudhry FA, Chen MH, Marshall JE, Porter TR, et al. Guidelines for Performance, Interpretation, and Application of Stress Echocardiography in Ischemic Heart Disease: From the American Society of Echocardiography. J Am Soc Echocardiogr. 2020;33(1):1-41.e8. doi: https://doi.org/10.1016/j.echo.2019.07.001

Review Article

The Role of Cardiac Magnetic Resonance in patients with Amyloidosis and Aortic Stenosis

O Papel da Ressonância Magnética Cardíaca em Pacientes com Amiloidose e Estenose Aórtica

Pedro Macedo Esmeraldo Barbosa[1]; *Tiago Augusto Magalhães*[1]
[1]*Hospital do Coração, São Paulo, SP, Brazil.*

Abstract

Cardiac magnetic resonance imaging (CMR) plays an important role in the diagnosis and prognosis of various heart diseases. The incidence of cardiac amyloidosis and aortic stenosis has been increasing in recent years, especially with the aging population, and their possible coexistence has created frequent diagnostic challenges in clinical practice. CMR assumes an important value in this context due to its unique capacity for multiparametric assessment evaluations that include anatomical, functional, and histopathological aspects. The present review aimed to increase our knowledge of the diagnosis and prognosis of amyloidosis in the presence of aortic stenosis and highlighted the importance of CMR in this scenario.

Introduction

The coexistence of cardiac amyloidosis (CA) and aortic stenosis (AS) has increasing relevance in clinical practice due to its high prevalence, diagnostic difficulty, and therapeutic management challenges. Primary CA forms feature amyloid light chain amyloidosis (AL) and transthyretin amyloidosis (ATTR) as the main presentations affecting up to 25% of octogenarians,[1] especially the latter. On the other hand, AS has a prevalence of up to 4% among individuals over 70 years,[2] with calcific degeneration as its main etiological landmark. CA[3] affects an estimated 5–16% of patients with major AS, reaching 30% in cases of low-flow low-gradient AS.[2]

The correlation between the two diseases can be explained by several factors, with the common prevalent age group being the most important. The second factor is related to the histological analysis of valves removed in valve replacement surgeries, demonstrating amyloid deposits in 74% of stenotic aortic valves, inferring the possibility of AS and CA having a similar pathophysiological pathway.[4] Another possible factor is mediated by increased AS afterload, which would potentially trigger amyloid protein accumulation in the ventricular myocardium.[4]

Keywords

Magnetic resonance imaging; Heart; Amyloidosis; Aortic valve stenosis.

Mailing Address: Tiago Augusto Magalhães •
Rua Desembargador Eliseu Guilherme, 147, Paraíso. CEP: 04004-030
São Paulo, SP, Brazil.
E-mail: tiaugusto@gmail.com
Manuscript received 6/24/2022; revised 7/11/2022; accepted 8/9/2022

Editor responsible for the review: Tiago Senra Garcia dos Santos

DOI: 10.47593/2675-312X/20223503eabc320i

The prognosis of patients with CA and AS tends to be worse than that of patients with isolated AS, which directly interferes with its therapeutic management. CA alone has a variable prognosis. The reported median survival of patients with ATTR is 24.1–69.2 months, while that of patients with AL is 3.5–26.4 months[5] (Figure 1). In a retrospective study, patients with ATTR + major AS had significantly better 1-year overall mortality than those with major AS alone (56% vs. 20%, $p < 0.0001$).[6] A study of patients with ATTR + AS versus AS alone showed that the former had an overall mortality that was almost twice as high (mean follow-up, 1.7 years) regardless of transcatheter aortic valve replacement (TAVR) or exclusive clinical maintenance (24.5% vs. 13.9%; $p < 0.05$). There is also evidence of no difference in 2-year mortality rates between patients with isolated ATTR and those with major ATTR + AS (33% vs. 37%, respectively; hazard ratio, 1.22; 95% confidence interval, 0.62–2.42; $p = 0.566$), even among the latter undergoing valve replacement, which suggests that ATTR would have a greater impact on mortality.[6] On the other hand, there is evidence of improved prognosis among patients with ATTR + AS undergoing valve replacement versus those remaining on clinical treatment,[3,7] while small studies reported the superiority of TAVR to surgical aortic valve replacement (SAVR) in patients with ATTR + AS.[2] Due to the higher prevalence of ATTR versus AL, it is important to emphasize that most patients with CA + AS included in the studies have the ATTR form.

Due to the high prevalence and impact of the association between CA and AS, it is essential to investigate CA in patients with AS who are eligible for valve replacement. Diagnostic flow involves three main steps: 1) identifying suspected signs; 2) performing scintigraphy/monoclonal protein peak surveys; and 3) defining the diagnosis (with vs. without biopsy or genotyping). Cardiac magnetic resonance imaging (CMRI) is a fundamental diagnostic method for CA in the presence of AS (Figure 2) due to its ability to detect relevant morphological functional changes. CMRI can also individualize the prognosis of CA and AS by aiding the identification of patients who will benefit most from valve replacement.

CMRI diagnosis

Cardiac adaptations to increased afterload by AS are similar to those that occur in CA (e.g., concentric left ventricle remodeling). In addition, the presence of other diseases, such as coronary insufficiency and systemic arterial hypertension, interferes with the accuracy of several methods in the diagnosis of AS-associated CA. In this context, CMRI performs well (sensitivity, 85%; specificity, 92%) for diagnosing CA.[8] Due to its multiparameter analysis, it is also fundamental in the diagnosis of AS-associated CA (Figure 2) or AS alone.

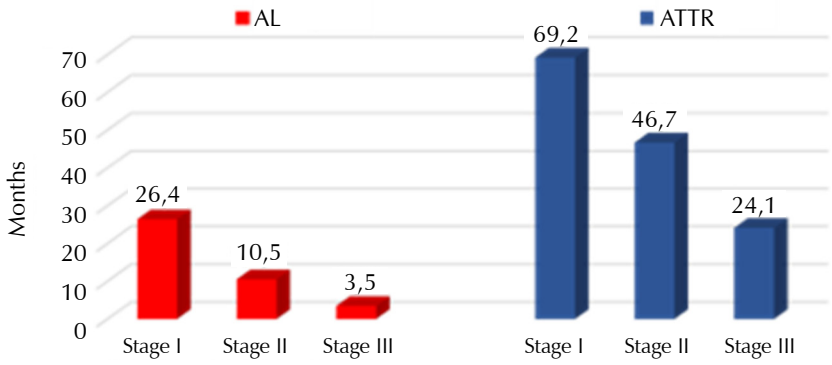

Source: adaptado de Cappelli et al.[5] AL amyloidosis staging: I: cTnI < 0.1 µg/L and NT-proBNP < 332 ng/L; II: cTnI ≥ 0.1 µg/L or NT-proBNP ≥ 332 ng/L; III: cTnI ≥ 0.1 µg/L and NT-proBNP ≥ 332 ng/L. ATTR amyloidosis staging: I: eGFR ≥ 45 mL/min/1.73 m2 Pand NT-proBNP ≤ 3000 ng/L; II: eGFR < 45 mL/min/1.73 m2 or NT-proBNP > 3,000 ng/L; III: eGFR < 45 mL/min/1.73 m2 and NT-proBNP > 3,000 ng/L eGFR, estimated glomerular filtration rate; NT-proBNP, N-terminal pro-brain natriuretic peptide; TnI, cardiac troponin I; TnT, cardiac troponin T .

Figure 1 – *Median survival of patients with AL vs. ATTR amyloidosis.*

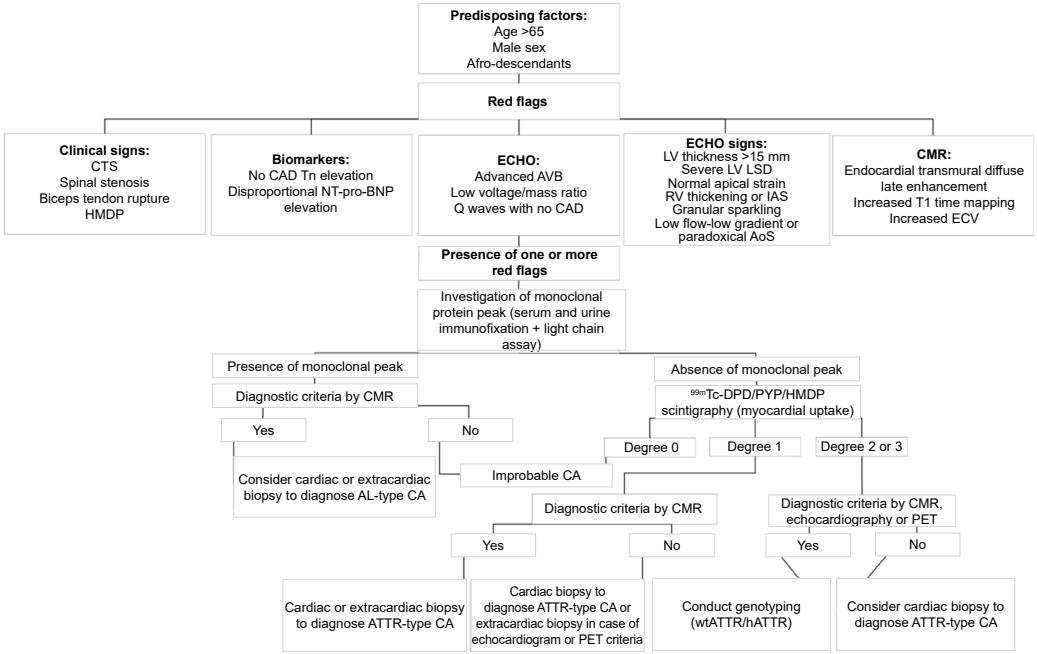

AL, light chain amyloidosis; ATTR, transthyretin amyloidosis; AVB, atrioventricular block; CA, cardiac amyloidosis; CTS, carpal tunnel syndrome; Tc-99m-DPD, technetium-99m with 3,3-diphosphono-1,2-propanedicarboxylic acid; ECV, extracellular volume; hATTR, hereditary transthyretin amyloidosis; HMDP, hydroxymethylenediphosphonate; LSD, longitudinal systolic dysfunction; PPM, permanent pacemaker; PYP, pyrophosphate; Tn, troponin; wATTR, wild (senile) transthyretin amyloidosis. Cardiac magnetic resonance imaging diagnostic criteria: myocardial thickening, ECV ≥ 40%, diffuse late myocardial enhancement, or myocardial inversion time < blood inversion time. Echocardiographic diagnostic criteria: myocardial thickening > 12 mm, apical longitudinal/mid-basal longitudinal strain > 1, or diastolic dysfunction grade ≥ 2.

Figura 2 – *Proposed diagnostic algorithm for CA in the presence of AS. Positron emission tomography diagnostic criteria: target–to–blood pool ratio > 1.5 or retention index > 0.030 min-1.*

Anatomical functional parameters

Left ventricular (LV) myocardial mass thickening and increases, atrial dilatation, and LV diastolic and systolic dysfunction are common in ATTR and AS but more severe when coexistent.

Patients with ATTR + AS versus AS alone have a higher LV mass index (105 ± 21 vs. 73 ± 21 g/m^2) as well as a lower LV ejection fraction and stroke volume (43 ± 17 vs. 52 ± 18% and 33 ± 10 vs. 44 ± 13 mL/m^2, respectively).[1] Myocardial thickening tends to be septally asymmetrical in the presence of ATTR, with a prevalence of 79%, versus concentrically thickened in AL.

Characteristics that are common in CA but uncommon in

AS are pericardial effusion, interatrial septal thickening, biatrial dilatation (Figure 3), atrioventricular valve thickening, and RV thickening (with or without isolated systolic RV dysfunction). Atrial wall thickening occurs in up to 70% of patients with ATTR + AS.[6]

Histological parameters

Noninvasive myocardial histological analysis by CMRI is based on the proton relaxation properties of each tissue used to identify the presence of localized or diffuse fibrosis. Different techniques (late enhancement, native myocardial T1 mapping, myocardial extracellular space volume calculations, myocardial-blood inversion time rate analysis, and myocardial edema investigation) can be used for cardiac tissue characterizations with quantitative measurements that assess the extent of damaged induced by amyloid substance deposits.

Native myocardial T1 mapping

Native myocardial T1 mapping, which analyzes the magnetic characteristic of tissue proton relaxation, is performed without a gadolinium injection. Its primary advantage involves the early identification of myocardial fibrosis, especially that with diffuse distribution, which may not be identified by late enhancement, making the diagnostic evaluation more sensitive. Normal myocardial T1 values may vary according to the machine used and are usually between 950 and 1,050 ms. Patients with isolated CA, CA + AS, or isolated AS may present with a prolonged T1, being significantly higher in patients with CA. Patients with ATTR + AS have higher native T1 values than those with isolated AS (native T1: 1,125 ± 49 vs. 1,035 ± 60 ms; $p = 0.002$).[6]

Myocardial edema research

Myocardial edema may be present in CA but is uncommon in isolated AS. It is diagnosed through T2 time mapping or specific T2-weighted sequences without the need for a gadolinium injection. The presence of myocardial edema with AS should prompt the investigation of other concomitant heart diseases.

Late myocardial enhancement

Late enhancement, which is based on preferential gadolinium uptake in tissues rich in extracellular matrix, aids in the contrast of healthy and pathological myocardium minutes after its administration. The enhancement pattern changes according to etiology. In ATTR, there a basal-apical enhancement distribution occurs that can spare the apical segments (Figure 4). AL has its own characteristics with circumferential subendocardial involvement. The presence of late enhancement in the atrial myocardium (Figure 5) or the RV is frequent in CA, with a prevalence of atrial enhancement of up to 90% and of RV enhancement of 37–97% of ATTR + AS cases.[6] Late enhancement occurs in up to 40% of isolated AS cases, being mainly present in the LV with a focal mesocardial pattern.

Extracellular volume (ECV) analysis is estimated based on native myocardial T1 time, post-contrast T1 time, and patient hematocrit at the time of the examination (normal ECV values are <25 to 27%).[9] Both CA and AS can increase myocardial ECV, but greater increases are seen in the presence of CA, particularly the ATTR type. Patients with ATTR + AS have higher ECV values than those with isolated AS (41.2 ± 16.7 vs. 27.9 ± 4.1%; $p < 0.001$).[6] ECV values > 40% are rare in diseases other than CA. In advanced CA stages, ECV can be more important for the diagnosis than T1 mapping.

Prognosis by CMRI

Patients with CA + AS lack formal therapeutic recommendations regarding the approach to AS, which makes its treatment challenging. A prognostic evaluation before valve replacement is essential, and CMRI can aid the decision, especially through late enhancement analysis and

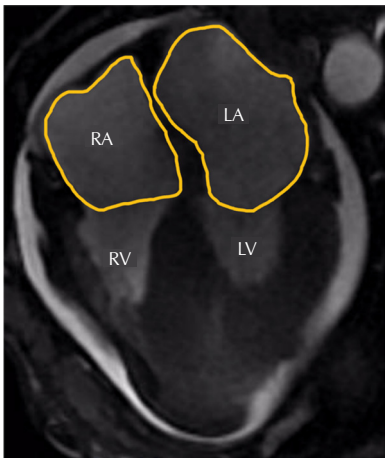

Source: collection Dr. Pedro Macedo. ATTR, transthyretin amyloidosis; LA, left atrium; LV, left ventricle; RA, right atrium; RV, right ventricle. .

Figure 3 – *Cine-resonance image taken of a patient with ATTR amyloidosis showing biatrial dilatation, increased myocardial thickness, and a mild pericardial effusion.*

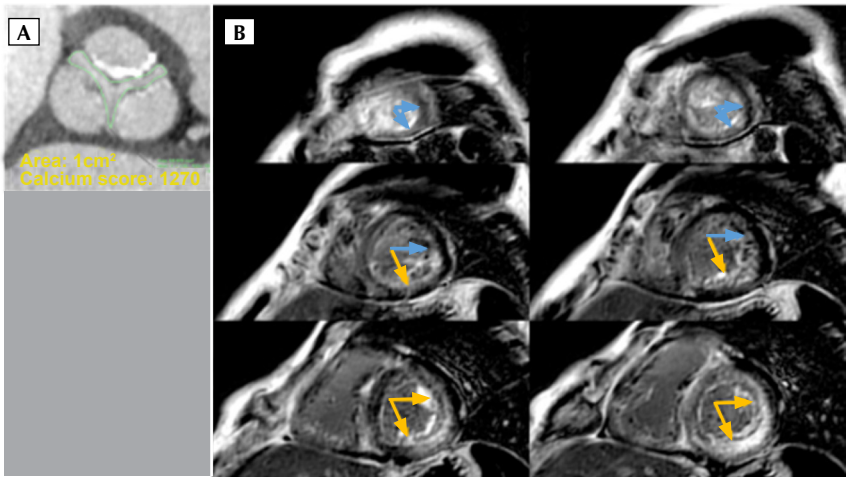

Source: collection Dr. Tiago Serna.

Figura 4 – *Images taken of a patient with AS and ATTR amyloidosis. (A) Computed tomography image demonstrating calcific AS (valve area, 1 cm2; valvular calcium score, 1,270). (B) Cardiac magnetic resonance images showing diffuse late myocardial enhancement more evident in the mid-basal segments compatible with the diagnosis of ATTR CA (orange arrow: late enhancement present; blue arrow: late enhancement absent).*

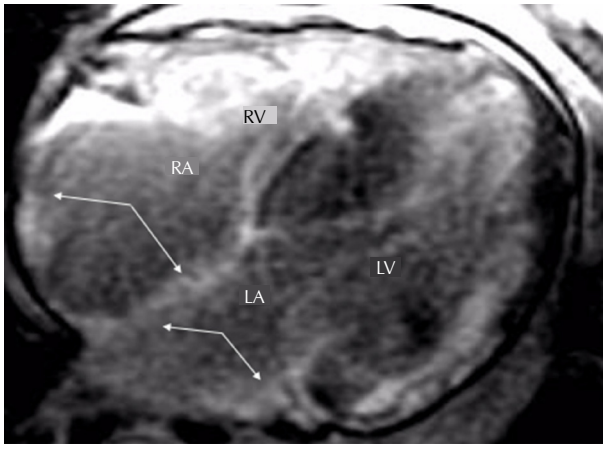

Source: collection Dr. Pedro Macedo. LA, left atrium; LV, left ventricle; RA, right atrium; RV, right ventricle.

Figure 5 – *Images of atrial fibrosis (white arrows) in a patient with ATTR amyloidosis.*

ECV. Late enhancement is a poor independent prognostic factor for all heart diseases. Moderate to severe AS carries an eight-fold increased risk of mortality regardless of stenosis severity. An increased relative risk of major cardiovascular events after aortic valve replacement in the presence of late enhancement has also been documented, as has the possibility of left ventricular dysfunction maintenance post-aortic valve replacement in the presence of late enhancement.[10]

ECV has excellent prognostic value in patients with ATTR + AS since it is correlated with mortality (Figure 6). An ECV < 25% is protective regardless of exclusive clinical treatment or valve replacement, with no reports of cardiovascular death within 1 year.[1]

Increased native myocardial T1 mapping interpreted in isolation showed only a tendency to be correlated with prognosis in patients with ATTR + AS, but the difference was not statistically significant (Figure 6).[1] Further studies with a greater number of patients may provide additional information about the use of native myocardial T1 mapping in the prognostic definition of this patient group.

Conclusion

CA and AS are increasingly encountered in clinical practice, mainly due to an increased number of diagnoses and continued population aging. The diagnosis of CA

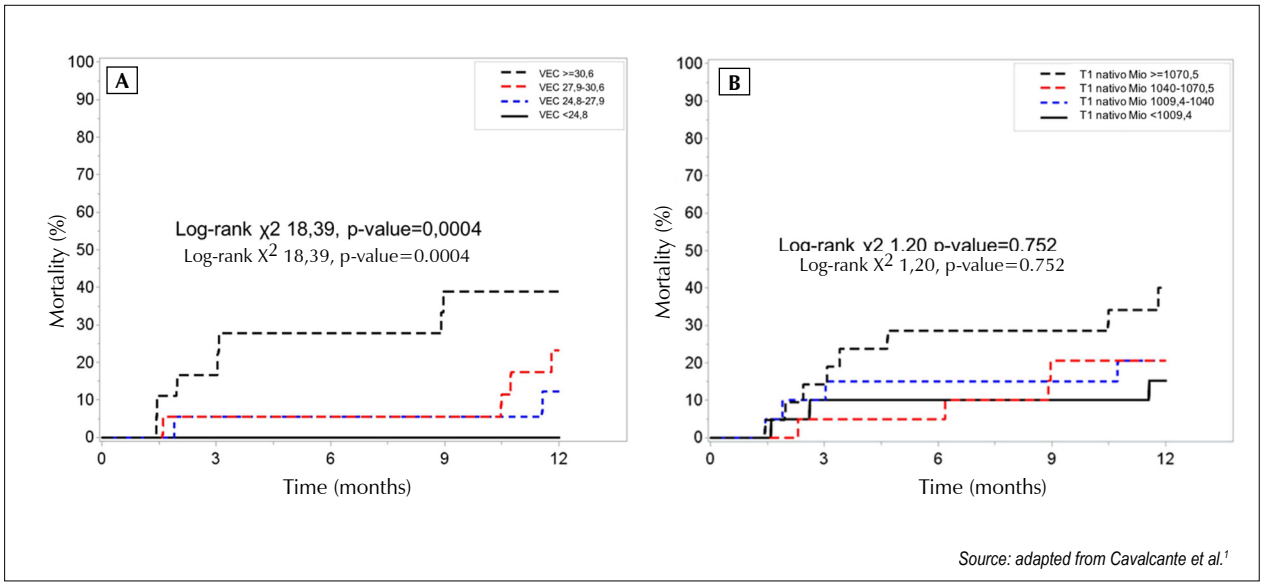

Figure 6 – *Mean survival of patients with CA + AS by ECV (A) or T1 time (B).*

should be considered in cases of suspicious signs or when phenotypic cardiac changes are noted beyond those expected according to AS severity. CMRI, which plays an important role in the diagnosis and prognosis of patients with CA + AS, is a fundamental test that enables more assertive therapeutic decisions.

Authors' contributions

Research conception and design: Barbosa PME, Magalhães TA; data collection: Barbosa PME, Magalhães TA; data analysis and interpretation: Barbosa PME, Magalhães TA; statistical analysis: Barbosa PME, Magalhães TA; funding: Barbosa PME, Magalhães TA; manuscript writing: Barbosa PME, Magalhães TA; critical review of the manuscript for important intellectual content: Barbosa PME, Magalhães TA.

Conflict of interest

The author declares that he has no conflict of interest

References

1. Cavalcante JL, Rijal S, Abdelkarim I, Althouse AD, Sharbaugh MS, Fridman Y, et al. Cardiac amyloidosis is prevalent in older patients with aortic stenosis and carries worse prognosis. J Cardiovasc Magn Reson. 2017;19(1):98. doi: https://doi.org/10.1186/s12968-017-0415-x
2. Ternacle J, Krapf L, Mohty D, Magne J, Nguyen A, Galat A, Gallet R, et al. Aortic Stenosis and Cardiac Amyloidosis: JACC Review Topic of the Week. J Am Coll Cardiol. 2019;74(21):2638-51. doi: https://doi.org/10.1016/j.jacc.2019.09.056
3. Nitsche C, Aschauer S, Kammerlander AA, Schneider M, Poschner T, Duca F, et al. Light-chain and transthyretin cardiac amyloidosis in severe aortic stenosis: prevalence, screening possibilities, and outcome. Eur J Heart Fail. 2020;22(10):1852-62. doi: https://doi.org/10.1002/ejhf.1756
4. Galat A, Guellich A, Bodez D, Slama M, Dijos M, Zeitoun DM, et al. Aortic stenosis and transthyretin cardiac amyloidosis: the chicken or the egg? Eur Heart J. 2016;37(47):3525-31. doi: https://doi.org/10.1093/eurheartj/ehw033
5. Cappelli F, Perfetto F, Martone R, Di Mario C. Cardiac Amyloidosis in Patients Undergoing TAVR: Why We Need to Think About It. Cardiovasc Revasc Med. 2021;22:109-14. doi: https://doi.org/10.1016/j.carrev.2020.06.005
6. Balciunaite G, Rimkus A, Zurauskas E, Zaremba T, Palionis D, Valeviciene N, Aidietis A, et al. Transthyretin cardiac amyloidosis in aortic stenosis: Prevalence, diagnostic challenges, and clinical implications. Hellenic J Cardiol. 2020;61(2):92-8. doi: https://doi.org/10.1016/j.hjc.2019.10.004
7. Griffin JM, Rosenthal JL, Grodin JL, Maurer MS, Grogan M, Cheng RK. ATTR Amyloidosis: Current and Emerging Management Strategies: *JACC: CardioOncology* State-of-the-Art Review. JACC CardioOncol. 2021;3(4):488-505. doi: https://doi.org/10.1016/j.jaccao.2021.06.006
8. Yilmaz A. The "Native T1 Versus Extracellular Volume Fraction Paradox" in Cardiac Amyloidosis: Answer to the Million-Dollar Question? JACC Cardiovasc Imaging. 2019;12(5):820-2. doi: https://doi.org/10.1016/j.jcmg.2018.03.029
9. Sado DM, Flett AS, Banypersad SM, White SK, Maestrini V, Quarta G, Lachmann RH, et al. Cardiovascular magnetic resonance measurement of myocardial extracellular volume in health and disease. Heart. 2012;98(19):1436-41. doi: https://doi.org/10.1136/heartjnl-2012-302346
10. Bohbot Y, Renard C, Manrique A, Levy F, Maréchaux S, Gerber BL, Tribouilloy C. Usefulness of Cardiac Magnetic Resonance Imaging in Aortic Stenosis. Circ Cardiovasc Imaging. 2020;13(5):e010356. doi: https://doi.org/10.1161/CIRCIMAGING.119.010356

11. Dorbala S, Ando Y, Bokhari S, Dispenzieri A, Falk RH, Ferrari VA, et al. ASNC/AHA/ASE/EANM/HFSA/ISA/SCMR/SNMMI expert consensus recommendations for multimodality imaging in cardiac amyloidosis: Part 2 of 2-Diagnostic criteria and appropriate utilization. J Nucl Cardiol. 2020;27(2):659-73. doi: https://doi.org/10.1007/s12350-019-01761-5. Erratum in: J Nucl Cardiol. 2021;28(4):1763-7.

12. Nitsche C, Scully PR, Patel KP, Kammerlander AA, Koschutnik M, Dona C, et al. Prevalence and Outcomes of Concomitant Aortic Stenosis and Cardiac Amyloidosis. J Am Coll Cardiol. 2021;77(2):128-39. doi: https://doi.org/10.1016/j.jacc.2020.11.006

13. Kristen AV, Schnabel PA, Winter B, Helmke BM, Longerich T, Hardt S, et al. High prevalence of amyloid in 150 surgically removed heart valves--a comparison of histological and clinical data reveals a correlation to atheroinflammatory conditions. Cardiovasc Pathol. 2010;19(4):228-35. doi: https://doi.org/10.1016/j.carpath.2009.04.005

14. Longhi S, Lorenzini M, Gagliardi C, Milandri A, Marzocchi A, Marrozzini C, et al. Coexistence of Degenerative Aortic Stenosis and Wild-Type Transthyretin-Related Cardiac Amyloidosis. JACC Cardiovasc Imaging. 2016;9(3):325-7. doi: https://doi.org/10.1016/j.jcmg.2015.04.012

15. Castaño A, Narotsky DL, Hamid N, Khalique OK, Morgenstern R, DeLuca A, Rubin J, et al. Unveiling transthyretin cardiac amyloidosis and its predictors among elderly patients with severe aortic stenosis undergoing transcatheter aortic valve replacement. Eur Heart J. 2017;38(38):2879-87. doi: https://doi.org/10.1093/eurheartj/ehx350

16. Scully PR, Patel KP, Treibel TA, Thornton GD, Hughes RK, Chadalavada S, et al. Prevalence and outcome of dual aortic stenosis and cardiac amyloid pathology in patients referred for transcatheter aortic valve implantation. Eur Heart J. 2020;41(29):2759-67. doi: https://doi.org/10.1093/eurheartj/ehaa170

17. Treibel TA, Fontana M, Gilbertson JA, Castelletti S, White SK, Scully PR, et al. Occult Transthyretin Cardiac Amyloid in Severe Calcific Aortic Stenosis: Prevalence and Prognosis in Patients Undergoing Surgical Aortic Valve Replacement. Circ Cardiovasc Imaging. 2016;9(8):e005066. doi: https://doi.org/10.1161/CIRCIMAGING.116.005066

18. Treibel TA, Fontana M, Gilbertson JA, Castelletti S, White SK, Scully PR, et al. Occult Transthyretin Cardiac Amyloid in Severe Calcific Aortic Stenosis: Prevalence and Prognosis in Patients Undergoing Surgical Aortic Valve Replacement. Circ Cardiovasc Imaging. 2016;9(8):e005066. doi: https://doi.org/10.1161/CIRCIMAGING.116.005066

Myocardial Work: a Systematic Review of Novel Echocardiography Method and Clinical Applications

Trabalho Miocárdio: uma Revisão Sistemática do Novo Método de Ecocardiografia e Aplicações Clínicas

Sidhi Laksono[1,2], Hillary Kusharsamita[3], Mefri Yanni[4], Astri Astuti[5]

[1]RS Pusat Pertamina, Department of Cardiology and Vascular Medicine, South Jakarta, Indonesia; [2]Universitas Muhammadiyah Prof Dr Hamka, Faculty of Medicine, Tangerang, Indonesia; [3]Universitas Diponegoro,Faculty of Medicine, Semarang, Indonesia; [4]University of Andalas, Medical Faculty, DR M Djamil Hospital, Department of Cardiology and Vascular Medicine, Padang, Indonesia; [5]Universitas Padjadjaran, Hasan Sadikin General Hospital, Department of Cardiology and Vascular Medicine, Bandung, Indonesia.

Abstract

Background: Myocardial work (MW) is a novel imaging modality that has emerged as a potential left ventricular (LV) function assessment in various clinical settings. MW calculates speckle-tracking echocardiography strain curves with an estimated LV pressure curve by non-invasively utilizing standard brachial blood pressure curves. Objective: This study aimed to provide a summary of current knowledge of non-invasive MW and its clinical applications, including in heart failure, coronary artery disease, cardiomyopathy, and hypertension. In addition, the limitations, and recommendations of MW in clinical practice are discussed. Methods: We searched the PubMed database using the following keywords: (myocardial constructive work) OR (wasted septal work) OR (global myocardial work) OR (myocardial work) OR (myocardial constructive work) OR (novel echocardiography). We further subjected 12 studies to full-text review and included them in this systematic review. Results: While MW indices, particularly global work index and global constructed work, have shown good correlations with ejection fraction (EF) and strain parameters, the opportunity of offering incremental information that is unaffected by loading conditions has made MW application particularly useful in a variety of clinical settings. Conclusion: Compared to EF and global longitudinal strain, MW is a promising test with higher sensitivity and accuracy for identifying individuals with cardiovascular disease. Clinicians should also evaluate symptoms and electrocardiographic findings until extensive multicenter studies validating this strategy are performed to establish the incremental value of MW in daily echocardiographic assessments.

Keywords

Myocardial Contraction, Left Ventricular Function, Echocardiography, Noninvasive Method.

Mailing Address: Sidhi Laksono •
Fakultas Kedokteran Universitas Muhammadiyah Prof Dr Hamka, Jl. Raden Patah No.01, RT.002/RW.006, Parung Serab, Kec. Ciledug, Kota Tangerang, Banten 13460.
E-mail: sidhilaksono@uhamka.ac.id
Manuscript received 4/29/2022; revised 6/15/2022; accepted 9/5/2022

Editor responsible for the review: Marco S. Lofrano Alves

DOI: 10.47593/2675-312X/20223504eabc299i

Introduction

The assessment of left ventricular (LV) systolic function is critical in all echocardiographic studies. The first-line method for describing LV systolic function is LV ejection fraction (LVEF). Despite its widespread usage, LVEF depends on geometric presumptions and is extremely load-dependent, resulting in substantial loss of reproducibility, and may be driven by changes in geometry and it is insufficiently sensitive at detecting decreasing ventricular function. All of these issues encouraged the exploration of novel myocardial function indicators.[1,2]

In the last decade, speckle-tracking echocardiography (STE) has transformed LV function evaluations. Peak global longitudinal strain (GLS), obtained from STE, has arisen as a highly sensitive method of detecting early LV dysfunction and has been utilized instead of LVEF in several clinical settings.[3] However, many studies have shown that GLS, similar to LVEF, has significant load dependency; hence, it is affected by elevated pre- or after-load.[4] In recent years, myocardial work (MW) has emerged as an alternative myocardial function assessment tool.

Russel et al. further evaluated MW non-invasively by coupling STE segmental strain curves with an estimated LV pressure curve in which systolic cuff pressure is employed as a substitute for LV peak pressure.[5] The method has been validated for many diseases, with high concordance to that of the invasive method.[6] This application is beneficial because it combines blood pressure measurements with a non-invasive approach using a simple brachial cuff, making the technology feasible in everyday practice in echocardiography facilities. As a result, MW is an alternate tool for assessing cardiac mechanics and a less load-dependent but non-invasive LV performance assessment method.[7,8]

Here we aimed to provide an up-to-date summary of the current understanding of non-invasive MW, its clinical application, future direction, limitation, and recommendation in clinical practice.

MW definition and analysis

The MW echocardiographic assessment procedure uses the same principle and practical approaches as the two-dimensional image capture process for GLS analysis by STE. The following are the MW and its component, namely global work index (GWI), global work efficiency (GWE), global constructed work (GCW), and global wasted work (GWW) presented in Table 1.

Using the same bull's-eye plot as for the GLS analysis, the

GWI bull's-eye canals are visually evaluated using a color scale, with red indicating high work, green indicating normal work, and blue indicating negative work. The shift from zero to a negative number on the color scale of wasted effort is shown in dark blue. As a result, lighter blue indicates decreased but still positive work, whereas deeper blue is used to code the transition to zero. On the other hand, GWE is also shown in a segmented bull's-eye format with numerical values and colored scaling. Green denotes locations with high efficiency (closer to 100%), while red denotes poor efficiency areas (closer to 0%).[9]

Table 1 - Definition of myocardial work components.[30]

Variable	Meaning
Global work index	Total work within the area of the left ventricular (LV) pressure-strain loop, from mitral valve closure to mitral valve opening
Global constructive work (GCW)	Myocardial work performed during LV shortening in systole and LV lengthening during the isovolumic relaxation phase
Global wasted work (GWW)	Myocardial work performed during LV lengthening in systole and LV shortening during the isovolumic relaxation phase
Global work efficiency	Calculated as the ratio of GCW/(GCW + GWW)

Method

This systematic review was designed and performed in accordance with the Preferred Reporting Items for Systematic Reviews and Meta-Analyses guidelines. We reviewed English-language studies published during the last 10 years that investigated the clinical application of MW in cardiovascular diseases, particularly heart failure (HF), coronary artery disease (CAD), cardiomyopathy (CMP), and hypertension (HTN).

Two independent authors searched the PubMed database on March 5, 2022, using the following keywords: (myocardial constructive work) OR (wasted septal work) OR (global myocardial work) OR (myocardial work) OR (myocardial constructive work) OR (novel echocardiography). Only studies that were previously peer-reviewed were considered for inclusion in our review. Reviews, case reports, editorials, comments, and letters were excluded. The study consort flowchart is shown in Figure 1.

Each abstract was examined separately by the authors. If at least one of the authors considered the research suitable, the full text was reviewed. In the event of disagreement, the authors discussed the reasons for their judgments before reaching a final resolution. Data were extracted from the studies, recorded in Microsoft Excel, and checked and confirmed by two authors (SL and HK). The extracted data of each study included the following: authors' names, outcome assessed, participants, and main result.

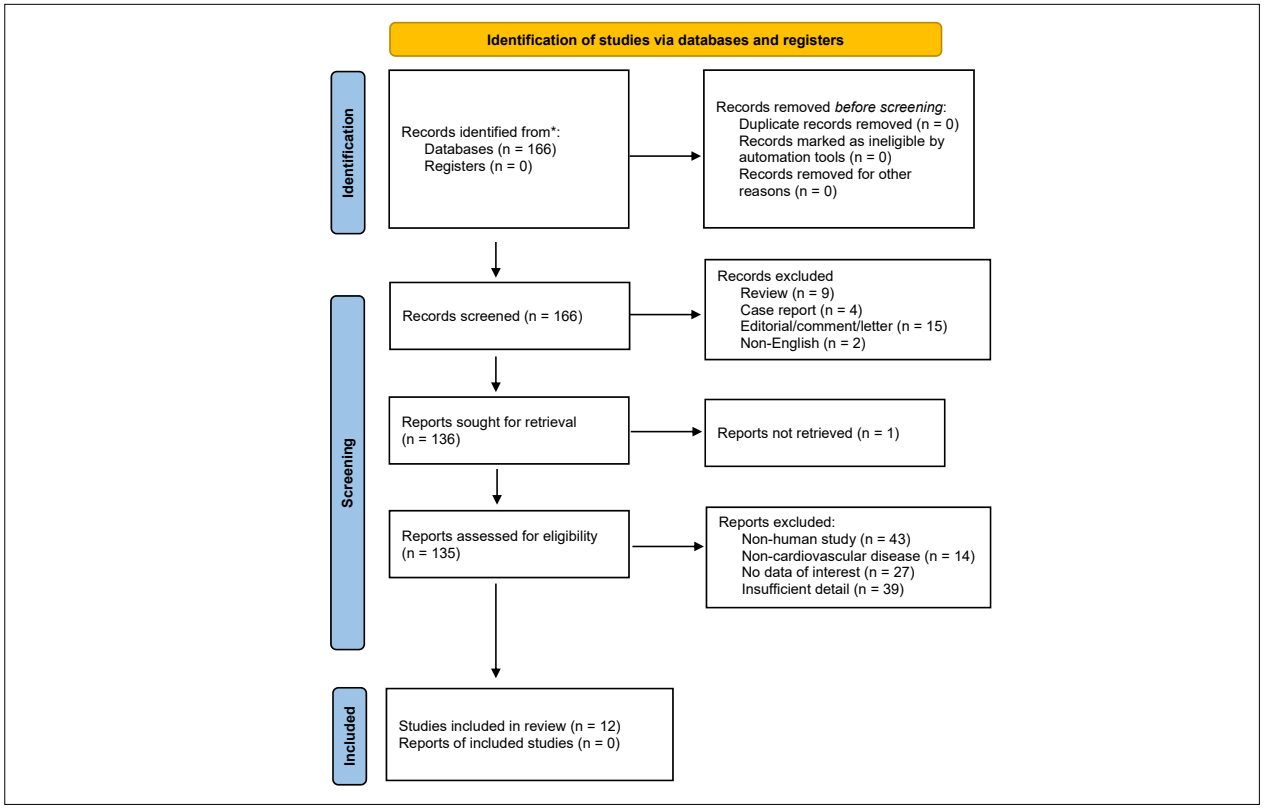

Figura 1 – *Fluxograma do consórcio de estudos da revisão sistemática.*

Results

A total of 166 were obtained from PubMed and subjected to title and abstract screening. Thereafter, 136 studies were subjected to full-text screening. One study was excluded because no full-text article was identified. After application of the inclusion and exclusion criteria, 12 studies were included in this systematic review.

The MW clinical applications in cardiovascular diseases assessed by the 12 studies differed: four assessed HF, two assessed CAD, five assessed CMP, and one assessed HTN. The baseline study information is shown in Table 2, while the baseline MW information in clinical applications is shown in Table 2.

Discussion

Clinical Application of MW

Heart failure

Predicting therapeutic advantages and outcomes in HF patients undergoing cardiac resynchronization therapy (CRT) was the first and most promising use of segmental MW. CRT is now used to treat symptomatic HF patients with an LVEF of 35% and a wide QRS complex.[10] MW appears to be capable of identifying patients who may benefit from cardiac resynchronization. According to a recent study, GWW

Table 2 - Baseline information of the myocardial work in clinical application.

No.	Study	Outcome assessed	Participants	Intervention	Main result
1	Vecera J, et al.[11]	HF	42 patients with HF (mean age, 72 ± 12 years;74% males) planned for CRT implantation	Clinical and echocardiographic data were collected before and at a median of 8 (IQR, 6–13) months after device implantation	GWW decreased from 39 ± 21% to 17 ± 7% with CRT (P,0.01) WW in the septum together with WMSI was a strong predictor of a CRT response
2	Galli E, et al.[8]	HF	97 patients with HF (ejection fraction: 27 ± 6%; QRS duration 164 ± 18 ms) underwent planned CRT implantation	STE was performed before CRT and at the 6-month follow-up. PSL analysis: calculation of CW and WW	>15% reduction in LV end-systolic volume at follow-up GCW was significantly increased in CRT responders
3	Wang CL, et al.[12]	HF	508 patients (mean age, 62.9 ± 15.8 years; 29.1% female) with LVEF ≤ 40%	Additional value of GMW for connection with composite outcome (all-cause death and HF hospitalization), clinical and echocardiographic variables	EF and GLS were not independent variables when GMW was included in the model Patients with a GMW < 750 mmHg% had a substantially higher risk of all-cause mortality and HF hospitalization (HR, 3.33; 95% CI, 2.31–4.80) than patients with a GMW > 750 mmHg%
4	Przewlocka-Kosmala M, et al.[31]	HF	114 patients (57 randomized to spironolactone, 57 to placebo)	At baseline and 6-month follow-up, resting and immediately post-exercise echocardiogram assessing GLS and MW indices	At follow-up, exercise intolerance in the spironolactone group was followed by a substantial improvement in GCW exertional rise (P = 0.002) but not GLS An increase in exercise capacity was independently linked with a change in exertional increase in GCW from baseline to follow-up (b = 0.24; P = 0.009) but not with GLS (P = 0.14) at 6 months. There was no significant interaction between spironolactone usage and peak VO_2 (P = 0.97).
5	Edwards NFA, et al.[15]	CAD	115 patients referred for coronary angiography who had an LVEF ≥ 55%, no resting regional wall motion abnormalities, and no chest pain	Three hours before cardiac catheterization, TTE was performed	Patients with significant CAD demonstrated a significantly reduced global MW (P < 0.001) versus those without CAD MW outperformed GLS (area under the curve = 0.693) as the most effective predictor of severe CAD (area under the curve = 0.786) The optimum global MW cut-off value for predicting substantial CAD was 1,810 mmHg% (sensitivity, 92%; specificity, 51%)
6	Lustosa RP, et al.[16]	CAD	600 STEMI patients divided according to the presence of LV remodeling	Non-invasive myocardial work indices were measured at 3 months after STEMI	The percentages of decreased GWI, GCW, and GWE as well as the percentage of increased GWW were found in patients with versus without LV remodeling: GWI (1,708 ± 522 mmHg% vs 1,979 ± 450 mmHg%; P < 0.001) GCW (1,941 ± 598 mmHg% vs 2,272 ± 519 mmHg%; P < 0.001) GWE (92% [range, 88–96%] vs 95% [range, 93–96%]; P < 0.001) GWW (116 mmHg% [range, 73–184 mmHg%] vs 91 mmHg% [range, 61–132 mmHg%]; P < 0.001).

7	Galli E, et al.[19]	CMP	82 patients with non-obstructive HCM and 20 age-matched healthy subjects (58 ± 7 years; P = 0.99) underwent STE	All HCM patients underwent clinical examination, standard and STE, 48-h Holter monitoring, and cardiopulmonary exercise test	GCW (1599 ± 423 vs 2248 ± 249 mmHg%; P < 0.0001) was significantly reduced in HCM versus control group No difference was observed in GWW (141 ± 125 mmHg% vs 101 ± 88 mmHg%; P = 0.18) and LVEF (63 ± 13% vs 66 ± 4%; P = 0.17) In HCM, GCW was the only predictor of LV fibrosis in the multivariable analysis (OR, 1.01; 95% CI, 0.99–1.08; P = 0.04). A cut-off value of 1,623 mmHg% was able to predict myocardial fibrosis with good sensitivity and fair specificity (82% and 67%, respectively)
8	Hiemstra YL, et al.[20]	CMP	110 patients with non-obstructive HCM and 35 healthy age- and sex-matched control subjects	Clinical data were collected from the department of cardiology information system and the first echocardiogram available was used	GCW (1,722 ± 602 vs 2,274 ± 574 mmHg%; P < 0.001) GWE (93% [89–95%] vs 96% [96–97%]; P < 0.001) GWI (1,534 ± 551 mmHg% vs 1,929 ± 473 mmHg%) were significantly reduced GWW (104 mmHg% [66–137 mmHg%] vs 71 mmHg% [49–92 mmHg%]; P < 0.001) was increased in patients with HCM versus control subjects Patients with a GCW > 1,730 mmHg% experienced better event-free survival than those with a GCW < 1,730 mmHg% (P < 0.001)
9	Chan J, et al.[21]	CMP	74 patients who underwent TTE and strain analysis before coronary angiography were divided into control, HTN, and CMP groups	TTE was performed immediately prior to coronary angiography	Increase in GCW and GWW. GLS, GWI, and GWE were significantly reduced in CMP (P < 0.05) GCW was elevated in HTN Grade1 but did not reach significant levels (P = 0.87; 2361 ± 377 mmHg%) and significantly elevated in HTN grade 2/3 (P = 0.0001; 3057 ± 403 mmHg%) when compared with controls (2184 ± 192 mmHg%) GWW was elevated in both HTN subgroups but not statistically significant
10	Cui C, et al.[22]	CMP	30 with DCM and 30 healthy patients as the control group	After 6 months of medical treatment, conventional echocardiography and MW were examined, and the measurements on the 6-min walk test were compared before and after therapy	GMW differences between controls and cases were significant (P < 0.05) The GWI and 6-min walking distance increased after treatment, while the LV ejection fraction and GLS did not change significantly GWI might be a marker of therapeutic efficacy
11	Clemmensen TS, et al.[24]	CMP	100 patients with CA	The patients were followed prospectively from the time of echocardiography until death or censoring on March 31, 2019; MACE and death during follow-up were registered	Patients with CA had significantly lower GWI and GWE than control subjects (P < 0.0001 for all) Patients with a GWI < 1,043 mmHg% had a higher MACE risk than patients with an LV myocardial work index > 1043 mmHg% (HR, 2.3; 95% CI, 1.2–4.3; P = 0.01) GWI <1039 mmHg% higher all-cause mortality risk than patients with LV GWI >1039 mmHg% (HR, 2.6; 95% CI, 1.2–5.5; P < 0.05).
12	Tadic M, et al.[26]	HTN	165 subjects (55 controls, 60 HTN patients without DM, and 50 HTN patients with DM)	This cross-sectional study performed a complete two-dimensional echocardiographic examination including two-dimensional STE	GWI gradually increased from controls to HTN patients to subjects with HTN and DM (1,887 ± 289 vs 2,073 ± 311 vs 2,144 ± 345 mmHg%, P = 0.001) DM demonstrated an additional negative effect on myocardial work in HTN patients

**CA, cardiac amyloidosis; CAD, coronary artery disease; CI, confidence interval; CMP, cardiomyopathy; DCM, dilated cardiomyopathy; DM, diabetes mellitus; EF, ejection fraction; GCW, global constructed work; GLS, global longitudinal strain; GWE, global work efficiency; GWI, global work index; HCM, hypertrophic cardiomyopathy; HF, heart failure; HR, hazard ratio; HTN, hypertension; LV, left ventricular; LVEF, LV ejection fraction; MACE, major adverse cardiac event; OR, odds ratio; STE, speckle-tracking echocardiography; STEMI, ST-elevated myocardial infarction; TTE, transthoracic echocardiography; WMSI, wall motion score index.*

evaluated at the septum was higher in CRT responders than non-responders, but these indices significantly dropped after CRT implantation, returning to normal cardiac values.[11] In a study of 97 patients, Galli et al. discovered that GCW is the sole predictor of CRT response at 6-month follow-up and closely associated with the idea of myocardial remodeling in ischemic and non-ischemic individuals.[8]

A recent study reported that MW was linked to HF hospitalizations and all-cause death. Patients with a GMW greater than 750 mmHg% had a significantly higher risk of all-cause mortality and HF hospitalization than patients with a GMW greater than 750 mmHg%. These results increase the use of MW in EF patients by 40% and provide a safe alternative to EF and GLS for evaluating patient survival and future hospitalization rates.[12]

Coronary artery disease

When wall motion abnormalities (WMA) are not seen in the coronary arteries, assessing individuals with coronary artery disease is difficult. GLS was previously shown to

be a good predictor of stable ischemic cardiopathy in the absence of WMA.[13] However, agreement is lacking on the appropriate GLS diagnostic cut-off value, which differs widely among investigations due to clinical features, afterload dependency, and inter-evaluator variance. Furthermore, the contractile characteristics of the ischemic myocardium are substantially controlled by loading conditions, with fast transitions from hypokinesis to dyskinesis after an abrupt increase in afterload, which serves as the primary constraint.[14] MW indices demonstrated that it can overcome this constraint and provide diagnostic and prognostic information in chronic and acute settings. Edwards et al. observed that, in patients with suspected CAD but normal systolic function, GWI, GCW, and GWE all decreased dramatically in the presence of obstructive illness, although GWW increased modestly.[15]

At the 3-month follow-up, ST-elevation myocardial infarction (STEMI) patients who exhibited LV ischemia remodeling had significantly lower GWI, GCW, and GWE values but significantly higher GWW values.[16] These results imply that MW deficiency manifests in changed (permanently anaerobic) energy metabolism in the rebuilt myocardium.[17] The regional MW index is superior to all other echocardiographic markers (GLS and LVEF) at detecting acute coronary artery blockages in non-ST-segment acute coronary syndrome.[18]

Cardiomyopathy

GCW was the single predictor of LV fibrosis when late gadolinium enhancement was used, and values <1,730 mmHg% were related to a poorer long-term prognosis.[19,20] Chan et al. described a significant decrease in GWI, GCW, and GWE and an increase in GWW in a subgroup of patients with dilated cardiomyopathy (DCM).[21] This finding resulted from a significant deterioration of cardiomyocytes contractile performance in DCM patients, whether ischemic or non-ischemic. Moreover, another benefit of MW measurement may be its use an indication in the assessment of therapy benefits in DCM patients.[22] Another therapeutic use for MW indicators might be in predicting significant cardiovascular events among patients with cardiac amyloidosis (CA).[23] Study by Clemmensen et al. examined the impact of LV MW in predicting prognosis in individuals with CA. They discovered that individuals with a GWI <1,043 mmHg% were at an increased risk of severe adverse cardiac events, while those with a GWI of <1,039 mmHg% were at an increased risk of all-cause death.[24]

Hypertension

In hypertensive individuals, the LV pumps against higher arterial pressure, reducing the LV stroke volume and increasing the energy required for LV pump function, hence elevating the global MW index.[25] Chan et al. discovered that patients with a systolic blood pressure (SBP) > 160 mmHg had substantially elevated GWI and GCW values. GWW steadily rose in patients with an SBP of 140–159 mmHg, peaking at 160 mmHg in those with an SBP > 160 mmHg.[21]

Additionally, Tadic et al. discovered that hypertension patients' MW values worsened compared to normotensive controls, but these values were considerably worse in hypertensive patients with concurrent diabetes mellitus. Only GCW was significantly greater in individuals with concurrent hypertension and diabetes mellitus than those with hypertension alone.[26] Moreover, Sahiti et al. investigated the correlation between MW with CV risk factors and sex and discovered that the link between hypertension and obesity and GWI was greater in women.[27]

Limitation and recommendation

Although an MW analysis may be conducted on a large proportion of patients, there are several limitations to consider. Because MW is based on the estimated non-invasive LV pressure from SBP measured with a cuff manometer, its use was not highly recommended for evaluation in pathologic situations such as aortic stenosis (AS) in which SBP is not reflective of LV peak systolic pressure due to the fixed obstruction caused by a stenotic valve. Jain et al. recently recommended that the total of the transaortic mean gradient and SBP be used to estimate the LV peak systolic pressure in a group of severe AS patients undergoing transcatheter aortic valve replacement (TAVR). When MW indicators were compared before and after TAVR, a substantial decrease in GWI and GCW was seen, contributing to the rapid relief of the increased oxygen demand associated with increased afterload.[28] These findings suggest that MW correction by the addition of a transaortic mean gradient to SBP is both possible and dependable. However, validation in larger AS patients undergoing TAVR is required before it can be used consistently.

Finally, MW is vendor platform–dependent and requires specialized software that is presently solely supported by General Electric and cannot be tested using other software. This fact restricts the number of patients whose data may be analyzed using this strategy and limits the comparison of the same patient's findings with items from multiple vendors.[9,29]

Conclusion

MW is a reasonable, feasible, and dependable method of non-invasive LV function assessment enabling the widespread use of MW measurement in the diagnostic and treatment evaluation of various cardiovascular diseases. MW improves LVEF and GLS assessments by minimizing their load dependence. While current information on MW alone is insufficient to guide further interventions, the development of an integrated method offering incremental value to conventional echocardiographic measures is expected. Clinicians also must rely on symptoms and electrocardiographic data until multicentered well-designed research validating this strategy in large populations is undertaken to establish its added value and MW indices are included in routine echocardiographic assessments.

Acknowledgments

The authors thank all who supported this systematic review.

Authors' contributions

Research conception and design: Laksono S, Kusharsamita H; data collection: Yanni M, Astuti A; data analysis and interpretation: Laksono S, Kusharsamita H; statistical analysis: Yanni M, Astuti A; obtaining funding: Yanni M, Astuti A; manuscript writing: Laksono S, Kusharsamita H; critical review of the manuscript for important intellectual content: Laksono S.

Conflict of interest

The authors have declared that they have no conflict of interest.

References

1. Marwick TH. Ejection Fraction Pros and Cons: JACC State-of-the-Art Review. J Am Coll Cardiol. 2018;72(19):2360-2379. doi: 10.1016/j.jacc.2018.08.2162.
2. Konstam MA, Abboud FM. Ejection Fraction: Misunderstood and Overrated (Changing the Paradigm in Categorizing Heart Failure). Circulation. 2017;135(8):717-719. doi: 10.1161/CIRCULATIONAHA.116.025795.
3. Zito C, Longobardo L, Citro R, Galderisi M, Oreto L, Carerj ML, et al. Ten Years of 2D Longitudinal Strain for Early Myocardial Dysfunction Detection: A Clinical Overview. Biomed Res Int. 2018;2018:8979407. doi: 10.1155/2018/8979407.
4. Reant P, Metras A, Detaille D, Reynaud A, Diolez P, Jaspard-Vinassa B, et al. Impact of Afterload Increase on Left Ventricular Myocardial Deformation Indices. J Am Soc Echocardiogr. 2016;29(12):1217-1228. doi: 10.1016/j.echo.2016.09.006.
5. Russell K, Eriksen M, Aaberge L, Wilhelmsen N, Skulstad H, Remme EW, et al. A novel clinical method for quantification of regional left ventricular pressure-strain loop area: a non-invasive index of myocardial work. Eur Heart J. 2012;33(6):724-33. doi: 10.1093/eurheartj/ehs016.
6. Hubert A, Le Rolle V, Leclercq C, Galli E, Samset E, Casset C, et al. Estimation of myocardial work from pressure-strain loops analysis: an experimental evaluation. Eur Heart J Cardiovasc Imaging. 2018;19(12):1372-1379. doi: 10.1093/ehjci/jey024.
7. Qin Y, Wu X, Wang J, Li Y, Ding X, Guo D, et al. Value of territorial work efficiency estimation in non-ST-segment-elevation acute coronary syndrome: a study with non-invasive left ventricular pressure-strain loops. Int J Cardiovasc Imaging. 2021 Apr;37(4):1255-1265. doi: 10.1007/s10554-020-02110-1.
8. Galli E, Leclercq C, Hubert A, Bernard A, Smiseth OA, et al. Role of myocardial constructive work in the identification of responders to CRT. Eur Heart J Cardiovasc Imaging. 2018;19(9):1010-1018. doi: 10.1093/ehjci/jex191.
9. Samset E. Evaluation of segmental myocardial work in the left ventricle. 2017. [Access on Sept 09, 2022]. Available from: https://www.gehealthcare.com/-/media/8cab29682ace4ed7841505f813001e33.pdf
10. Brignole M, Auricchio A, Baron-Esquivias G, Bordachar P, Boriani G, Breithardt OA, et al. ESC Guidelines on cardiac pacing and cardiac resynchronization therapy: the Task Force on cardiac pacing and resynchronization therapy of the European Society of Cardiology (ESC). Developed in collaboration with the European Heart Rhythm Association (EHRA). Eur Heart J. 2013;34(29):2281-329. doi: 10.1093/eurheartj/eht150.
11. Vecera J, Penicka M, Eriksen M, Russell K, Bartunek J, Vanderheyden M, et al. Wasted septal work in left ventricular dyssynchrony: a novel principle to predict response to cardiac resynchronization therapy. Eur Heart J Cardiovasc Imaging. 2016;17(6):624-32. doi: 10.1093/ehjci/jew019.
12. Wang CL, Chan YH, Wu VC, Lee HF, Hsiao FC, Chu PH. Incremental prognostic value of global myocardial work over ejection fraction and global longitudinal strain in patients with heart failure and reduced ejection fraction. Eur Heart J Cardiovasc Imaging. 2021;22(3):348-356. doi: 10.1093/ehjci/jeaa162.
13. Choi JO, Cho SW, Song YB, Cho SJ, Song BG, Lee SC, et al. Longitudinal 2D strain at rest predicts the presence of left main and three vessel coronary artery disease in patients without regional wall motion abnormality. Eur J Echocardiogr. 2009;10(5):695-701. doi: 10.1093/ejechocard/jep041.
14. Skulstad H, Edvardsen T, Urheim S, Rabben SI, Stugaard M, Lyseggen E, Ihlen H, Smiseth OA. Postsystolic shortening in ischemic myocardium: active contraction or passive recoil? Circulation. 2002;106(6):718-24. doi: 10.1161/01.cir.0000024102.55150.b6.
15. Edwards NFA, Scalia GM, Shiino K, Sabapathy S, Anderson B, Chamberlain R, et al. Global Myocardial Work Is Superior to Global Longitudinal Strain to Predict Significant Coronary Artery Disease in Patients With Normal Left Ventricular Function and Wall Motion. J Am Soc Echocardiogr. 2019;32(8):947-957. doi: 10.1016/j.echo.2019.02.014.
16. Lustosa RP, van der Bijl P, El Mahdiui M, Montero-Cabezas JM, Kostyukevich MV, Ajmone Marsan N, et al. Noninvasive Myocardial Work Indices 3 Months after ST-Segment Elevation Myocardial Infarction: Prevalence and Characteristics of Patients with Postinfarction Cardiac Remodeling. J Am Soc Echocardiogr. 2020;33(10):1172-1179. doi: 10.1016/j.echo.2020.05.001.
17. Azevedo PS, Minicucci MF, Santos PP, Paiva SA, Zornoff LA. Energy metabolism in cardiac remodeling and heart failure. Cardiol Rev. 2013;21(3):135-40. doi: 10.1097/CRD.0b013e318274956d.
18. Boe E, Russell K, Eek C, Eriksen M, Remme EW, Smiseth OA, et al. Non-invasive myocardial work index identifies acute coronary occlusion in patients with non-ST-segment elevation-acute coronary syndrome. Eur Heart J Cardiovasc Imaging. 2015;16(11):1247-55. doi: 10.1093/ehjci/jev078.
19. Galli E, Vitel E, Schnell F, Le Rolle V, Hubert A, Lederlin M, et al. Myocardial constructive work is impaired in hypertrophic cardiomyopathy and predicts left ventricular fibrosis. Echocardiography. 2019;36(1):74-82. doi: 10.1111/echo.14210.
20. Hiemstra YL, van der Bijl P, El Mahdiui M, Bax JJ, Delgado V, Marsan NA. Myocardial Work in Nonobstructive Hypertrophic Cardiomyopathy: Implications for Outcome. J Am Soc Echocardiogr. 2020;33(10):1201-1208. doi: 10.1016/j.echo.2020.05.010.
21. Chan J, Edwards NFA, Khandheria BK, Shiino K, Sabapathy S, Anderson B, et al. A new approach to assess myocardial work by non-invasive left ventricular pressure-strain relations in hypertension and dilated cardiomyopathy. Eur Heart J Cardiovasc Imaging. 2019;20(1):31-39. doi: 10.1093/ehjci/jey131.
22. Cui C, Liu L, Li Y, Liu Y, Huang D, Hu Y, et al. Left Ventricular Pressure-Strain Loop-Based Quantitative Examination of the Global and Regional Myocardial Work of Patients with Dilated Cardiomyopathy. Ultrasound Med Biol. 2020;46(10):2834-2845. doi: 10.1016/j.ultrasmedbio.2020.06.008.
23. Roger-Rollé A, Cariou E, Rguez K, Fournier P, Lavie-Badie Y, Blanchard V, et al; Toulouse Amyloidosis Research Network collaborators. Can myocardial work indices contribute to the exploration of patients with cardiac amyloidosis? Open Heart. 2020;7(2):e001346. doi: 10.1136/openhrt-2020-001346.
24. Clemmensen TS, Eiskjær H, Ladefoged B, Mikkelsen F, Sørensen J, Granstam SO, et al. Prognostic implications of left ventricular myocardial work indices in cardiac amyloidosis. Eur Heart J Cardiovasc Imaging. 2021;22(6):695-704. doi: 10.1093/ehjci/jeaa097.

25. Kuznetsova T, Nijs E, Cauwenberghs N, Knez J, Thijs L, Haddad F, et al. Temporal changes in left ventricular longitudinal strain in general population: Clinical correlates and impact on cardiac remodeling. Echocardiography. 2019;36(3):458-468. doi: 10.1111/echo.14246.

26. Tadic M, Cuspidi C, Pencic B, Grassi G, Celic V. Myocardial work in hypertensive patients with and without diabetes: An echocardiographic study. J Clin Hypertens (Greenwich). 2020;22(11):2121-2127. doi: 10.1111/jch.14053.

27. Sahiti F, Morbach C, Cejka V, Tiffe T, Wagner M, Eichner FA, et al. Impact of cardiovascular risk factors on myocardial work-insights from the STAAB cohort study. J Hum Hypertens. 2022;36(3):235-245. doi: 10.1038/s41371-021-00509-4.

28. Jain R, Bajwa T, Roemer S, Huisheree H, Allaqaband SQ, Kroboth S, et al. Myocardial work assessment in severe aortic stenosis undergoing transcatheter aortic valve replacement. Eur Heart J Cardiovasc Imaging. 2021;22(6):715-721. doi: 10.1093/ehjci/jeaa257.

29. Papadopoulos K, Özden Tok Ö, Mitrousi K, Ikonomidis I. Myocardial Work: Methodology and Clinical Applications. Diagnostics (Basel). 2021;11(3):573. doi: 10.3390/diagnostics11030573.

30. Galli E, John-Matthwes B, Rousseau C, Schnell F, Leclercq C, Donal E. Echocardiographic reference ranges for myocardial work in healthy subjects: A preliminary study. Echocardiography. 2019;36(10):1814-1824. doi: 10.1111/echo.14494.

31. Przewlocka-Kosmala M, Marwick TH, Mysiak A, Kosowski W, Kosmala W. Usefulness of myocardial work measurement in the assessment of left ventricular systolic reserve response to spironolactone in heart failure with preserved ejection fraction. Eur Heart J Cardiovasc Imaging. 2019;20(10):1138-1146. doi: 10.1093/ehjci/jez027.

Primary Cardiac Angiosarcoma Evaluated on PET/CT

Angiossarcoma Primário Cardíaco Avaliado em PET/TC

Pedro Henrique Rodrigues da Silva[1], Carlos Eduardo Lucena Montenegro[2], Maria Eduarda Duarte de Mello Flamini[1], Mariana Vila Nova de Oliveira Pontual[1], Simone Cristina Soares Brandão[1,2]

[1]Federal University of Pernambuco, Hospital das Clínicas, Serviço de PET/CT, Recife, PE, Brazil; [2]University of Pernambuco, Pernambuco Cardiological Emergency Room (PROCAPE), Recife, PE, Brazil.

Introduction

Cardiac angiosarcoma is a rare malignant endothelial tumor that is aggressive and has an adverse prognosis.[1,2] It features a high mortality rate because of the tendency for local recurrence and high incidence of systemic metastases.[1] Therefore, its early diagnosis is very important, as is the determination of its local and distant extension, to ensure its proper therapeutic management. The objective of this case report was to show the value of positron emission tomography associated with computed tomography with 18-fluorodeoxyglucose (^{18}F-FDG PET/CT) in the diagnosis and staging of cardiac angiosarcoma.

Caso Report

A 39-year-old man with dyspnea and palpitations at rest for approximately 15 days was admitted to the emergency room with signs of cardiac tamponade and underwent pericardiocentesis. During the hospitalization, the pericardial effusion recurred, which required a pericardial window and biopsy. The pericardial fluid showed a hematic aspect and high cellularity with a predominance of lymphomonocytic and low glucose, motivating empirical treatment with rifampicin, isoniazid, pyrazinamide, and ethambutol for possible tuberculosis.

Transthoracic echocardiography showed a fixed mass adherent to the lateral wall of the right ventricle (RV), right atrium (RA), and posterior tricuspid leaflet measuring approximately 30 mm × 34 mm. Transesophageal echocardiography showed a solid homogeneous mass adherent to the lateral wall of the RA projecting into the RV inlet and causing a flow obstruction with dimensions of 58 mm × 47 mm and without vascularization by microbubbles.

As the patient's condition failed to improve despite treatment, it was necessary to continue the investigation to better diagnose the cardiac mass. Magnetic resonance imaging (MRI) was not possible because of hemodynamic instability (lipothymia) at the time of the examination.

Keywords

Angiosarcoma; Positron-emission tomography; Diagnostic imaging.

Mailing Address: Simone Cristina Soares Brandão •
Av. Beira Rio, 360, Apto 201. Ilha do Retiro, Recife, PE, Brazil,
Postal Code: 50750-400.
E-mail: simone.brandao@ufpe.br
Manuscript received 8/23/2022; revised 9/15/2022; accepted 10/20/2022

Editor responsible for the review: Rafael Lopes

DOI: 10.47593/2675-312X/20223504eabc337i

Therefore, the patient was referred for ^{18}F-FDG PET/CT imaging. This examination revealed a cardiac mass with an epicenter in the RA (Figures 1 and 2), heterogeneous density, a more inferior solid component, and a superior area of necrosis/liquefaction measuring approximately 75 mm × 60 mm × 86 mm with a maximum standardized uptake value (SUVmax) of ^{18}F-FDG of 19.6. Diffuse nodular thickening of the entire pericardium, including its recesses (SUVmax of 16.0) and hypermetabolic thoracic lymph nodes, was also observed with no evidence of distant metastases.

These findings were suggestive of a high-grade primary malignant cardiac tumor. An anatomopathological study revealed that it was a fusocellular neoplasm (Figure 3), and the immunohistochemical study findings were compatible with angiosarcoma, with positive Ki-67 staining in 50% of the neoplastic cells.

Discussion

Primary cardiac angiosarcoma is a clinically rare cardiac neoplasm, with approximately 200 cases described to date[1] and an incidence of approximately 0.017%.[2] It is highly invasive and has a poor prognosis.[1,2] This tumor can occur in any part of the heart, but it most frequently occurs on the right side, especially in the RA, and rarely in the epicardium, pericardium, and RV.[2] It usually causes chest pain, vomiting, cough, hemoptysis, shortness of breath, fatigue, and arrhythmia. It has a high mortality rate owing to the tendency for local recurrence and high incidence of systemic metastases.[1]

The late diagnosis and rarity of these tumors makes it difficult to define the best treatment and prognostic factors. In addition, they are resistant to radiation and chemotherapy,[2] therefore, surgical resection is currently considered the ideal treatment modality. In the present case, surgical excision was not possible because of the extent of cardiac involvement. One week after the biopsy, the patient experienced new cardiac tamponade, underwent another pericardial window, and on the 3rd day after the procedure died suddenly.

With the development of new imaging techniques, an increasing number of cases are being diagnosed earlier.[3] CT, MRI, and ^{18}F-FDG PET/CT can help determine the extent of infiltration and presence of potential metastases. On contrast-enhanced CT, cardiac angiosarcomas commonly show inhomogeneous centripetal enhancement. Cardiac MRI allows for better characterization of the soft tissues and tumor in addition to being superior to CT in the assessment of myocardial and pericardial infiltration.[2]

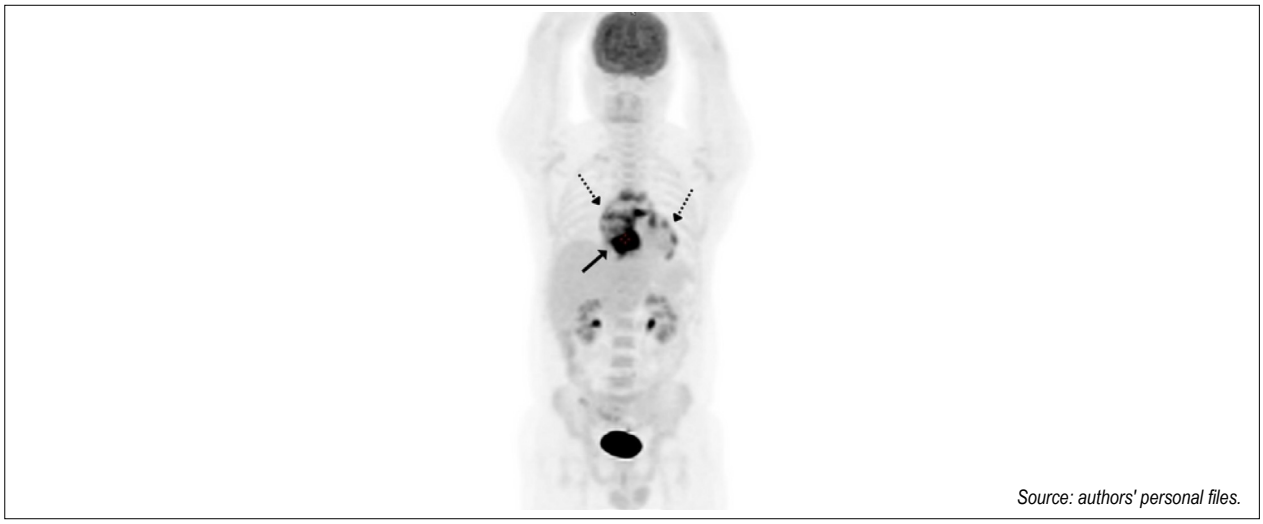

Source: authors' personal files.

Figure 1 – *Maximum intensity projection image of positron emission tomography associated with computed tomography with 18-fluorodeoxyglucose showing a marked increase in glycolytic metabolism in the cardiac mass involving the right atrium and ventricle (solid black arrow) with extension to the pericardium (dotted black arrows).*

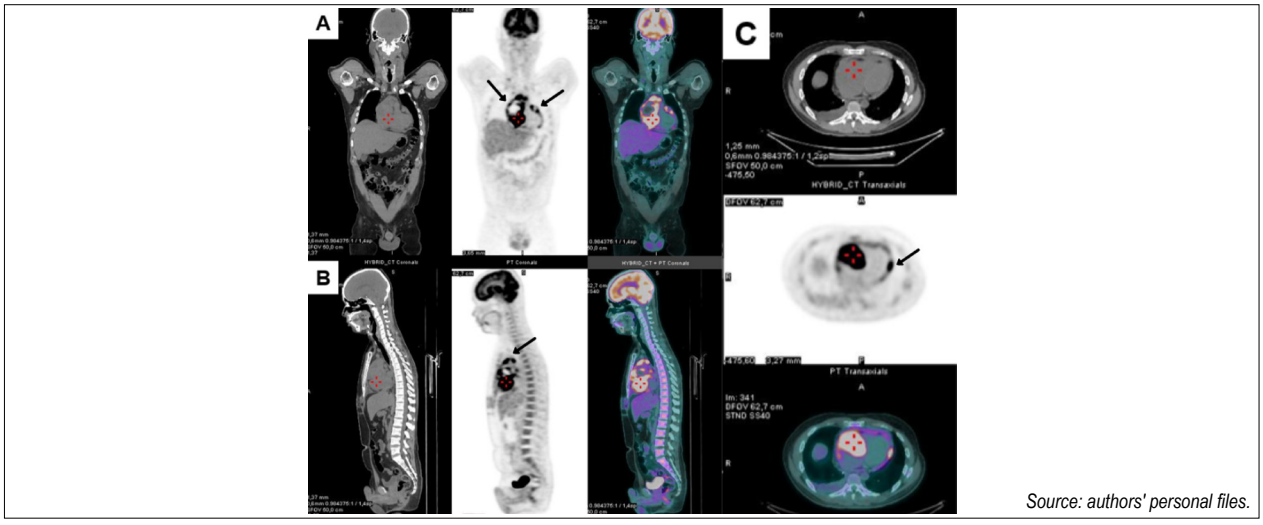

Source: authors' personal files.

Figure 2 – *Positron emission tomography (PET) associated with computed tomography (CT) with 18-fluorodeoxyglucose (18F-FDG) images (A, coronal CT, PET, and PET/CT sections; B, CT, PET, and PET/CT sagittal sections; C, CT, PET, and PET/CT axial sections) showing marked accumulation of 18F-FDG in the tumor (red cross marker) and sparse hypermetabolic foci in the pericardium (black arrows).*

Moreover, ^{18}F-FDG PET/CT has been used to better characterize and stage these tumors, as it aids the accurate determination of the tumor's extent, metabolic activity, and potential metastases, as it is a whole-body examination.[1,4] In addition, it makes it possible to characterize a malignant tumor in a non-invasive way,[4] which is very important for sparing the heart muscle.

The tumor metabolic characterization on ^{18}F-FDG PET/CT is based on the calculation of the SUVmax of FDG on the tumor mass versus the glucose uptake of the blood pool and the normal myocardium, permitting differentiation between hypermetabolic tumors and myocardial physiological uptake. In such a way that uptake is low in the blood pool and normal myocardium, it is higher in benign tumors and significantly higher in malignant primary tumors. Using a SUVmax cutoff of 3.5, the sensitivity in determining malignancy can reach 100%, while at a cutoff of slightly higher than 4.6, the specificity increased to 100%, although sensitivity decreased to 94%. Therefore, the use of an SUVmax cutoff of 3.5–4.6 has good accuracy for the diagnosis of malignant cardiac tumors.[5]

In the present case, ^{18}F-FDG PET/CT clearly demonstrated the extent of the primary tumor and the high uptake of ^{18}F-FDG in the cardiac lesion (SUVmax of 19.6), indicating the malignant nature of the tumor. This diagnostic approach makes it possible to characterize a malignant tumor noninvasively. Here we highlight the potential of ^{18}F-FDG PET/CT for diagnosing and staging primary cardiac angiosarcoma.

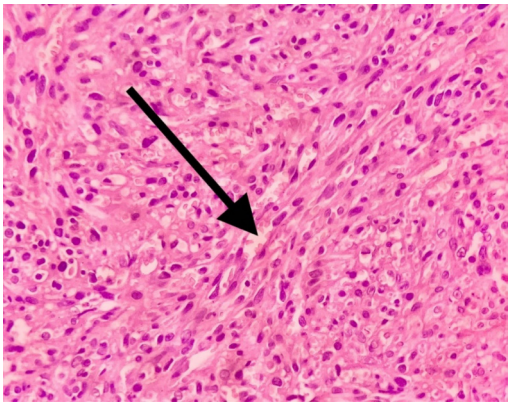

Source: authors' personal files.

Figure 3 – *Fusocellular neoplasm composed of cells with moderate atypia that outlines the vascular spaces (black arrow).*

Authors' contributions

Data collection and analysis: Silva PHR, Montenegro CEL, Flamini MEDM, Pontual MVNO and Brandão SCS; Manuscript writing: Silva PHR; Critical review of the article: Montenegro CEL and Brandão SCS, Consent to be responsible for all aspects of the work: Silva PHR, Montenegro CEL, Flamini MEDM, Pontual MVNO and Brandão SCS.

Conflict of interest

The authors have declared that they have no conflict of interest.

References

1. Dhull VS, Sharma P, Mukherjee A, Jana M, Bal C, Kumar R. 18F-FDG PET-CT for Evaluation of Cardiac Angiosarcoma: A Case Report and Review of Literature. Mol Imaging Radionucl Ther. 2015;24(1):32-6. doi: https://doi.org/10.4274/mirt.02486.
2. Yu JF, Cui H, Ji GM, Li SQ, Huang Y, Wang RN, et al. Clinical and imaging manifestations of primary cardiac angiosarcoma. BMC Med Imaging. 2019;19(1):16. doi: https://doi.org/10.1186/s12880-019-0318-4.
3. Zhang C, Huang C, Zhang X, Zhao L, Pan D. Clinical characteristics associated with primary cardiac angiosarcoma outcomes: a surveillance, epidemiology and end result analysis. Eur J Med Res. 2019;24(1):29. doi: https://doi.org/10.1186/s40001-019-0389-2
4. Soares Brandão SC, Dompieri LT, Tonini RC, Grativvol PS, Gama JD, Calado EB, et al. Cardiac Malignant Peripheral Nerve Sheath Tumor Accessed By 18F-FDG PET/CT. Can J Cardiol. 2020;36(6):967.e17-967.e19. doi: https://doi.org/10.1016/j.cjca.2019.12.035
5. Brandão SC, Dompieri LT. Aplicações da PET-TC 18F-FDG nos tumores cardíacos. Arq Bras Cardiol: imagem cardiovasc. 2019;32(4):309-17.

Real-time Three-Dimensional Echocardiogram in the Identification of Late Complications in the Follow-Up After Mitraclip® Implantation

Aplicação do Ecocardiograma Tridimensional em Tempo Real para Detecção de Complicações Tardias no Seguimento Pós-Implante de MitraClip®

Alexandre Costa[1], Bruna de Mattos Ivo Junqueira[1], Carolina Thé Macedo[1], Marcus Vinicius Silva Freire de Carvalho[1], Cristiano Guedes Bezerra[1], Rodrigo Morel Vieira de Melo[1]

[1]Hospital São Rafael, Salvador, BA, Brazil.

Introduction

Conventional surgery is the treatment of choice for severe mitral valve regurgitation.[1] However, it is not feasible for patients at high surgical risk, who have high morbidity and mortality rates despite clinical treatment. Percutaneous valve treatment (*MitraClip*) has been evolving as a therapeutic perspective for this population, with reduced heart failure (HF) hospitalization and all-cause mortality rates.[2,3,4]

Three-dimensional transesophageal echocardiography (3DTEE) has an additive role during clinical follow-up, especially in cases of suspected late complications with high detail of valve anatomy and clip positioning with cardiac structures. Additionally, due to the greater anatomical accuracy of this test, complications resulting from the procedure can be safely detected in real time.

This report describes a case of 3DTEE use in the diagnosis and evaluation of complications in the traditional follow-up of *MitraClip* implantation.

Case report

A 67-year-old man with a history of hypertension with dilated cardiomyopathy and significant functional mitral regurgitation who underwent *MitraClip* implantation in October 2021 was admitted five months after the procedure with chest pain and dyspnea on usual exertion. A transthoracic echocardiogram (TTE) showed two clips in the mitral position and significant mitral regurgitation in addition to significant bi-atrial and left ventricular enlargement with diffuse hypokinesia (25% ejection fraction calculated by the Simpson method).

Real-time 3DTEE to confirm mitral regurgitation and loss of the late result demonstrated that one of the clips had lost the capture zone related to the posterior leaflet. (Figure 1 and Video 1) Color Doppler showed two eccentric regurgitant jets, one directed at the interatrial septum and the other, of greater magnitude, related to the lateral wall of the left atrium (Figure 2 and Video 2), totaling a significant degree of regurgitation (*Vena Contracta* 3D: 0.9 cm^2). The patient's HF was compensated for with clinical measures and diuretic therapy, and the heart team chose a new outpatient percutaneous approach with a third clip implant strategy to treat the lateral mitral regurgitation jet (A1/P1 segments).

In April 2022, the patient was electively admitted for 3DTEE-guided implantation of the third clip without complications. This new implanted clip stabilized the one that had lost capture of the posterior leaflet and treated the lateral regurgitation jet (A1/P1) with consequent mitral regurgitation reduction. (Figure 3 and Video 3)

Discussion

Real-time 3DTEE, a fundamental imaging modality for the careful evaluation of patients eligible for *MitraClip* implantation, plays an important role in all stages of the procedure. Its role was established in the assessment of patient eligibility for device implantation through a systematic evaluation and use of recommended objective measurements.[4,5] Moreover, 3DTEE aids the dynamic intraoperative assessment of each procedural step.[5,6]

The *MitraClip* system is safe and features low rates of adverse events. Although the complication rate is low, the ideal format for clinical and echocardiographic follow-up should be better understood.[5] This case report reinforces the additional value of the three-dimensional resource in pre- and intraoperative assessments as well as in the late follow-up of patients undergoing percutaneous mitral valve repair (*MitraClip*).

In the case described here, conventional echocardiography showed signs of device failure with recurrent severe mitral regurgitation. The use of real-time 3DTEE provided detailed anatomical data of the different segments of the mitral valve with anatomic correlation and allowed the exact identification of the mechanism of mitral regurgitation, showing that *MitraClip* failure captured the posterior leaflet of the mitral valve and related clip hypermobility. TTE was limited by artifacts generated by the attached clip, which impaired the identification of the cause of the loss of the late result by the device. Moreover, 3DTEE allowed the topographical identification of the segment related to loss of capture (A1/P1) and helped plan treatment with an additional clip to approach the residual lateral insufficiency jet.

Keywords

Echocardiography, Three-Dimensional; Mitral Valve Insufficiency; Postoperative Complications, Cardiovascular Surgical Procedures.

Mailing Address: Alexandre Costa Souza •
Hospital São Rafael, Av. São Rafael, 2.152, São Marcos. CEP: 41253-190 – Salvador, BA, Brazil.
E-mail: alexandrecostahsr@gmail.com
Manuscript received 4/26/2022; revised 7/6/2022; accepted 8/8/2022

Editor responsible for the review: Daniela do Carmo Rassi Frota

DOI: 10.47593/2675-312X/20223504eabc298i

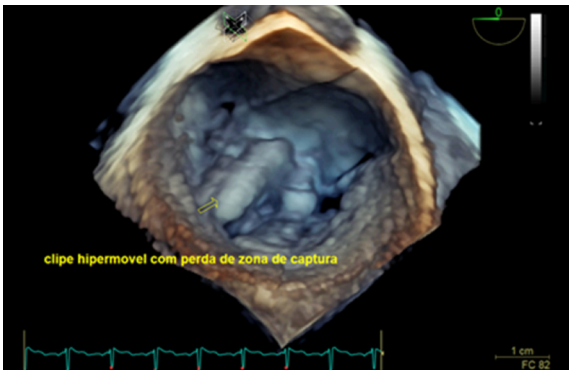

Figure 1 – *Three-dimensional transesophageal echocardiogram (3DTEE) with three-dimensional reconstruction showing MitraClip capture loss.*

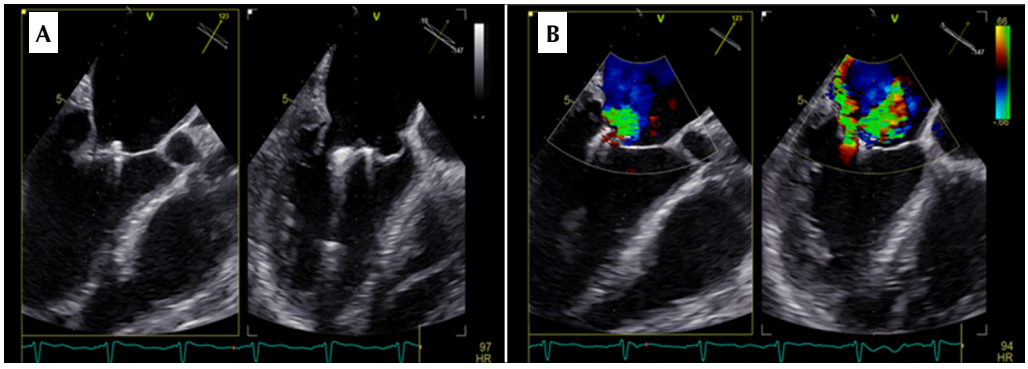

Figure 2 – *(A) TEE with multiplanar slices showing the MitraClip with loss of the posterior leaflet capture zone. (B) The presence of two jets, one eccentric, directed to the lateral wall and compatible with significant mitral valve regurgitation in the post-MitraClip implantation follow-up.*

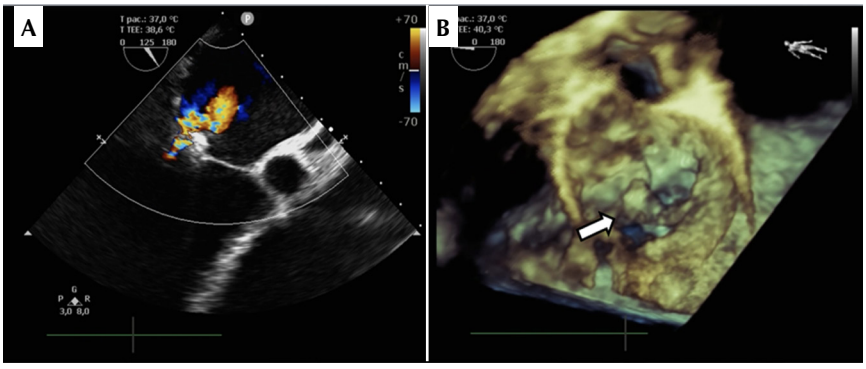

Figure 3 – *(A) TEE showing mild mitral valve regurgitation in intraoperative control after implantation of the third MitraClip. (B) Three-dimensional reconstruction of the mitral valve with the presence of a double fenestration and a percutaneous device (MitraClip).*

Mitral regurgitation severity was assessed using conventional parameters and 3D color Doppler echocardiography with quantification of the *Vena Contracta* 3D area. Buck *et al*. demonstrated that mitral valve geometry and left ventricle size and function may be associated with mitral regurgitation progression in the post-*MitraClip*[6] follow-up; such parameters, especially those related to the complex geometry of the mitral valve and its annulus, can be assessed through the three-dimensional resource. Partial clip displacement was described in 4–10% of cases.[7,8] Decisions about patient management should consider new clip implantation and optimal clinical therapy. In exceptional cases, mitral valve surgery may be indicated, but it

must always be a shared heart team decision since most patients, especially those with HF, are at high surgical risk.

The amount of leaflet tissue captured at the time of device implantation and aspects related to mitral valve and left ventricle geometry influence the late outcomes of patients undergoing *MitraClip* device implantation. Follow-up should include TTE and, in cases of suspected results loss, 3DTEE is indicated since it can add relevant anatomical information to aid our understanding of the exact mechanism of result failure and subsequent planning.

Authors' contributions:

Research conception and design: Costa A, Junqueira BMI; data collection: Macedo CT, Carvalho MVSF, Bezerra CG; manuscript writing: Costa A, Junqueira BMI; critical review of the manuscript: Melo RMV, Costa A

Conflict of interest

The authors have declared that they have no conflict of interest.

References

1. Mackensen GB, Lee JC, Wang DD, Pearson PJ, Blanke P, Dvir D, et al. Role of Echocardiography in Transcatheter Mitral Valve Replacement in Native Mitral Valves and Mitral Rings. J Am Soc Echocardiogr. 2018;31(4):475-90. doi: https://doi.org/10.1016/j.echo.2018.01.011
2. Obadia JF, Messika-Zeitoun D, Leurent G, Iung B, Bonnet G, Piriou N, et al.; MITRA-FR Investigators. Percutaneous Repair or Medical Treatment for Secondary Mitral Regurgitation. N Engl J Med. 2018;379(24):2297-306. doi: 10.1056/NEJMoa1805374
3. Feldman T, Foster E, Glower DD, Kar S, Rinaldi MJ, Fail PS, et al.; EVEREST II Investigators. Percutaneous repair or surgery for mitral regurgitation. N Engl J Med. 2011;364(15):1395-406. doi: 10.1056/NEJMoa1009355. Epub 2011 Apr 4. Erratum in: N Engl J Med. 2011 Jul 14;365(2):189. Glower, Donald G [corrected to Glower, Donald D].
4. Wunderlich NC, Siegel RJ. Peri-interventional echo assessment for the MitraClip procedure. Eur Heart J Cardiovasc Imaging. 2013;14(10):935-49. doi: 10.1093/ehjci/jet060
5. Schnitzler K, Hell M, Geyer M, Kreidel F, Münzel T, von Bardeleben RS. Complications Following MitraClip Implantation. Curr Cardiol Rep. 2021;23(9):131. doi: 10.1007/s11886-021-01553-9.
6. Buck T, Eiswirth N, Farah A, Kahlert H, Patsalis PC, Kahlert P, et al. Recurrence of Functional Versus Organic Mitral Regurgitation After Transcatheter Mitral Valve Repair: Implications from Three-Dimensional Echocardiographic Analysis of Mitral Valve Geometry and Left Ventricular Dilation for a Point of No Return. J Am Soc Echocardiogr. 2021;34(7):744-56. doi: 10.1016/j.echo.2021.02.017.
7. Franzen O, Baldus S, Rudolph V, Meyer S, Knap M, Koschyk D, et al. Acute outcomes of MitraClip therapy for mitral regurgitation in high-surgical-risk patients: emphasis on adverse valve morphology and severe left ventricular dysfunction. Eur Heart J. 2010;31(11):1373-81.
8. Gheorghe L, Ielasi A, Rensing BJ, Eefting FD, Timmers L, Latib A, et al. Complications Following Percutaneous Mitral Valve Repair. Front Cardiovasc Med. 2019;6:146. doi: 10.3389/fcvm.2019.00146

Percutaneous Closure of Multiple Atrial Septal Defects with Hemodynamic Repercussions: Report of Two Cases in First-Degree Related Adult Patients

Fechamento Percutâneo de Comunicação Interatrial Múltipla com Repercussão Hemodinâmica: Relato de Dois Casos em Pacientes Adultos Parentes de Primeiro Grau

Débora Freire Ribeiro Rocha[1,2], Henrique Lima Guimarães[1], Maurício Prudente Lopes[1], João Batista Masson Silva[1,2], Giulliano Gardenghi[1]

[1]Hospital ENCORE, Goiânia, GO; [2]Federal University of Goiás, Hospital das Clínicas, Goiânia, Goiânia, GO, Brazil.

Introduction

Atrial septal defects (ASD) account for 7–10% of congenital heart anomalies.[1,2] ASD are classified as three anatomical types: ostium secundum (OS) (70% of cases), ostium primum (15–20% of cases), and sinus venosus (5–10% of cases) defects. OS involves the fossa ovalis region and results from poor embryological development of septum secundum or excessive absorption of septum primum resulting in the lack of a septum in the fossa ovalis.[1]

Affected patients are usually asymptomatic. Exercise intolerance in the form of dyspnea or fatigue is the most common initial presentation.[1] Echocardiography is a fundamental tool in the diagnosis and management of patients with ASD. Transthoracic echocardiography (TTE) identifies ASD type and size, shunt direction, and the presence of anomalous sinus venous drainage. Three-dimensional transesophageal echocardiography (3DTEE) details the morphology and anatomical relationships of the atrial septum, providing fundamental information for choosing treatment.[1,3]

Based on European guidelines for the diagnosis and treatment of congenital heart diseases, the indications for ASD closure are the presence of atrial and/or right ventricular (RV) dilatation on echocardiography, magnetic resonance imaging (MRI), or computed tomography with no severe pulmonary hypertension and presenting one or more of the following: minimum 10-mm ASD diameter on echocardiography, or Qp/Qs ratio > 1.5:1 measured by echocardiography or contrast-enhanced MRI (class I recommendation; level of evidence, B). Sinus venosus, coronary sinus, or ostium primum ASD must be surgically repaired.[3]

ASD with hemodynamic repercussions should be closed to improve right chamber size, decrease pulmonary arterial pressure, and improve symptoms of reduced functional limitation.[3] Several hospital services implemented the percutaneous closure of OS ASD due to shorter hospitalization time and fewer complications than surgical treatment. Thus, this study aimed to report the presence of OS ASD with hemodynamic repercussions in two first-degree related adults undergoing percutaneous treatment.

The study was approved by the Research Ethics Committee of Hospital de Urgências de Goiânia (CAAE number 85497418.2.0000.0033).

Case 1

RCAS, a 41-year-old man, asymptomatic from the cardiovascular point of view, underwent TTE on February 20, 2018, which showed a patent foramen ovale (PFO) with large passage of microbubbles and a large interatrial septum aneurysm associated with ASD with hemodynamic repercussions (Qp: QS 2 and moderate right chamber enlargement).

On April 6, 2018, a 3DTEE was performed for the morphological and functional assessment of the ASD closure procedure. A multi-fenestrated ASD was visualized in a predominantly posteroinferior location of the septum and PFO (Figures 1A, 1B). The three-dimensional image was fundamental in choosing the device to be implanted, as it showed the reconstructed image of the interatrial septum in which each fenestration and edge was demonstrated in relation to the adjacent structures.

Thus, the multi-fenestrated ASD was occluded with the PFO from the successful implantation of two Amplatzer ASD® cribriform prostheses of 30 and 25 mm without clinical or angiographic complications or residual shunt (Figures 2A, 2B).

The patient's condition progressed without clinical or hemodynamic complications in the immediate postoperative period, and he was discharged on April 8, 2018. He returned to the service on September 1, 2021, for a late follow-up 3DTEE, which showed an intact interatrial and interventricular septum, well-positioned occluding devices in the topography of the interatrial septum, and no residual shunt after an agitated saline injection (microbubble test) (Figures 3A, 3B).

Case 2

RPASC was a 39-year-old woman with dyspnea on minimal exertion and slowly progressing exercise intolerance.

Keywords

Heart Septal Defects, Atrial; Echocardiography; Hemodynamics.

Mailing Address: Giulliano Gardenghi •
Rua Gurupi, Quadra 25, Lote 6 a 8, Vila Brasília. CEP 74905-350 – Aparecida de Goiânia, GO, Brazil.
E-mail: ggardenghi@encore.com.br
Manuscript received 9/1/2022; revised 9/30/2022; accepted 10/30/2022

Editor responsible for the review: Daniela do Carmo Rassi Frota

DOI: 10.47593/2675-312X/20223504eabc345i

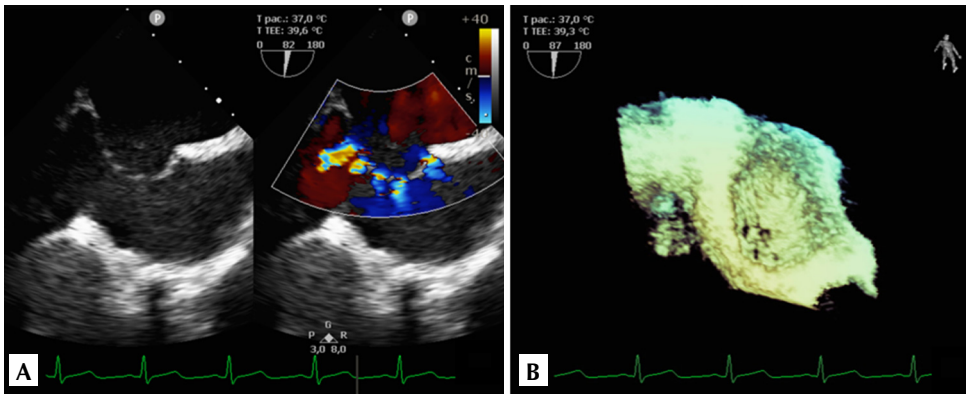

Figure 1 – *Transthoracic echocardiography pre-percutaneous closure procedure performed on April 6, 2018. A. Two-dimensional image of a multi-fenestrated atrial septal defect (ASD; five fenestrations). B. Three-dimensional image of a multi-fenestrated ASD.*

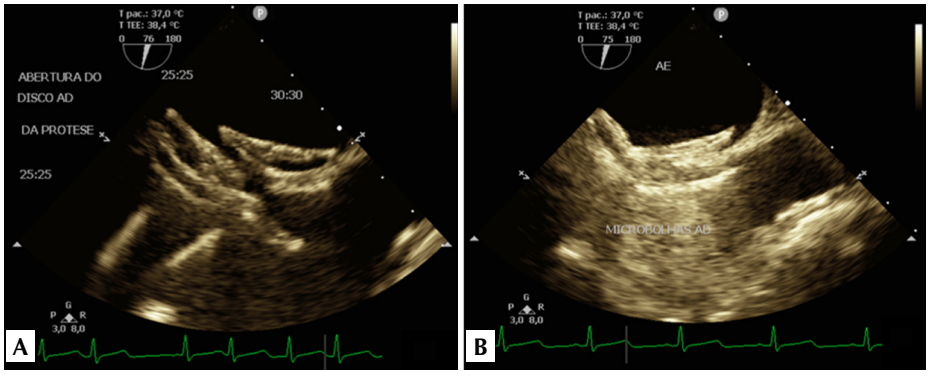

Figure 2 – *Percutaneous procedure for closing a multi-fenestrated atrial septal defect (ASD) with patent foramen ovale on April 6, 2018. A. The implantation of two Amplatzer ASD cribriform prostheses (30 and 25 mm). B. Microbubble test showing no residual shunt.*

On November 10, 2021, a TTE showed slight RV enlargement with preserved systolic function (S', 10 cm/s; tricuspid annular plane systolic excursion, 19 mm; fractional area change, 42%; no indirect signs of pulmonary hypertension pulmonary artery trunk, 21 mm in diameter; inferior vena cava (IVC), 12 mm in diameter; respiratory variability, greater than 50%; and estimated pulmonary arterial systolic pressure, 24 mmHg]), and the presence of two OS ASD, one more anterior measuring 18 × 9 mm and another closer to the IVC measuring 6 × 5 mm, with hemodynamic repercussions. The estimated Qp/Qs was 1.7 with septal borders greater than 5 mm. A 3DTEE performed in another service showed two OS ASD measuring 12 × 14 mm and 4 × 4.3 mm and 12 mm apart with hemodynamic repercussions.

Therefore, percutaneous treatment was indicated due to the presence of an ASD with hemodynamic repercussions (right chamber dilation, Qp/Qs > 1.5).

On November 11, 2021, the patient was taken to the hemodynamics service for intraoperative 3DTEE, which revealed two ASD, the larger one 15 mm and the smaller one 4.3 mm, separated by 14 mm of septal tissue, with moderate hemodynamic repercussion (Qp/Qs, 2) and no other heart diseases (Figures 4A–4C). Thus, the intracardiac ASD was percutaneously closed with two ASD® Amplatzer prostheses (one 24 mm, the other 6 mm) in the major and minor ASD, respectively, guided by 3DTEE without residual shunt or clinical or angiographic complications (Figures 5A, 5B).

The patient's condition progressed with significant clinical improvement in the immediate postoperative period and no hemorrhagic or hemodynamic complications. She returned for a control TTE on December 11, 2021, which showed two occluding devices in the interatrial septum and no residual shunt (Figures 6A, 6B).

Discussion

The decision to repair any type of ASD is based on clinical and echocardiographic information, including signs and symptoms of right heart failure, defect size and location, magnitude and hemodynamic impacts of the left-to-right shunt, and the presence and degree of pulmonary hypertension. Elective closure is recommended for all ASD cases with echocardiographic evidence of RV overload or a clinically significant Qp/Qs ratio greater than 1.5.[4]

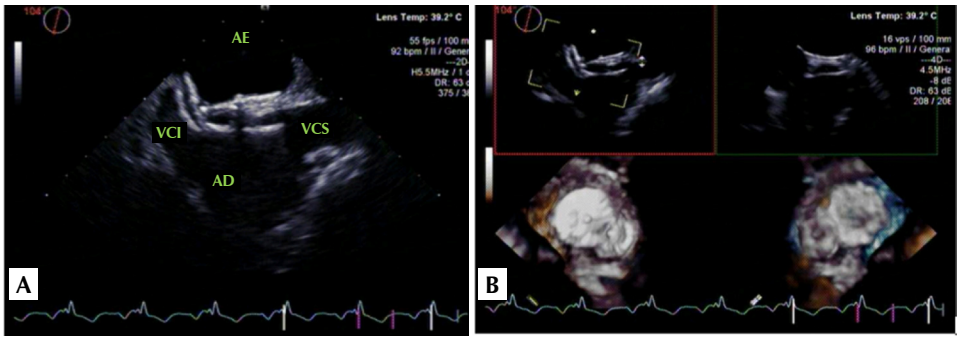

AE: left atrial; VCS: superior vena cava; AD: right atrium; VCI: inferior vena cava.

Figure 3 – *Echocardiogram performed on September 1, 2021, in the late postoperative period of percutaneous closure of the multi-fenestrated atrial septal defect. A. Two-dimensional image of the occluding device in the topography of the interatrial septum. B. Three-dimensional image of the prosthesis.*

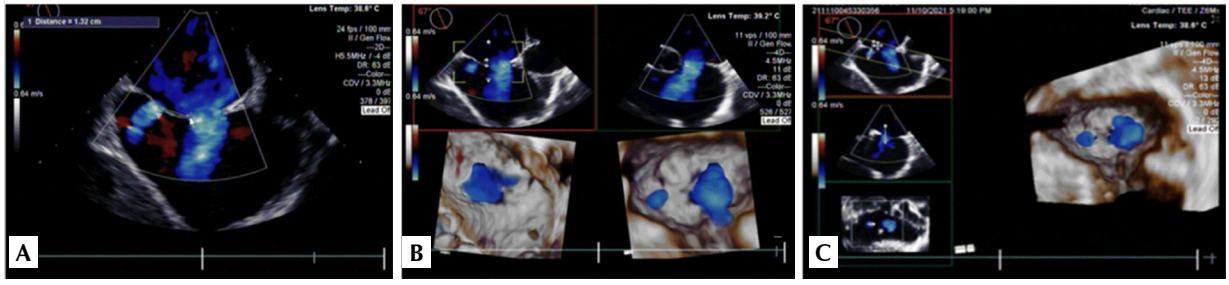

Figure 4 – *Three-dimensional transesophageal echocardiogram taken on November 11, 2021, showing an ostium secundum atrial septal defect (2 fenestrations) with hemodynamic repercussions.*

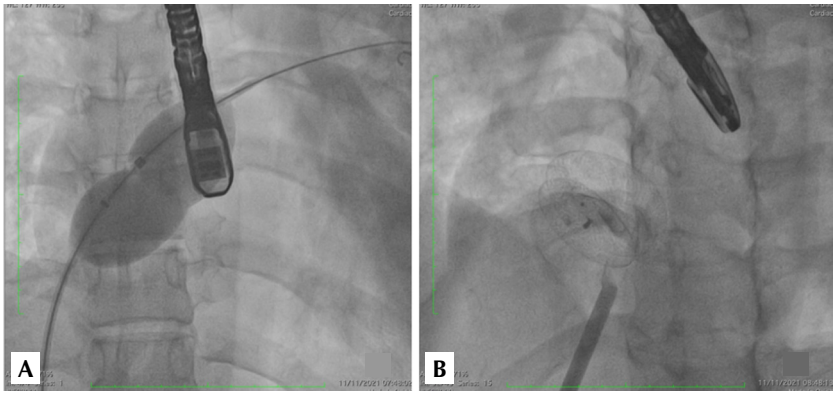

Figure 5 – *Percutaneous closure of two atrial septal defects (ASD) with Amplatzer ASD prostheses on November 11, 2021. A. Balloon sizing. B. Final result.*

Current criteria for the percutaneous treatment of OS ASD include a defect size ≤ 32 mm and a 5-mm rim of atrial septal tissue around the defect, flow through the defect predominantly directed from the left to right atrium, presence of signs of right chamber volumetric overload (increased RV diameter, presence of paradoxical movement in the interventricular septum), no fixed pulmonary hypertension, and no associated defects requiring surgery.[4]

Contraindications to percutaneous treatment include cases in which the defect is small enough to not generate hemodynamic repercussions or severe pulmonary arterial hypertension with indexed pulmonary vascular resistance above 5.0 w.m^2 refractory to pulmonary vasodilator testing.[5]

Interatrial communication has a complex anatomy when presenting the following characteristics: stretched diameter greater than 26 mm; deficient borders measuring less than 4 mm in the anterior, posterior, or inferior region of the septum; two distant fenestrations; multi-fenestrated interatrial

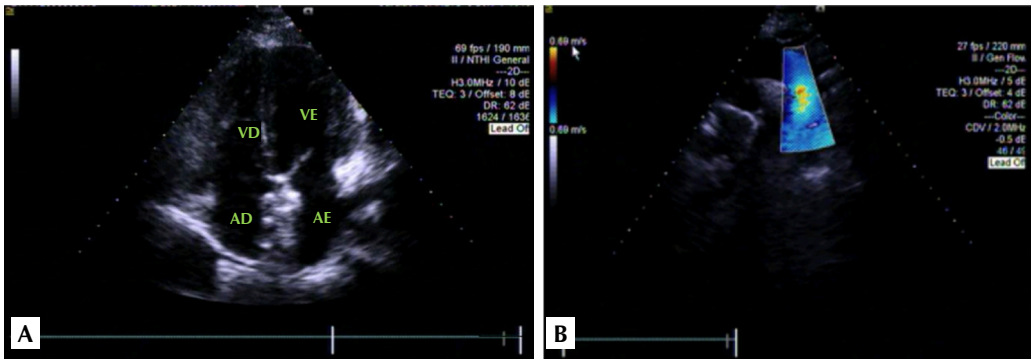

VE: Left ventricle; AE: left atrial; AD: right atrium; VD: right ventricular.

Figure 6 – *Transthoracic echocardiogram taken on November 12, 2021, showing two occluding devices in the interatrial septum (A) and no residual shunt (B).*

septum and interatrial septal aneurysm (redundant and mobile interatrial septum with an excursion greater than 10 mm).[7]

The presence of two or more defects detectable on 3DTEE and distant from one another is amenable to a transcatheter approach since two or more devices can be safely and efficiently implanted simultaneously. In such situations, it is important to individually assess each of the defects. Very small defects (2–3 mm) less than 5 mm away from the largest OS ASD can be indirectly occluded by being covered by the disk of the implanted prosthesis. Multiple small OS ASD (multi-fenestrated septum), provided they are in a region with a diameter of 30–35 mm, can also be percutaneously treated through the implantation of a prosthesis specifically for this purpose.[5]

This prosthesis must have a diameter 20–30% greater than the basal ASD diameter. In cases of multi-fenestrated ASD, the prosthesis must be specific for this type of defect, with two retention disks joined by a thin waist. The device must be implanted through the most central fenestration to allow its disks cover the surrounding fenestrations.[5]

In this context, TTE provides evidence of the shunt through the interatrial septum, cardiac chamber size, RV function, Qp/Qs calculation, and pulmonary pressure estimation, as an insufficient left atrial size can prevent percutaneous ASD closure.[6]

Interestingly, 3DTEE is performed using a sizing catheter to determine the specific anatomical properties of the ASD such as size, location, adequate borders (aortic, mitral, and superior, inferior, and posterior vena cava) and defect relation with adjacent heart structures. In addition, during the procedure, it enables visualizing of the catheters, guiding them through the defect. Color flow Doppler allows defect sizing and helps selecting the proper device size for implantation, confirms the correct device position, evaluates and grades the presence of residual leaks, when possible, checks the need for a second device, and identifies the presence of surgical complications.[6]

The advantages of 3DTEE in the study of ASD include the clear demonstration of the characteristics of the interatrial septum and its defects with special visualization of the extension of the anterosuperior border that established the defect shape and fenestration size. This imaging modality allows an *en face* communication analysis that mimics the surgeon's view with the advantage of being dynamic during the cardiac cycle. After the prosthesis implantation, 3D reconstruction can help identify device position, demonstrate and locate the arms or disks protruding into the right atrium. This method can also be used to assess and measure residual defects.[7]

This procedure presents a low complication rate. Serious complications such as malposition and subsequent surgery occur at a frequency of 1–5%, device embolization in 0.4–4%, stroke in 0.1–0.3%, cardiac tamponade in 0.1%, cardiac perforation in 0.03%, and endocarditis in 0.03%.[4]

An interesting fact in our report was the presence of ASD in non-syndromic siblings. The literature shows reports of patients with OS ASD with a positive family history of this defect or other congenital heart malformations and co-existing heart block. Although an autosomal dominant mode of inheritance for familial ASD was described in some families, the incidence of this defect in these families is many times lower than expected for single-gene defects. Therefore, a multifactorial mode of inheritance has been postulated due to the presence of clinical phenotype diversity combined with generational leaps.[8] According to Benson et al., the familial ASD locus is located in the telomeric region of chromosome 5p. It is a genetically heterogeneous disorder of incomplete penetrance and variable expressivity that results in the significant underestimation of the hereditary nature (multifactorial etiology with complex polygenic interaction and environmental factors) of this condition. The author also suggests that the identification of ASD or other congenital heart defects (such as interatrial septal aneurysm, persistent left superior vena cava, bicuspid aortic valve, which occur in 0.5–1% of cases) in more than one family member should lead to the clinical and genetic evaluation of their relatives. Furthermore, the author emphasized that the identification of other familial genes of ASD should provide new insights about important cardiac morphogenesis steps that lead to atrial septation.[9]

Conclusion

ASD are frequent congenital heart diseases, and a positive family history of this defect should prompt the

investigation of other cardiac anomalies in the index case in addition to the investigation of first-degree relatives. OS ASD occlusion by percutaneous implantation is a safe and effective alternative to traditional surgical closure, but the procedure is not risk-free and must be performed in specialized centers by trained operators. In this context, we highlight the role of echocardiography given the diversity of important data obtained in the pre-, intra-, and postoperative periods of ASD correction as well as in the late follow-up of these patients.

Authors' contributions

Research conception and design: Lopes MP; data collection and manuscript writing: Rocha DFR; critical review of the manuscript for intellectual content: Guimarães HL, Silva JBM and Gardenghi G.

Conflict of interest

The authors have declared that they have no conflict of interest.

References

1. Bigarelli RK, Caixe SH, Martins WP. Defeitos do septo atrial: diagnóstico e tratamento. EURP. 2009;1(2):66-76. [2022 Maio 27] Disponível em: https://issuu.com/fatesa/docs/v1n2abr-mar2009.
2. Ribeiro MS, Costa RN, Pedra SR, Kreuzig DL, Fontes VF, Pedra CA. Estado atual do tratamento dos defeitos do septo atrial. Rev Soc Cardiol Estado de São Paulo. 2017 [citado 2022 Out. 13];27(1):39-48. Disponível em: https://docs.bvsalud.org/biblioref/2021/08/836944/05_revistasocesp_v27_01.pdf
3. Baumgartner H, De Backer J, Babu-Narayan SV, Budts W, Chessa M, Diller GP, et al.; ESC Scientific Document Group. 2020 ESC Guidelines for the management of adult congenital heart disease. Eur Heart J. 2021;42(6):563-645. doi: https://doi.org/10.1093/eurheartj/ehaa554
4. Comissão Nacional de Incorporação de Tecnologia do SUS (Conitec). Procedimento para fechamento percutâneo de comunicação interatrial septal com dispositivo intracardíaco. Relatório de Recomendação. Brasília, DF: Conitec; 2018 [citado 2022 Out. 13]. Disponível em: https://www.gov.br/conitec/pt-br/midias/relatorios/2018/relatorio_oclusores_fechamentopercutaneo.pdf
5. Pedra SR, Pontes Júnior SC, Cassar RS, Pedra CA, Braga SL, Esteves CA, et al. O papel da ecocardiografia no tratamento percutâneo dos defeitos septais. Arq Bras Cardiol. 2006;86(2).
6. Lee MS, Naqvi TZ. A practical guide to the use of echocardiography in assisting structural heart disease interventions. Cardiol Clin. 2013;31(3):441-54. doi: https://doi.org/10.1016/j.ccl.2013.04.004.
7. Gelernter-Yaniv L, Lorber A. The familial formo f atrial septal defect. Acta Paediatrica. 2007;96:726-30. doi: https://doi.org/10.1111/j.1651-2227.2007.00240.x
8. Benson DW, Sharkey A, Fatkin D, Lang P, Basson CT, McDonough B, et al. Reduced penetrance, variable expressivity, and genetic heterogeneity of familial atrial septal defects. Circulation. 1998;97(20):2043-8. doi: https://doi.org/10.1161/01.cir.97.20.2043

Apical Occupation by Endomyocardiofibrosis Associated with Thrombus Diagnosed with Contrast Echocardiography and Resolved with Clinical Treatment

Ocupação Apical por Endomiocardiofibrose Associada a Trombo Diagnosticada com Ecocardiografia de Contraste e Resolvida com Tratamento Clínico

André Timóteo Sapalo[1], Rodolpho Cunha[1], Luis Gustavo Gali[1], Minna Moreira Dias Romano[1]

[1]University of São Paulo, School of Medicine of Ribeirão Preto, Department of Clinical Medicine, Cardiology Center, Laboratory of Echocardiography, Ribeirão Preto, SP, Brazil.

Abstract

Endomyocardial fibrosis (EMF) is a neglected but prevalent disease in underdeveloped countries. Despite its frequency, it is still considered a rare disease. It is marked by the following findings: architectural distortion, ventricular filling changes, and segmental mobility changes affecting not only diastolic and systolic dynamics but also heart valve function. Apical thrombi can be formed in more advanced disease. In this case report, we revisit EMF and present the challenging case of a 52-year-old woman with New York Heart Association (NYHA) functional classification (FC) IV heart failure. Resting electrocardiography revealed sinus rhythm with left ventricular (LV) overload, high voltage vectors, rectified ST-segment depression, and a negative T-wave in the anterolateral region compatible with the strain pattern. The evaluation of echocardiographic images showed marked left atrial dilation, no ventricular dilatation, and hyper-refringent apical occupation within the LV suggestive of a large sessile thrombus superimposed on the endocardial fibrous layer. Although surgery is the most supported approach in the literature in such situations, this patient was treated with oral anticoagulants (OAC) for 1 month and 24 days. The patient progressed well with an improved NYHA FC. Endocavitary contrast echocardiography performed 2 months after OAC initiation showed regression of the apical thrombus image.

Introduction

Endomyocardial fibrosis (EMF) is a neglected but prevalent disease in underdeveloped countries. Global estimates show that approximately 10–12 million people have EMF, mainly in sub-Saharan African and some Latin America regions.[1] In Brazil, the prevalence of the disease is 2%, with a higher incidence in women and a female-to-male ratio of 5:1.[2]

Keywords

Thrombus, Contrast Echocardiography, Oral Anticoagulation.

Mailing Address: Minna Moreira Dias Romano •
R: Ten. Catão Roxo, 3900, Vila Monte Alegre, Ribeirão Preto, SP, Brazil, Postal Code: 14015-010.
E-mail: minna@fmrp.usp.br
Manuscript received 9/20/2022; revised 10/28/2022; accepted 11/3/2022

Editor responsible for the review: Daniela do Carmo Rassi Frota

DOI: 10.47593/2675-312X/20223504eabc349i

The etiology of EMF remains uncertain, but its main morphological characteristic is endocardial layer fibrosis, predominantly in the apical region, that causes architectural distortion, ventricular filling changes, and segmental mobility changes affecting not only diastolic and systolic dynamics but also heart valve functions. In addition, apical occupation by thrombi is found in more advanced disease stages.[3]

Thus, the non-consolidation of the pathophysiological and etiological mechanisms involved in EMF exacerbation complicates therapeutic conduct decisions. In most cases, treatment is based on symptomatic control of heart failure and other cardiomyopathies; in more severe situations, surgical intervention and even heart transplantation are recommended.[4]

Case report

Here we describe the clinical case of a 52-year-old woman with a history of systemic arterial hypertension, hypothyroidism, hepatic steatosis, and gouty arthritis. She presented with short-duration atypical stabbing chest pain (10–15 minutes) of moderate intensity unrelated to physical exertion and without triggering or improving factors at 2 months after the initial appointment.

Resting electrocardiography (ECG) revealed sinus rhythm with left ventricular (LV) overload, high voltage vectors, rectified ST-segment depression, and a negative T-wave in the anterolateral region that may be compatible with the strain pattern (Figure 1).

Transthoracic echocardiography (TTE) at the time of the initial diagnosis revealed a predominantly apical increased myocardial thickness suggestive of differential diagnoses such as apical hypertrophic cardiomyopathy or EMF. Cardiac magnetic resonance imaging (CMR) suggested endomyocardial fibrosis as a cause of the apical occupancy (Figure 2).

A few months later, the patient demonstrated clinical worsening with restrictive syndrome for which she was hospitalized. A new TTE with sulfur hexafluoride contrast (SonoVue) revealed marked left atrial (LA) dilation with an indexed volume of 102 mL of 56 mL/m^2 (greater than in the previous test), and a hyper-refringent apical LV occupancy image suggested a large sessile thrombus superimposed on the endocardial fibrous tissue measuring 24 × 21 mm that was not present on a previous test (Figure 3).

The patient's LV ejection fraction was preserved (58%

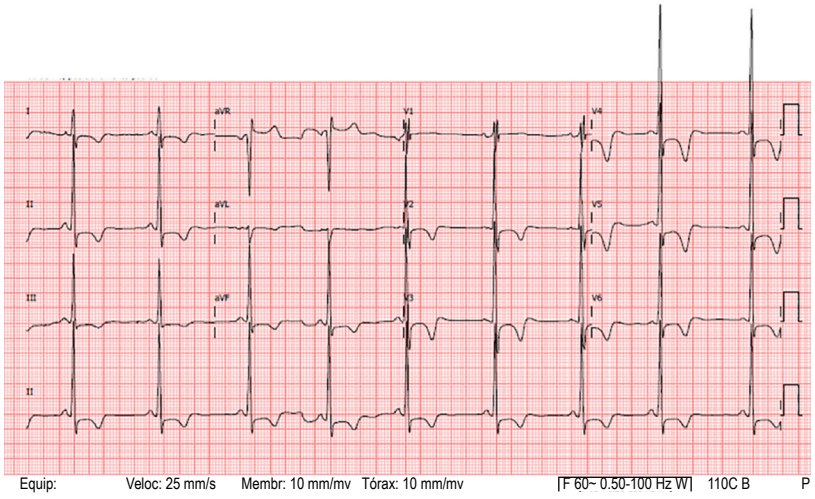

Figure 1 – *Twelve-lead electrocardiogram.*

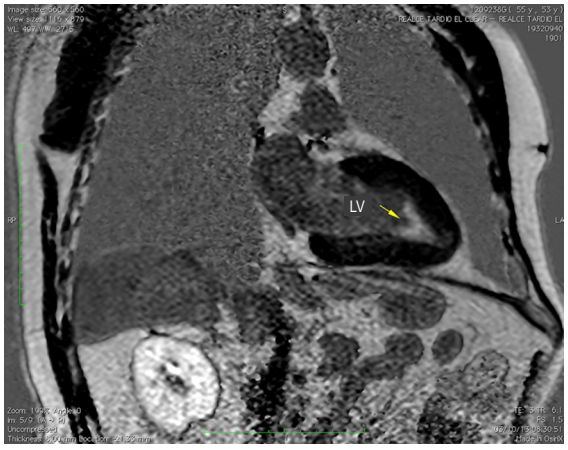

LV: Left ventricle

Figure 2 – *Cardiac magnetic resonance image on which the yellow arrow shows endocardial fibrosis confirming endomyocardial fibrosis.*

using Simpson's method), although there were signs of severe diastolic dysfunction (grade III) typical of EMF (E/A ratio = 2.9). Tissue Doppler analysis showed a reduced mitral annulus velocity (septal e` = 3.7 cm/s; lateral e` = 5.8 cm/s; E/e´ ratio = 17.3) (Figure 4).

Oral anticoagulants (OAC) provided symptom relief. A third TTE 2 months thereafter showed almost complete thrombus resolution and reduced LA dimensions (Figure 5).

Discussion

This is an infrequent clinical case that lacks conduct based on robust scientific evidence. Although its etiology is still poorly understood, other publications such as that of Tharakan[5] corroborate our findings, emphasizing that LV EMF is characterized by several degrees of endocardial obliteration that is usually limited to the endocardium and presents only secondary effects in the myocardium without significant pericardial involvement. LV morphology may present a dilation spectrum in the transverse axis of the basal region assuming a spherical shape. ECG abnormalities reflect hemodynamic changes (LA overload) that depend on diastolic dysfunction and mitral regurgitation degree.

TTE, associated with other imaging methods such as CMR, is essential for the morphological diagnosis. While TTE can be used to perform diagnostic and sequential evaluations at lower cost and with greater availability with the use of new techniques such as cavity contrast, which can improve the definition of apical images for both ventricles, CMR provides better spatial resolution and detects late gadolinium enhancement in the endocardial layer of the ventricular apex.[6,7]

As previously emphasized, the therapeutic approaches to this heart disease are quite challenging. The current

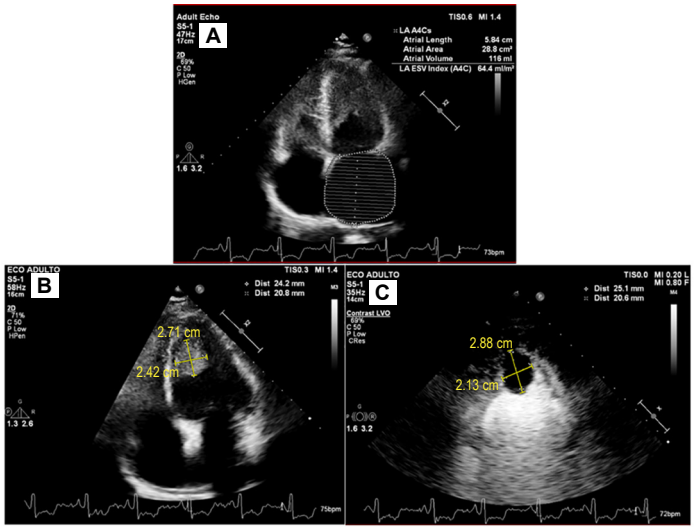

Figure 3 – *(A) Measurement of left atrial volume using Simpson's method; (B) Intracavitary thrombus measurement; (C) Use of contrast to increase thrombus enhancement*

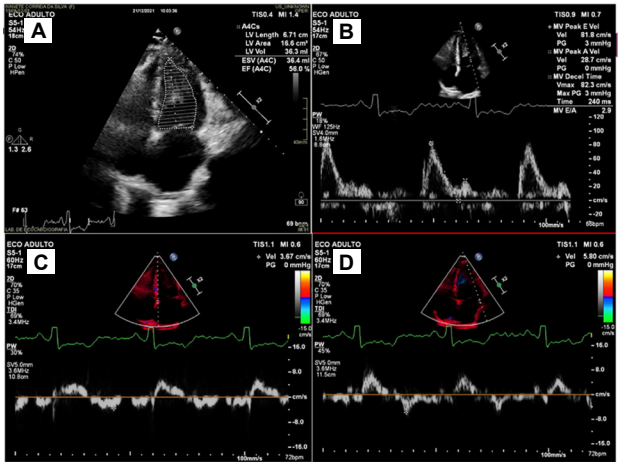

Figure 4 – *(A) Ejection fraction measurement; (B) Doppler transmitral flow; (C) Movement of the septal mitral annular plane by tissue Doppler; (D) Movement of the lateral mitral annular plane.*

treatment is based on the symptomatic control of heart failure. Surgical intervention for apical evacuation is beneficial in patients with signs of severe ventricular restriction and New York Heart Association functional class III or IV heart failure.[8]

In contrast, here we demonstrated a case of good clinical progression after symptomatic treatment with OAC that could not only be diagnosed with multimodality support, its follow-up and apical thrombus resolution was supported by TTE with cavity contrast.

Authors' contributions

Manuscript Writing, Data Analysis and Interpretation: Sapalo AT; Data Collection: Cunha R, Gali LG; Critical Review of the Manuscript for Importante Intellectual Contente: Romano MMD.

Conflict of interest

The authors have declared that they have no conflict of interest.

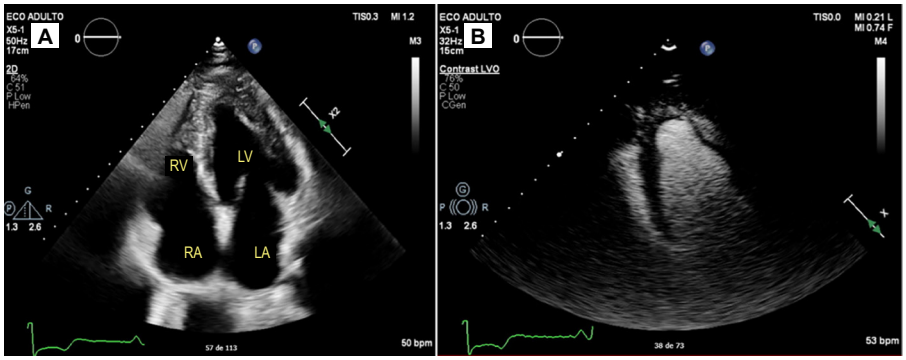

LA, left atrium; LV, left ventricle; RA, right atrium; RV, right ventricle.

Figura 5 – *(A) Apical window showing complete thrombus removal and LA diameter reduction; (B) Use of contrast to increase enhancement of the thrombus region.*

References

1. Bukhman G, Ziegler J, Parry E. Endomyocardial fibrosis: still a mystery after 60 years. PLoS Negl Trop Dis. 2008;2(2):e97. doi: 10.1371/journal.pntd.0000097
2. da Costa FD, Moraes CR, Rodriques JV, de Mendonça JT, de Andrade JC, Buffolo E, et al. Early surgical results in the treatment of endomyocardial fibrosis. A Brazilian cooperative study. Eur J Cardiothorac Surg. 1989;3(5):408-13. doi: 10.1016/1010-7940(89)90049-3
3. Iglezias SD, Benvenuti LA, Calabrese F, Salemi VM, Silva AM, Carturan E, et al. Endomyocardial fibrosis: pathological and molecular findings of surgically resected ventricular endomyocardium. Virchows Arch. 2008;453(3):233-41. doi: 10.1007/s00428-008-0652-3
4. Beaton A, Mocumbi AO. Diagnosis and management of endomyocardial fibrosis. Cardiol Clin. 2017;35(1):87-98. Available from: http://dx.doi.org/10.1016/j.ccl.2016.08.005
5. Tharakan JA. Electrocardiogram in endomyocardial fibrosis. Indian Pacing Electrophysiol J. 2011;11(5):129-33. PMID: 21994470.
6. Salemi VM, Rochitte CE, Shiozaki AA, Andrade JM, Parga JR, de Ávila LF, et al. Late gadolinium enhancement magnetic resonance imaging in the diagnosis and prognosis of endomyocardial fibrosis patients. Circ Cardiovasc Imaging. 2011;4(3):304-11. doi: 10.1161/CIRCIMAGING.110.950675
7. Mocumbi AO, Carrilho C, Sarathchandra P, Ferreira MB, Yacoub M, Burke M. Echocardiography accurately assesses the pathological abnormalities of chronic endomyocardial fibrosis. Int J Cardiovasc Imaging. 2011;27(7):955-64. doi: 10.1007/s10554-010-9753-6.
8. Moraes F, Lapa C, Hazin S, Tenorio E, Gomes C, Moraes CR. Surgery for endomyocardial fibrosis revisited. Eur J Cardiothorac Surg. 1999 Mar;15(3):309-12; discussion 312-3. doi: 10.1016/s1010-7940(99)00027-5.